sid.inpe.br/mtc-m21d/2021/12.07.02.34-TDI

APPLICATION OF THE SDRE TECHNIQUE IN THE SATELLITE ATTITUDE AND ORBIT CONTROL SYSTEM WITH NONLINEAR DYNAMICS

Alessandro Gerlinger Romero

Doctorate Thesis of the Graduate Course in Space Engineering and Technology, guided by Drs. Luiz Carlos Gadelha de Souza, and Antonio Fernando Bertachini de Almeida Prado, approved in December 07, 2021.

URL of the original document:
<http://urlib.net/8JMKD3MGP3W34T/45TQ5D8>

INPE
São José dos Campos
2021

PUBLISHED BY:

Instituto Nacional de Pesquisas Espaciais - INPE
Coordenação de Ensino, Pesquisa e Extensão (COEPE)
Divisão de Biblioteca (DIBIB)
CEP 12.227-010
São José dos Campos - SP - Brasil
Tel.:(012) 3208-6923/7348
E-mail: pubtc@inpe.br

sid.inpe.br/mtc-m21d/2021/12.07.02.34-TDI

APPLICATION OF THE SDRE TECHNIQUE IN THE SATELLITE ATTITUDE AND ORBIT CONTROL SYSTEM WITH NONLINEAR DYNAMICS

Alessandro Gerlinger Romero

Doctorate Thesis of the Graduate Course in Space Engineering and Technology, guided by Drs. Luiz Carlos Gadelha de Souza, and Antonio Fernando Bertachini de Almeida Prado, approved in December 07, 2021.

URL of the original document:
<http://urlib.net/8JMKD3MGP3W34T/45TQ5D8>

INPE
São José dos Campos
2021

Cataloging in Publication Data

Romero, Alessandro Gerlinger.

R664a Application of the SDRE technique in the satellite attitude and orbit control system with nonlinear dynamics / Alessandro Gerlinger Romero. – São José dos Campos : INPE, 2021.

xxvi + 111 p. ; (sid.inpe.br/mtc-m21d/2021/12.07.02.34-TDI)

Thesis (Doctorate in Space Engineering and Technology) – Instituto Nacional de Pesquisas Espaciais, São José dos Campos, 2021.

Guiding : Drs. Luiz Carlos Gadelha de Souza, and Antonio Fernando Bertachini de Almeida Prado.

1. Nonlinear control. 2. SDRE. 3. H_∞. I.Title.

CDU 629.7.062.2:521.31

MINISTÉRIO DA CIÊNCIA, TECNOLOGIA E INOVAÇÕES

INSTITUTO NACIONAL DE PESQUISAS ESPACIAIS
Serviço de Pós-Graduação - SEPGR

DEFESA FINAL DE TESE DE ALESSANDRO GERLINGER ROMERO
BANCA Nº 278/2021, REG 107697/2017

No dia 07 de dezembro de 2021, as 10h, por teleconferência, o(a) aluno(a) mencionado(a) acima defendeu seu trabalho final (apresentação oral seguida de arguição) perante uma Banca Examinadora, cujos membros estão listados abaixo. O(A) aluno(a) foi APROVADO(A) pela Banca Examinadora, por unanimidade, em cumprimento ao requisito exigido para obtenção do Título de Doutor em Engenharia e Tecnologia Espaciais/Mecânica Espacial e Controle.

Título: "APPLICATION OF THE SDRE TECHNIQUE IN THE SATELLITE ATTITUDE AND ORBIT CONTROL SYSTEM WITH NONLINEAR DYNAMICS".

Membros da Banca:

Dr. Mario César Ricci – Presidente – INPE
Dr. Luiz Carlos Gadelha de Souza - Orientador UFABC
Dr. Antonio Fernando Bertachini de Almeida Prado – Orientador INPE
Dr. Valdemir Carrara – Membro Externo – ITA
Dr. Alain Giacobini de Souza -Membro Externo - ITA

Documento assinado eletronicamente por **Antonio Fernando Bertachini de Almeida Prado**, **Chefe do Serviço de Pós-Graduação**, em 20/12/2021, às 11:06 (horário oficial de Brasília), com fundamento no § 3º do art. 4º do Decreto nº 10.543, de 13 de novembro de 2020.

Documento assinado eletronicamente por **alain giacobini de souza (E)**, **Usuário Externo**, em 20/12/2021, às 12:51 (horário oficial de Brasília), com fundamento no § 3º do art. 4º do Decreto nº 10.543, de 13 de novembro de 2020.

Documento assinado eletronicamente por **Luiz Carlos Gadelha de Souza (E)**, **Usuário Externo**, em 20/12/2021, às 15:56 (horário oficial de Brasília), com fundamento no § 3º do art. 4º do Decreto nº 10.543, de 13 de novembro de 2020.

Documento assinado eletronicamente por **Valdemir Carrara (E)**, **Usuário Externo**, em 20/12/2021, às 18:40 (horário oficial de Brasília), com fundamento no § 3º do art. 4º do Decreto nº 10.543, de 13 de novembro de 2020.

Documento assinado eletronicamente por **Mario Cesar Ricci**, **Tecnologista**, em 21/12/2021, às 11:31 (horário oficial de Brasília), com fundamento no § 3º do art. 4º do Decreto nº 10.543, de 13 de novembro de 2020.

A autenticidade deste documento pode ser conferida no site http://sei.mctic.gov.br/verifica.html, informando o código verificador **8402175** e o código CRC **6C316CF9**.

Referência: Processo nº 01340.007649/2021-04 SEI nº 8402175

"DK 21B34. But as for certain truth, no man has known it,
Nor will he know it; neither of the gods,
Nor yet of all the things of which I speak.
And even if by chance he were to utter
The final truth, he would himself not know it:
For all is but a woven web of guesses.

DK B18. The gods did not reveal, from the beginning,
All things to us; but in the course of time,
Through seeking we may learn, and know things better."

Xenophanes of Colophon,
c. 570 – c. 478 BC, translated from Greek by Karl Raimund Popper in "The World of Parmenides: Essays on the Presocratic Enlightenment, 2002."

This thesis is dedicated to the eternal women:
Graziela**, **Gabriela** and **Sheila

ACKNOWLEDGEMENTS

"*Quod potui feci; veniam da mihi, posteritas* – What I could have done, me you will (please forgive), posterity" - The epitaph of Leonardo da Vinci

I would like to thank prof. Gadelha, who supported this endeavor across the inevitable storms. I also would like to thank prof. Bertachini, who joined us later and helped to conclude such the endeavor. In some way, they know "*Yes, there were times I'm sure you knew when I bit off more than I could chew but through it all when there was doubt I ate it up and spit it out*".

I would like to thank my parents, Sheila and Waldomiro, because they taught me by example and then "*I faced it all and I stood tall and did it my way*".

Finally, I would like to thank my daughters, Graziela and Gabriela since the more I live with them, the more I know "*the gods did not reveal, from the beginning, all things to us; but in the course of time, through seeking we may learn, and know things better*". I understand better than ever we always will be together somehow.

ABSTRACT

The satellite attitude and orbit control subsystem (AOCS) can be designed with success by linear control theory if the satellite has slow angular motions. However, for fast maneuvers, the linearized models are not able to represent all the perturbations due to the effects of the nonlinear terms present in the dynamics which compromises the system's performance. Therefore, in such cases, it is expected that nonlinear control techniques yield better performance than the linear control techniques, improving the AOCS pointing accuracy without requiring a new set of sensors and actuators. Nonetheless, these nonlinear control techniques can be more sensitive to uncertainties. One candidate technique for the design of AOCS control law under a fast maneuver is the State-Dependent Riccati Equation (SDRE). SDRE provides an effective algorithm for synthesizing nonlinear feedback control by allowing nonlinearities in the system states while offering great design flexibility through state-dependent weighting matrices. The Brazilian National Institute for Space Research (INPE, in Portuguese) was demanded by the Brazilian government to build remote-sensing satellites, such as the Amazonia-1 and the CONASAT missions. In the Amazonia-1 mission, the AOCS must stabilize the satellite in three-axes so that the optical payload can point to the desired target. Currently, the control laws of AOCS are designed and analyzed using linear control techniques in commercial software. In this work, we present research focused on modeling and analysis, through simulation using open-source software based on Java, of control laws, applying SDRE and SDRE extended with H_∞ techniques, for attitude control as nonlinear systems tackling the regulator problem in the presence of hard nonlinearities and uncertainties. Moreover, we present a methodology to evaluate a possible quantifiable increment in the robustness of SDRE and SDRE extended with H_∞ when compared to linear techniques.

Keywords: Nonlinear control. SDRE. H_∞.

APLICAÇÃO DA TÉCNICA SDRE NOS SISTEMAS DE CONTROLE DE ATITUDE E ÓRBITA DE SATÉLITES COM DINÂMICA NÃO LINEAR

RESUMO

O subsistema de controle de atitude e órbita de um satélite (AOCS, do Inglês, Attitude and Orbit Control subsystem) pode ser projetado com sucesso pela teoria do controle linear se o satélite exibir movimentos angulares lentos. No entanto, para manobras rápidas, os modelos linearizados não são capazes de representar todas as perturbações devido aos efeitos dos termos não lineares presentes na dinâmica o que compromete o desempenho do sistema. Portanto, nesses casos, espera-se que as técnicas de controle não-lineares apresentem melhor desempenho do que as técnicas de controle linear, melhorando a precisão de apontamento do AOCS sem exigir um novo conjunto de sensores e atuadores. No entanto, essas técnicas de controle não lineares podem ser mais sensíveis a incertezas. Uma técnica candidata para o projeto da lei de controle do AOCS para manobras rápidas é a equação de Riccati dependente do estado (SDRE, do Inglês, State-Dependent Riccati Equation). O SDRE fornece um algoritmo eficaz para sintetizar o controle baseado em feedback, permitindo não linearidades nos estados do sistema, oferecendo grande flexibilidade de projeto por meio de matrizes peso dependentes do estado. O Instituto Nacional de Pesquisas Espaciais (INPE) é demandado pelo governo brasileiro para a construção de satélites de sensoriamento remoto, como a missão Amazônia-1 e a missão CONASAT. Na missão Amazonia-1, o AOCS deve estabilizar o satélite em três eixos, para que a carga óptica possa apontar para o alvo desejado. Atualmente, as leis de controle do AOCS são projetadas e analisadas usando técnicas de controle linear em software comercial. Neste trabalho, apresentamos uma pesquisa voltada para modelagem e análise, por meio de simulação usando software livre baseado em Java, de leis de controle, aplicando SDRE e SDRE estendido com H_∞, para controle de atitude como sistemas não lineares focada no problema do regulador na presença de incertezas e não linearidades rígidas. Além disso, apresentamos uma metodologia para avaliar um possível incremento quantificável na robustez do SDRE e do SDRE estendido com H_∞ quando comparado às técnicas lineares.

Palavras-chave: Controle Não Linear. SDRE. H_∞.

LIST OF FIGURES

Page

LIST OF TABLES

Page

LIST OF ABBREVIATIONS

ARE	–	Algebraic Riccati Equation
AWGN	–	Additive White Gaussian Noise
DCM	–	Direction Cosine Matrix
ECI	–	Earth-centered inertial
LFT	–	Linear Fractional Transformation
LQR	–	Linear Quadratic Regulator
LTI	–	Linear Time Invariant
INPE	–	National Institute for Space Research (Instituto Nacional de Pesquisas Espaciais)
MRPs	–	Modified Rodrigues Parameters
NP	–	Nominal Performance
NS	–	Nominal Stability
ROA	–	Region of Attraction
RP	–	Robust Performance
RS	–	Robust Stability
SDC	–	State-Dependent Coefficients
SDRE	–	State-Dependent Riccati Equation

LIST OF SYMBOLS

A, B, C, D	–	matrices that represent the linear state-space
A(x), B(x), C(x), D(x)	–	functions of the state that represent the pseudo-linear state-space
$\dot{x}$	–	the derivative, with respect to time, of x
$\mathbb{R}$	–	the set of real numbers
$\|\|\ \|\|_2$	–	L2 norm
$\|\|\ \|\|_\infty$	–	L-infinity norm

CONTENTS

Page

1 INTRODUCTION

> "Dogmatism and skepticism are both, in a sense, absolute philosophies; one is certain of knowing, the other of not knowing. What philosophy should dissipate is certainty, whether of knowledge or ignorance." - Bertrand Russel

In this chapter, the motivation of the thesis is explored and the problem is stated. Subsequently, the hypotheses and goals are described, which support the presentation of contributions. Finally, the outline of this thesis is presented.

1.1 Motivation

In the design of a satellite attitude and orbit control subsystem (AOCS), the one in charge of the attitude control, which involves plant uncertainties, large angle maneuvers, and fast attitude control following a stringent pointing, requires nonlinear control methods in order to satisfy performance and robustness requirements. An example is a typical mission of the Brazilian National Institute for Space Research (INPE), in which the AOCS must stabilize a satellite in three-axes so that the optical payload can point to the desired target with few arcsecs of pointing accuracy, e.g., Amazonia-1 (SILVA et al., 2014). Another example is the Nano-satellite Constellation for Environmental Data Collection (CONASAT) (CARVALHO, 2010; MESQUITA et al., 2017), a set of remote sensing CubeSats of the INPE, in which the AOCS must stabilize the satellite in two-axes in order to maximize the receiving of environment data sent by platforms in the Brazilian territory.

One candidate method for a nonlinear AOCS control law is the State-Dependent Riccati Equation (SDRE) method, originally proposed by Pearson (1962) and then explored in detail by Cloutier et al. (1996), Cloutier (1997), Çimen (2008), Çimen (2010). SDRE provides an effective algorithm for synthesizing nonlinear feedback control by allowing nonlinearities in the system states while offering great design flexibility through state-dependent weighting matrices.

In this thesis, we present research focused on modeling and analysis, through simulation using open-source software, of control laws, applying State-Dependent Riccati Equation (SDRE) and SDRE extended with H_∞, for attitude control in AOCSs as nonlinear systems tackling the regulator problem.

1.2 Problem, hypothesis, and goals

1.2.1 Problem

Statement of the problem

Brazilian National Institute for Space Research (INPE) has been demanded by the Brazilian government to build satellites and CubeSats, such as Amazonia-1 and CONASAT missions, respectively. Currently, the control laws of the attitude control system are designed and analyzed using linear control techniques in commercial software (CARVALHO, 2010; MESQUITA et al., 2017; SILVA et al., 2014). However, for fast maneuvers, the linearized models are not able to represent all the perturbations that can compromise the system's performance. Additionally, the pressure to reduce costs may force, or at least stimulate, the usage of open-source software for the analysis through simulation.

Area

Control Engineering

Subject

Modeling and analysis, through simulation using open-source software, of control laws, applying State-Dependent Riccati Equation (SDRE) and SDRE extended with H_∞, for attitude control systems as nonlinear systems tackling the regulator problem.

Main question

Do the modeling of attitude control systems as nonlinear systems and applying to such models SDRE and SDRE extended with H_∞ as controllers for the regulator problem provide a quantifiable increment in the robustness when compared to linear techniques?

Explained main question

Although linear control techniques have been applied with success to the INPE's satellites, it may be the case that there are opportunities to increment the robustness of satellites built by INPE, such as Amazonia-1, by modeling them as a nonlinear system and applying to such models the SDRE and SDRE extended with H_∞ techniques as the controller for the regulator problem.

In particular, for fast maneuvers, the linearized models, which rely on the key assumption of small range operation, are not able to represent all the perturbations due to the effects of the nonlinear terms present in the dynamics. Moreover,

the uncertainties (structured and unstructured) can lead to significant performance degradation or even instability, when not taken into account.

Furthermore, the stringent requirements for reduction of volume, mass, and power in conjunction with pointing accuracy can pose challenges to the current techniques, based on linear control. CONASAT is a well-known example of the former three requirements since they determine a CubeSat for the space segment.

Problem rationale

Linear control techniques have been applied with success by INPE, therefore, it is natural for one to wonder why to investigate a nonlinear control technique, in particular, SDRE using open-source software.

There are many reasons for that investigation ranging from the demand to push the science borders to opportunities for the improvement of robustness in the practical day-to-day. For this work, the main reasons to investigate a nonlinear control technique can be summarized as:

- **Improvement of existing systems** - the linearized models, which rely on the key assumption of small range operation, are not able to use the potential from the system, in the sense that, the maneuvers in the attitude control are neither optimal nor suboptimal for some to be defined cost function, in such a way that there are wasting of energy and, consequently, wasting of hardware equipment;
- **Hard nonlinearities** - another assumption of linear control is that the dynamics is linearizable. However, there are nonlinearities whose discontinuous nature does not allow linear approximation, the "hard nonlinearities", e.g., the saturation of the reaction wheels;
- **Uncertainties** - linear controllers usually assume that the parameters and the dynamics of the system are reasonably well known. However, the attitude and orbit control of satellites involves uncertainties in the parameters (structured uncertainty) and in the model of the systems' dynamics (unstructured uncertainties).
- **Potential new requirements** - for example, for fast maneuvers, the linearized models, which rely on the previously cited key assumption, are not able to represent all the perturbations due to the effects of the nonlinear terms;

The next fundamental question is why to investigate SDRE but not another nonlinear control technique.

There is a plethora of nonlinear control techniques, these include any technique based on some sort of linearization, e.g, feedback linearization (SLOTINE; LI, 1991); and nonlinear techniques not based on linearization such as sliding control (SLOTINE; LI, 1991), adaptative control (SLOTINE; LI, 1991; KHALIL, 2002) and control-Lyapunov function (BACCIOTTI A.; ROSIER, 2005; KHALIL, 2002).

Lesser-known nonlinear technique is SDRE (CLOUTIER, 1997), which was originally proposed by (PEARSON, 1962) and then explored, decades later, in detail by (CLOUTIER et al., 1996; CLOUTIER, 1997; ÇIMEN, 2008; ÇIMEN, 2010). Pearson (PEARSON, 1962) observed that one of the difficulties of controlling a nonlinear dynamic system is that optimal control policies are not generally easy to implement so a lengthy preliminary computation is required which presents quite unwieldy solutions for the controller to realize. In other words, in general, the embedded required computations are too expensive as well as their certification so the idea is starting with a nonlinear control problem, a linear time and state varying model is constructed. Such a model is treated as an instantaneously stationary linear system and then optimized using the usual techniques.

The SDRE technique, as a suboptimal nonlinear control technique, has three major advantages: (a) simplicity, (b) numerical tractability (for embedded computation), and (c) flexibility for the designer (ÇIMEN, 2008).

Therefore, the reasons to investigate SDRE as the nonlinear control technique in this work can be summarized as follows: (1) suboptimal results; (2) less known, consequently, it exhibits more opportunities for extension; (3) numerical tractability for embedded computation so it can be applied in the practical day to day; and (4) flexibility for the designer.

There is a plethora of linear control techniques that could be used for the evaluation proposed. The selection of LQR as the linear control technique is rooted in two reasons: (1) LQR is the linear counterpart of SDRE (see Section 2); and, (2) this thesis assumes that $x(t)$ is known exactly (KALMAN, 1960a), consequently, the well-known weakness of LQR regarding sensitivity to perturbation on the state acquisition is not relevant.

The analysis through simulation is the current practice of control engineering, fur-

thermore, it is based on commercial software usually. The usage of open-source software is an alternative to reduce costs. Therefore, the selection of the programming language that supports the open-source software for the investigation of SDRE is the final topic in the present problem rationale.

One can argue that open-source software can be defined using a commercial programming language, however, such argument remits to licensing costs readily. Therefore, an "open-source" programming language shall be used to support the open-source software. Figure 1.1 shows the most popular programming languages in the major repository of open-source software available (GITHUT, 2020).

Figure 1.1 - Language popularity in the major open-source repository.

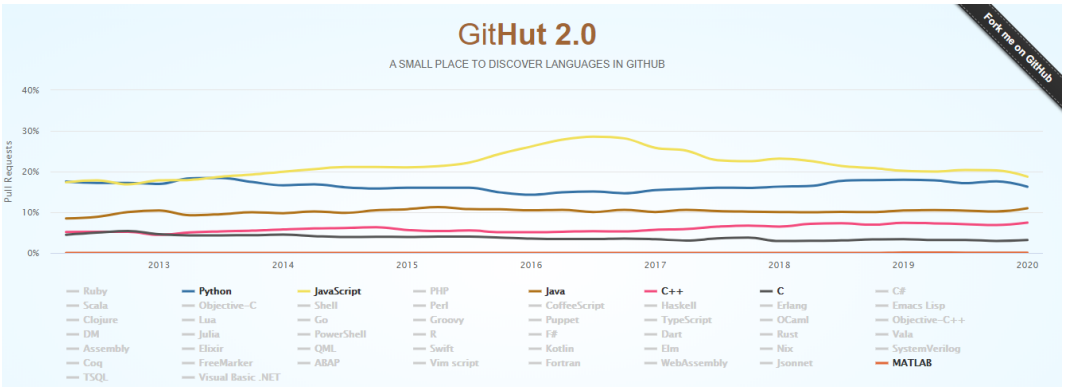

SOURCE: GitHut (2020).

The top three programming languages are Javascript, Python, and Java, respectively. Those three programming languages can run in a variety of runtime environments, in addition, the former two programming languages are dynamic-typed languages while the latter is a static-typed language. It is well-known that static-typed programming languages make sure that there were not any type violations applying static analysis techniques, which are requirements for certification processes generally. Moreover, taking into account the CubeSats, in particular, PhoneSats, it is public that the major open platform for phone development, Android platform (GOOGLE, 2020), supports two static-typed languages, namely, Kotlin and Java. Finally, there is research evaluating the embedding of Java software in avionics (ARMBRUSTER et al., 2007) and in mission-critical large-scale embedded systems (SHARP et al., 2003).

Therefore, the reasons to use Java as the programming language that supports the open-source software can be summarized as follows: (1) static-typed language more friendly to certification process; (2) a programming language for PhoneSats based on Android platform; (3) popularity, which means, among other aspects, the availability of professional resources; and (4) in theory, embeddable.

To the best of our knowledge the hypothesis, presented in the next section, is original, general, and largely applicable.

1.2.2 Hypothesis

H_0: There is no significant quantifiable increment of robustness between LQR, a linear control technique, and SDRE control technique in the INPE's missions.

H_1: There is a significant quantifiable increment of robustness between LQR, a linear control technique, and SDRE control technique in the INPE's missions.

1.2.3 Goal

Investigate and compare the quantifiable results of the application of SDRE and SDRE extended with H_∞ techniques in the satellite attitude control system with nonlinear dynamics. In particular, modeling and analysis, through simulation using open-source software based on Java, of control laws, applying State-Dependent Riccati Equation (SDRE) and SDRE extended with H_∞ techniques, for attitude control as nonlinear systems tackling the regulator problem in the presence of hard nonlinearities and uncertainties.

Specific goals

a) Mathematical modeling and evaluation of uncertainties using SDRE and SDRE extended with H_∞ in the presence of hard nonlinearities

b) Evaluation of the stability through the determination of the region of attraction of LQR, SDRE, and SDRE extended with H_∞ in the presence of hard nonlinearities and uncertainties

c) Compare the quantifiable results, using Monte Carlo perturbation models, between a linear control technique (LQR) and its counterpart nonlinear technique SDRE as well as SDRE extended with H_∞ in the presence of hard nonlinearities and uncertainties

1.2.4 Delimitations

It is beyond the scope of the present thesis the following related topics: orbital dynamics control and simulation (HUGHES, 1986; SIDI, 2006; OREKIT..., 2017), attitude estimation based on noisy sensor measurements (HUGHES, 1986; SIDI, 2006), and real-time implementation concerns of an SDRE controller based on the Java software (ARMBRUSTER et al., 2007; SHARP et al., 2003) or other software languages as C (MENON et al., 2002).

1.3 Contribution

The major significance of the current work is centered on the engineering contribution presented in the next subsection.

1.3.1 Engineering contribution

The appropriately tackling of uncertainties for nonlinear systems in the context of SDRE and SDRE extended with H_∞ may be a significant contribution to the research field of control engineering.

In addition, for INPE, such contribution may have direct results in cheaper and longer space missions. In particular, replacing the linear models/control with nonlinear/suboptimal control maneuvers may save energy and, consequently, hardware equipment, which in turn may increase the lifecycle of space missions reducing costs. Moreover, the space missions may be more robust to imperfections in the building as well as to perturbations in the space environment. Finally, more stringent requirements may be fulfilled using the same set of sensors and actuators.

The drawback of the suboptimal control using SDRE is that its implementation requires more computing resources and tends to exhibit difficulties for verification.

1.3.2 Strategic contribution

Space agencies around the world are heavily working on open-source software. Indeed, it is a trend for space agencies due to the generally perceived benefits ((ESA), 2020):

- increases software quality;
- reduces development and maintenance costs for the individual users;
- avoids vendor lock-in;

- facilitates rapid evolution of the software;
- encourages reuse of software;
- fosters industrial competitiveness;
- develops lucrative consulting, training, and support services offering.

Furthermore, space agencies have specific programs for open-source development, e.g., NASA (AERONAUTICS; (NASA), 2020) and CNES (CNES, 2020). Indeed, the library used in this work for flight-dynamics, Orekit (OREKIT..., 2017), is sponsored by a relevant company in the aerospace market.

Therefore, the open-source software, based on an open programming language and available at the major open-source repository, may have strategic significance for INPE and can serve as one more step in the direction of following other space agencies (a minor strategic contribution).

Finally, the open-source software, already available, can run on a variety of platforms - including an Android operating system in a CubeSat - as well as it has lower costs.

1.4 Outline

This thesis draft is organized as follows. This Section 1, presents the problem, the hypothesis, goals, delimitations, and contributions. In Section 2, a review of the preliminaries is shared. In Section 3, the state of the art is presented. In Section 4, the methodology is presented. The models are shared in Section 5 and the preliminary results are presented in Section 6. Finally, the conclusions and future work are shared in Section 7.

2 PRELIMINARIES

This chapter presents the preliminaries that support this work. The first section briefly reviews the attitude for a rigid-body, indeed, the satellites are treated as rigid-bodies in this work. The last section shares the preliminaries related to attitude control.

2.1 Rigid-body attitude

This section presents the preliminaries for the satellite attitude dynamics, indeed, in this work, a rigid-body. Recall orbital dynamics is out of the scope of the present work.

2.1.1 Kinematics

Given the Earth-centered inertial (ECI) reference frame ($\mathfrak{F}_i$) and the frame defined in the satellite with origin in its centre of mass (the body-fixed frame, $\mathfrak{F}_b$), then a rotation $R \in SO(3)$ - $SO(3)$ is the set of all attitudes of a rigid body described by 3×3 orthogonal matrices whose determinant is one - represented by a unit quaternion $Q = [q_1\ q_2\ q_3 \mid q_4]^T$ as well as a direction cosine matrix (DCM) C_{body_eci} can define the attitude of the satellite.

Defining the angular velocity $\vec{\omega} = [\omega_1\, \omega_2\, \omega_3]^T$ of $\mathfrak{F}_b$ with respect to $\mathfrak{F}_i$ measured in the $\mathfrak{F}_b$, the kinematics can be described by Equation 2.1 (CARRARA, 2012; HUGHES, 1986).

$$\begin{aligned} \omega^{\times}_{body\_eci} &= -\dot{C}_{body\_eci} C^T_{body\_eci} \\ \dot{C}_{body\_eci} &= C_{body\_eci} \omega^{\times}_{body\_eci} \end{aligned} \tag{2.1}$$

where $\omega^{\times}$ is the anti-symmetric matrix that represents the cross product.

Equation 2.1 allows the prediction of the satellite's attitude if it is available the initial attitude and the history of the change in the angular velocity ($\dot{\theta} = F(\omega, t)$).

2.1.1.1 Euler angles

Using the Euler angles (non-classic Euler angles 3-2-1, indeed, Cardan angles), the kinematics can also be defined by Equation 2.2 (HUGHES, 1986).

$$S = \begin{bmatrix} -\sin\theta_2 & 0 & 1 \\ -\cos\theta_2 \sin\theta_3 & \cos\theta_3 & 0 \\ \cos\theta_2 \cos\theta_3 & -\sin\theta_3 & 0 \end{bmatrix}$$
$$\begin{bmatrix} \omega_1 \\ \omega_2 \\ \omega_3 \end{bmatrix} = S \begin{bmatrix} \dot{\theta}_1 \\ \dot{\theta}_2 \\ \dot{\theta}_3 \end{bmatrix} \tag{2.2}$$

In order to model how the satellite attitude changes depending on angular velocity, the matrix S is inverted as shown in Equation 2.3 (it has a discontinuity at 90° since $\cos\frac{\pi}{2} = 0$).

$$S^{-1} = \begin{bmatrix} 0 & \frac{\sin\theta_3}{\cos\theta_2} & \frac{\cos\theta_3}{\cos\theta_2} \\ 0 & \cos\theta_3 & -\sin\theta_3 \\ 1 & \frac{\sin\theta_3 \sin\theta_2}{\cos\theta_2} & \frac{\cos\theta_3 \sin\theta_2}{\cos\theta_2} \end{bmatrix}$$
$$\begin{bmatrix} \dot{\theta}_1 \\ \dot{\theta}_2 \\ \dot{\theta}_3 \end{bmatrix} = S^{-1} \begin{bmatrix} \omega_1 \\ \omega_2 \\ \omega_3 \end{bmatrix} \tag{2.3}$$

2.1.1.2 Quaternions

It is common to avoid the singularities that are inherent in the Euler angles using quaternions (HUGHES, 1986; CARRARA, 2012). Equation 2.4 shows the kinematics

represented using quaternions $Q = [q_1\ q_2\ q_3 \mid q_4]^T$.

$$\dot{Q} = \frac{1}{2}\Omega(\omega)Q = \frac{1}{2}\Xi(Q)\omega$$

$$\Omega(\omega) \triangleq \begin{bmatrix} 0 & \omega_3 & -\omega_2 & \omega_1 \\ -\omega_3 & 0 & \omega_1 & \omega_2 \\ \omega_2 & -\omega_1 & 0 & \omega_3 \\ -\omega_1 & -\omega_2 & -\omega_3 & 0 \end{bmatrix} \tag{2.4}$$

$$\Xi(Q) \triangleq \begin{bmatrix} q_4 & -q_3 & q_2 \\ q_3 & q_4 & -q_1 \\ -q_2 & q_1 & q_4 \\ -q_1 & -q_2 & -q_3 \end{bmatrix},$$

where the quaternion $Q = [q_1\, q_2\, q_3\, q_4]^T$ satisfies the following identity:

$$q_1^2 + q_2^2 + q_3^2 + q_4^2 = 1 \tag{2.5}$$

Nonetheless, it is worthy to mention that although the definition of the unit quaternion is global in the sense that it can represent all attitudes, each physical attitude $R \in SO(3)$ is represented by a pair of unit quaternions $\pm Q \in \mathbf{S}^3$ (FORTESCUE; SWINERD, 2011). This characteristic can produce undesirable effects in control as *unwind*, in which the trajectories of the closed-loop system start close to the desired attitude and yet travel a large distance before returning to the desired attitude (FORTESCUE; SWINERD, 2011).

2.1.1.3 Gibb's vector

Equation 2.4 can be rewritten to separate terms with q_4 (scalar term) from other elements of the quaternion. Define a vector part of the first three components of the quaternion (complex or vectorial terms) and denote this by g (Gibbs vector or Rodrigues parameter) as $Q = [g^T | q_4]^T$.

$$\dot{Q} = -\frac{1}{2}\begin{bmatrix} \omega^{\times} \\ \omega^T \end{bmatrix}\begin{bmatrix} q_1 \\ q_2 \\ q_3 \end{bmatrix} + \frac{1}{2}q_4\begin{bmatrix} I_{3\times 3} \\ 0_{1\times 3} \end{bmatrix}\omega \tag{2.6}$$

Note the Gibbs vector is geometrically singular since it is not defined for 180° of rotation (FORTESCUE; SWINERD, 2011), nonetheless, the Equation (2.6) is global.

2.1.2 Rotational dynamics

In order to know the history of the change in the angular velocity, it is necessary to understand the history of the change in the angular acceleration ($\dot{\omega} = G(\tau, t)$) of the satellite. According to the Euler-Newton formulation of the rotational motion, angular acceleration is caused by torques, in other words, the change in the angular momentum $\dot{\vec{h}}$ is equal to the net torques $\vec{g}$ applied in the satellite, see Equation 2.7 (the present subsection is derived based on the centre of mass of the satellite, for the general case, see Carrara (2012), Hughes (1986)).

$$\dot{\vec{h}} = \vec{g} \tag{2.7}$$

The angular momentum is also known as the moment of momentum since it defines the moment of a given momentum $\vec{p}$ ($\vec{p} \triangleq m\vec{v}$) about a given point P_{cm}. See Equation 2.8, in which r locates a given point p with respect to P_{cm}.

$$\vec{h} = \vec{r} \times \vec{p} \tag{2.8}$$

Now, taking into account the motion of the body-fixed frame $\mathfrak{F}_b$ with respect to the ECI $\mathfrak{F}_i$ and an angular velocity ω of $\mathfrak{F}_b$ with respect to $\mathfrak{F}_i$ measured in the $\mathfrak{F}_b$, the derivative of the angular momentum in $\mathfrak{F}_b$ is defined by Equation 2.9.

$$\dot{\vec{h}} = \vec{g} - \vec{\omega} \times \vec{h} \tag{2.9}$$

Furthermore, $\dot{\vec{h}} = \vec{I}\dot{\vec{\omega}}$ and $\vec{h} = \vec{I}\vec{\omega}$, which results in the Equation 2.10.

$$\vec{I}\dot{\vec{\omega}} = \vec{g} - \vec{\omega} \times (\vec{I}\vec{\omega}) \tag{2.10}$$

Recall the satellite has a set of 3 reaction wheels, each one aligned with its principal axes of inertia, furthermore, such type of actuator, momentum exchange actuators, does not change the angular momentum of the satellite. Consequently, it is mandatory to model their influence in the satellite, in particular, the angular momentum, in the scalar form, of the satellite is defined by Equation 2.11.

$$\vec{h} = (I - \sum_{n=1}^{3} I_{n,s} a_n a_n^T)\vec{\omega} + \sum_{n=1}^{3} h_{w,n}\vec{a_n} \tag{2.11}$$

where $I_{n,s}$ is the inertia moment of the reaction wheels in their symmetry axis a_n, $h_{w,n}$ is the angular momentum of the n reaction wheel about its centre of mass ($h_{w,n} = I_{n,s}a_n^T\omega + I_{n,s}\omega_n$) and ω_n is the angular velocity of the n reaction wheel.

One can define I_b using the Equation 2.12.

$$I_b \triangleq I - \sum_{n=1}^{3} I_{n,s}a_n a_n^T \tag{2.12}$$

Using I_b, the motion of the satellite is described by Equation 2.13 (expanded until the applied equation).

$$\begin{aligned} I_b\dot{\omega}^b = g_{cm} - \omega^\times(I_b\omega + \sum_{n=1}^{3} h_{w,n}a_n) - \sum_{n=1}^{3} g_n a_n \implies \\ \dot{\omega}^b = I_b^{-1}g_{cm} - I_b^{-1}\omega^\times I_b\omega - I_b^{-1}\omega^\times \sum_{n=1}^{3} h_{w,n}a_n - I_b^{-1}\sum_{n=1}^{3} g_n a_n \end{aligned} \tag{2.13}$$

where g_{cm} is the net external torque; and g_n are the torques generated by the reactions wheels ($\dot{h_{w,n}} = g_n$).

2.2 Control

The **classical control** techniques developed up to the 1940s were concerned with the *regulator problem* (in which a steady state is to be maintained) and *tracking problem* (in which a defined trajectory is to be followed) of linear single input systems, which can be described by linear differential equations with constant coefficients and have a single control input. The design techniques were analytical and graphical since they were limited by the computational tools and simulations facilities available (BENNETT, 1979). One set of techniques, the frequency response techniques, based on the use of Nyquist, Bode, or Nichols charts, evaluates performance in terms of bandwidth, resonances, and gain and phase margins. A complementary set of techniques, the time response techniques, are based on the use of the Laplace transform to express performance in terms of rise time, percentage overshoot, steady-state error, and damping. Regarding damping and resonances, another technique is root locus, which provides a method of assessing performance based on frequency response ideas (BENNETT, 1979).

Experience during Second World War showed that to obtain high performance - fast response, high accuracy, good rejection of noise and external perturbations - required more than linear analysis could provide (BENNETT, 1979).

The recognition of the more general nature of the control problem arose from the immediate post war work on aircraft and missile control systems. In these systems, the motion can be modified by several different available controls, and hence the systems are multivariable (BENNETT, 1979).

A second realization was that systems possess uncertainties, which were listed as by Bennett (1979):

a) error in the parameters that appear in differential equations of motion;

b) errors inherent in modeling a physical system by means of mathematical equations;

c) sensor errors and related noise in measurements;

d) exogenous stochastic perturbations that influence the time evolution of the systems state variables in a random manner.

Such sources of uncertainty may be grouped into two main classes: (A) **structured**, or parametric, in which the structure of the system is known, but some of the parameters are uncertain, therefore, uncertainty is modeled in a structured manner; (B) **unstructured** in which the structure of the system is in error because of missing dynamics either through deliberate neglect or because of a lack of understanding of the physical system - any model of a real system contains this source of uncertainty (SKOGESTAD; POSTLETHWAITE, 2005).

Taking into account the previous two realizations - the necessity for more than analysis of linear single input systems and the uncertainty in the systems, Bennett (1979) points out, the development of **model control** theory was strongly influenced by two factors: first, the nature of the problem that society saw as important - the launching, maneuvering, guidance, and tracking of missiles and space vehicles; and secondly by the advent of the digital computer. The problem was essentially one of the control of ballistic objects and hence detailed physical models could be constructed in terms of differential equations. A consequence was to focus attention once again on the differential equation approach to the analysis and design of control systems.

To deal with the multivariate nature of the problem, engineers working in the aerospace realm turned to formulating the general differential equations in terms of a set of first order equations. This was a technique of which Poincaré was first

to see the significance and first to exploit. The whole approach became know as the "**state-space** approach" (BENNETT, 1979).

Indeed, one can decompose an nth order time-invariant differential equation ($\dot{x} = f(x)$) into an equivalent system of n first order differential equations (PARKS, 1966), in the form:

$$\begin{aligned} \dot{x}_i(t) = f_i(x_1, x_2, ..., x_n) \;\; (i = 1, 2, 3, 4, ..., n) \\ x_1(t) = x(t) \\ x_2(t) = \dot{x}(t) \\ x_{...}(t) = x^{(...)}(t) \\ x_{(n)}(t) = x^{(n)}(t) \end{aligned} \tag{2.14}$$

Such a system of differential equations is known as the **state-space** description and the variables x_i as state variables. They need not be physical quantities and to a large extent can be chosen arbitrarily. Moreover, the state-space description is not unique, in fact, all statespace vectors describing a particular system are interchangeable, i.e., through a similarity transformation spanning the same statespace (PARKS, 1966). The state-space description is generally expressed in the form:

$$\begin{aligned} \dot{x} &= Ax + Bu \\ y &= Cx \end{aligned} \tag{2.15}$$

where $x \in \mathbb{R}^n$ is the state vector, $u \in \mathbb{R}^m$ is the control vector, $y \in \mathbb{R}^l$ is the output vector and A, B, C are real matrices having the appropriate dimensions.

The formulation of control problem in statespace led to extensive and deep studies of mathematical problems of control. Furthermore, the growing availability of the digital computer, during the late 1950s, made a recursive algorithm possible, as opposed to the search for a closed form solution in the classical approach (BENNETT, 1979).

In fact, regarding the initial value problem, which one that uses the initial condition to predict future states of a given system:

$$x_0 = x(t_0), \; \textit{compute } x(t) \; \forall \, t > t_0 \tag{2.16}$$

The closed form solution of non-linear time-invariant dynamic systems are in general very difficult to find and for many problems no explicit solutions are known (PARKS,

1966).

Therefore, it is of interest to know whether a particular non-linear time-invariant dynamic system has solutions and whether these solutions are unique. Suppose that $f_i(x)$ are defined in a given region Γ of the state-space, then: (1) if all $f_i \in C^0$ (continuous) then a solution exists, and (2) if all $f_i \in C^1$ ($\partial f_i/\partial x_j$ are continuous) then the solution is unique (PARKS, 1966).

The developments during the 1950s converge to the ground-breaking paper *"On the general theory of control systems"* presented by Kalman (1960b), which established the state-space approach as the basis for the following definitions:

a) **Controllability**: A state x of a system is said to be "controllable" if there exists a control signal $u(t)$ defined over a finite interval $0 < t < t_1$ such that $f(x)_{t_1} = O$. In general, the time t_1 will depend on x. If every state is controllable (the $pair(A, B)$), the system is said to be "completely controllable" (KALMAN, 1960b).

b) **Observability**: A costate x^* (an element x^* of the space of all functions on X) is said to be "observable" if its exact value at any state x at time 0 can be determined from the measurements of the output signal y over the finite interval $0 < t < t_2$. The time t_2 will depend on x^*. If every costate is observable (the $pair(A, C)$), the system is said to be "completely observable" (KALMAN, 1960b).

c) **Optimal Regulator Problem**: to optimize a regulating system, it is necessary to introduce a performance index. This is usually taken as the integrated error along with the motions of the system. It is convenient to define the error as a positive definite quadratic form $x^T\mathbf{Q}x$ (^{T} meaning the transposed vector), where $\mathbf{Q}$ is positive definite matrix ($\mathbf{Q}\ positive\, definite \implies x^T\mathbf{Q}x > 0, \forall x \in \mathbb{R}^p$). Being Q positive-definite, $(x^T\mathbf{Q}x)^{\frac{1}{2}}$ is the *generalized euclidean norm*, furthermore, if $\mathbf{Q} = 1$ it is the L2-norm. Then the performance index is a function given by:

$$V(x) = \int_0^\infty x^T\mathbf{Q}x\ dt \tag{2.17}$$

and the optimal regulator problem is: *find a control such that 2.17 is minimized for every initial state x*. It was remarkable that: *If $\mathbf{Q}$ in 2.17 is positive definite, the solution of the optimal regulator problem exists if and*

only if the system is completely controllable. Moreover, the resulting control systems has the following properties: the closed loop system is asymptotically stable, and $V(x)$ is one of its Lyapunov functions (KALMAN, 1960b).

d) **Principle of Duality**: Considering the class of feedback system with linear control law, the dual plant defined in X^* is obtained by the following steps: (i) replace f by its dual f^*, (ii) interchange input and output constraints, and (iii) reverse the direction of time (KALMAN, 1960b). Therefore, the duality of the optimal regulator problem and optimal estimation problem is well-established. In other words, a system with real matrices (A, B, C) is controllable if and only if the system with the real matrices (A^*, C, B^*) is observable.

The weaker definitions of controllability and observability are, respectively:

a) **Stabilizability**: A system is stabilizable if all states x that cannot be controlled decay to zero;

b) **Detectability**: A system is detectable if all costates x^* that cannot be observable decay to zero.

Another ground-breaking paper is *"Contributions to the Theory of Optimal Control"* presented also by Kalman (1960a), which is the first paper to deal with linear-quadratic feedback control setting the stage for what came to be known as LQR (Linear-Quadratic-Regulator) control, which is explored after the next subsection that presents the linearization method.

2.2.1 Linear control

In order to apply the linear control techniques, linear models must be obtained through the linearization method, which can be described by the following steps given a nonlinear state-space model (SKOGESTAD; POSTLETHWAITE, 2005):

a) Determine the steady-state operating point (or trajectory) about which to linearize.

b) Introduce the deviation variables and linearize the model. There are essentially three parts to this step:

Linearize the equations using a Taylor expansion where second- and higher-order terms are omitted.

Introduce the deviation variables, e.g., $\delta x(t)$ defined by $\delta x(t) = x(t) - x^*$ where the superscript * denotes a steady-state operating point or trajectory along which the model is to be linearized.

Subtract the steady-state (or trajectory) to eliminate the terms involving only steady-state quantities.

These three parts are usually accomplished together. For example, for a nonlinear state-space model of the form

$$\dot{x} = f(x, u) \tag{2.18}$$

the linearized model in deviation variables $(\delta x, \delta u)$ is

$$\dot{\delta x}(t) = \frac{\partial f}{\partial x}^* \delta x(t) + \frac{\partial f}{\partial u}^* \delta u(t) \tag{2.19}$$

where x and u are real vectors and then its first-order partial derivatives are matrices (Jacobians).

Note the linearization method (which, today, is sometimes incorrectly referred to as Lyapunov's first method) is simply given as an example of application of the *direct* (or second) method in Lyapunov's original work. The *first method* in Lyapunov's original work was the so-called method of exponents, which is used today in the analysis of chaos (SLOTINE; LI, 1991)

2.2.1.1 Linear quadratic regulator (LQR)

Once a linearized model for the application of the linear control techniques is available, it is time to come back to the second ground-breaking paper *"Contributions to the Theory of Optimal Control"* presented by Kalman (1960a).

The term "linear" comes from the fact that the systems considered were assumed linear, and the term "quadratic" comes from the use of performance indexes that involve the square of an error signal. Therefore, regarding the regulator problem, linear quadratic regulator (LQR). Kalman's formulation in terms of finding the least squares control that evolves from an arbitrary initial state is a precise formulation of the least squares optimal control problem (KALMAN, 1960a). This problem can be solved by the Hamilton-Jacobi theory (KALMAN, 1960b), by the minimum principle

of Pontryagin (KUCERA, 1973), by the dynamic programming of Bellman (KALMAN, 1960b), or by the direct method of Lyapunov (KALMAN, 1960b; KUCERA, 1973) (see Subsection 2.2.2.1).

The system model in Equation (2.15) is subject to the cost functional described in Equation (2.20).

$$J(x_0, u) = \frac{1}{2}\int_0^\infty (x^T Q x + u^T R u) dt \tag{2.20}$$

where $Q \in \mathbb{R}^{n\times n}$ and $R \in \mathbb{R}^{m\times m}$.

According to LQR theory (KALMAN, 1960a) and Equation (2.15) and (2.20), the state-feedback control law is $u = -Kx$ and the gain K is obtained by Equation (2.21) (KALMAN, 1960a; ÇIMEN, 2010).

$$K = R^{-1}B^T P \tag{2.21}$$

where P is the unique, symmetric, positive-definite solution of the algebraic Riccati equation (ARE) given by Equation (2.22) (KALMAN, 1960a; ÇIMEN, 2010).

$$PA + A^T P - PBR^{-1}B^T P + Q = 0 \tag{2.22}$$

Finally, the conditions for the application of the LQR technique in a given system model are (ÇIMEN, 2010; KALMAN, 1960a):

a) $A \in C^1(\mathbb{R}^w)$

b) $B, C, Q, R \in C^0(\mathbb{R}^w)$

c) Q is positive definite and R is symmetric positive definite

d) $Ax \implies A0 = 0$, i.e., the origin is an equilibrium point

e) $pair(A, B)$ is stabilizable (a sufficient test for stabilizability is to check the rank of controllability matrix)

f) $pair(A, Q^{\frac{1}{2}})$ is detectable (a sufficient test for detectability is to check the rank of observability matrix)

The LQR theory offered the following advantages over existing design techniques (DORATO et al., 2000):

a) It allowed for optimization over finite intervals;

b) It was applicable to time-varying systems;

c) It dealt in a relatively simple way with multivariable systems.

However, LQR did not deal with another central issue associated with the design of feedback control systems: uncertainty either structured or unstructured.

2.2.1.2 H-infinity

Motivated by the previously mentioned shortcomings of linear-quadratic control, there was a significant shift in the 1980s towards H_∞ optimization for robust control. In fact, the interest in H_∞ optimization for robust control of linear plants is mostly attributed to the influential work of Zames (1981), in which the problem of sensitivity reduction by feedback is formulated as an optimization problem.

Indeed, as stated by Zames (1981), two opposing tendencies can be found in most feedback systems. On the one hand, to the extent that feedback reduces sensitivity, it reduces the need for plant identification. On the other hand, the less information is available about the plant, the less possible it is to select a feedback to reduce sensitivity. The balance between these tendencies establishes a *maximum to the amount of tolerable plant uncertainty* and, equivalently, a minimum to the amount of identification needed.

Regarding plant uncertainty, for a given nominal plant model (G), one can study the behavior of a family of plants $G_p = G + E$, where plant uncertainty (E) is bounded, but otherwise unknown. In such a study, the resulting controlled system may have the following properties (SKOGESTAD; POSTLETHWAITE, 2005):

- **Nominal Stability (NS)** - The system is stable with no plant uncertainty;
- **Nominal Performance (NP)** - The system satisfies the performance specification with no plant uncertainty;
- **Robust Stability (RS)** - The system is stable about the nominal plant up to the worst-case plant uncertainty;
- **Robust Performance (RP)** - The system satisfies the performance specifications about the nominal plant up to the worst-case plant uncertainty.

Figure 2.1 - General control configuration.

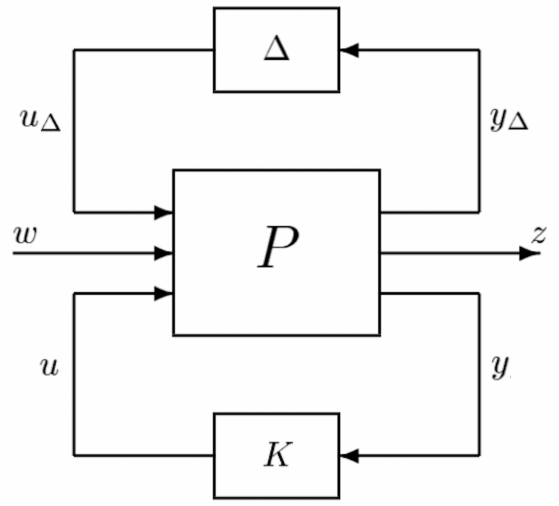

SOURCE: Skogestad and Postlethwaite (2005).

RS and RP are usually assessed using the general method of formulating control problems introduced by Doyle (SKOGESTAD; POSTLETHWAITE, 2005) depicted in Figure 2.1, in which P is the generalized plant for G, w is the exogenous input signals, z is the exogenous output signals, u is the control signals and y is the sensed output signals.

The statespace representation of the generalized plant P is (SKOGESTAD; POSTLETHWAITE, 2005):

$$\begin{aligned} \dot{x} &= Ax + B_1 w + B_2 u \\ z &= C_1 x + D_{11} w + D_{12} u \\ y &= C_2 x + D_{21} w + D_{22} u \end{aligned} \tag{2.23}$$

where $x \in \mathbb{R}^n$ is the state vector, $u \in \mathbb{R}^m$ is the control vector, $w \in \mathbb{R}^m$ is the input vector of exogenous signals (e.g., perturbations) and $z \in \mathbb{R}^n$ is the output vector of "error" signal which is to be minimized in some sense to meet control objectives. Furthermore, D_{12} and D_{21} have full rank, the pair(A,B_1), pair(A,B_2), pair(A,C_1) and pair (A,C_2) are stabilizable and detectable, respectively.

The block diagram in Figure 2.1 in terms of P may be transformed into the block diagram in Figure 2.2 in terms of N (for analysis) by using K to close a lower loop around P. If P is partitioned to be compatible with the controller K, then a

Figure 2.2 - NΔ - structure.

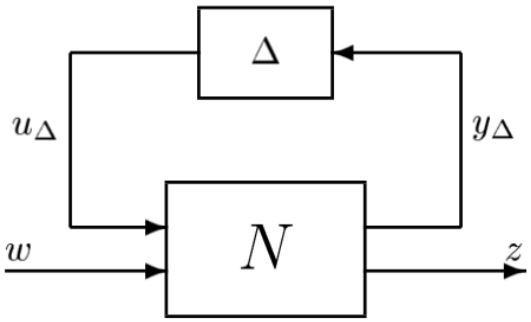

SOURCE: Skogestad and Postlethwaite (2005).

lower linear fractional transformation (LFT, F_l) can be found for $N = F_l(P, K) = P_{11} + P_{12}K(I - P_{22}K)^{-1}P_{21}$ (SKOGESTAD; POSTLETHWAITE, 2005).

To evaluate the uncertain closed-loop transfer function from external input w to external output z, $z = Fw$, one can use Δ to close the upper loop around N, resulting in an upper LFT (F_u) (SKOGESTAD; POSTLETHWAITE, 2005):

$$F_u(N, \Delta) = N_{22} + N_{21}\Delta(I - N_{11}\Delta)^{-1}N_{12} \tag{2.24}$$

In fact, the overall control objective is to minimize some norm of the transfer function from w to z, e.g., the H_∞ norm (SKOGESTAD; POSTLETHWAITE, 2005).

Assume (I) the system is NS (with $\Delta = 0$) in such a way that N is stable (which means that the whole of N, and not only N_{22}, must be stable); and, (II) Δ is stable. The only source of instability in Equation (2.24) is the term $(I - N_{11}\Delta)^{-1}$, therefore, for **RS in the presence of unstructured uncertainties**, it is sufficient to analyze the so-called "$M\Delta$-structure" depicted in Figure 2.3 where $M = N_{11}$ is the transfer function from the output to the input of the perturbations.

It is time to briefly review the small-gain theorem: assume two stable systems S_1 and S_2 are connected in a feedback loop, then the closed-loop system is stable if $||S_1||_\infty||S_2||_\infty < 1$.

Applying small-gain theorem to the "$M\Delta$-structure", the **theorem RS for unstructured perturbations** can be stated: **assume that the nominal system M is stable (NS) and that the perturbation Δ is stable. Then the "$M\Delta$-**

Figure 2.3 - MΔ - structure.

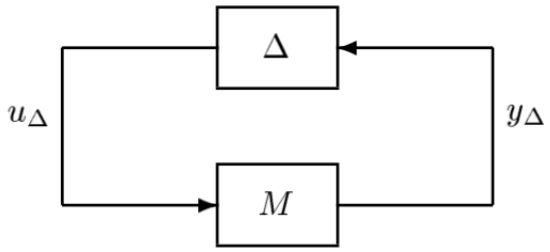

SOURCE: Skogestad and Postlethwaite (2005).

system" is stable for all perturbations Δ satisfying $||\Delta||_\infty \leq 1$ if an only if $||M||_\infty < 1$ (SKOGESTAD; POSTLETHWAITE, 2005).

There is research arguing that unstructured uncertainty has a substantial advantage over structured uncertainty in the fact that not only changes in parameters can be taken into consideration (MATU et al., 2011). Nonetheless, unstructured uncertainty is well-known by its conservatism in description and, consequently, in the RS analysis.

Glover and McFarlane (1989) addressed the problem of RS of a family of plants in the case where such family was characterized by H_∞ *bounded perturbations of a normalized left coprime factorization of a nominal plant*. In such a way that the attention is moved to the size of error signals (in the same spirit of the performance index studied by Kalman (1960b) focusing on state-space) and away from the size and bandwidth of selected closed-loop transfer function (SKOGESTAD; POSTLETHWAITE, 2005). In fact, the coprime uncertainty description provides a good "generic" uncertainty description for cases where one does not use any specific *a priori* uncertainty information and is focused on maximizing the magnitude of the uncertainty such that RS is maintained (SKOGESTAD; POSTLETHWAITE, 2005).

Now consider the stabilization of a nominal plant G which has a normalized left coprime factorization (GLOVER; MCFARLANE, 1989; SKOGESTAD; POSTLETHWAITE, 2005):

$$G = M_l^{-1} N_l \tag{2.25}$$

then a perturbed plant model G_p can be written as (SKOGESTAD; POSTLETHWAITE, 2005):

$$G_p = (M_l + \Delta_M)^{-1}(N_l + \Delta_N) \tag{2.26}$$

where Δ_M, Δ_N are stable unknown transfer functions which represent the uncertainty for the nominal plant G.

The objective of robust stabilization H_∞ is to stabilize not only the nominal plant G, but a family of perturbed plants defined by (GLOVER; MCFARLANE, 1989; SKOGESTAD; POSTLETHWAITE, 2005):

$$G_p = \{(M_l + \Delta_M)^{-1}(N_l + \Delta_N) :: ||[\Delta_N \ \Delta_M]||_\infty < \epsilon\} \tag{2.27}$$

where $\epsilon > 0$ is the stability margin, i.e., the maximum value while retaining stability (RS). Hence, ϵ is a limitation on the size of perturbation that can exist without destabilizing the closed-loop system of Figure 2.4 (GLOVER; MCFARLANE, 1989).

The condition for RS in such systems can be derived rearranging the block diagram in Figure 2.4 to match the $M\Delta$-structure in Figure 2.3, which in turn is the transfer function from θ to $\begin{bmatrix} u \\ y \end{bmatrix}$, i.e., the transfer function from the output (Δu in Figure 2.3) to the input (Δy in Figure 2.3) of the perturbations Δ, which results in:

$$\begin{aligned} u &= \frac{KM_l^{-1}}{I - M_l^{-1}N_lK}\theta_1 = \frac{KM_l^{-1}}{I - GK}\theta_1 = K(I - GK)^{-1}M_l^{-1}\theta_1 \\ y &= \frac{M_l^{-1}}{I - M_l^{-1}N_lK}\theta_2 = \frac{M_l^{-1}}{I - GK}\theta_2 = (I - GK)^{-1}M_l^{-1}\theta_2 \\ \Delta &= [\Delta_N \ \Delta_M] \\ M &= \begin{bmatrix} K \\ I \end{bmatrix}(I - GK)^{-1}M_l^{-1} \end{aligned} \tag{2.28}$$

Therefore, applying the **theorem RS for unstructured perturbations** (SKOGESTAD; POSTLETHWAITE, 2005), RS is satisfied for all $||\Delta_N \ \Delta_M||_\infty \leq \epsilon$ if and only if $||M||_\infty < \epsilon^{-1}$.

To maximize this stability margin (ϵ) is the problem of H_∞ robust stabilization of normalized coprime factor plant descriptions (GLOVER; MCFARLANE, 1989). For the positive feedback of Figure 2.4, the perturbed plant is RS if and only if the nominal feedback is stable and:

$$\left\| \begin{bmatrix} K \\ I \end{bmatrix}(I - GK)^{-1}M^{-1} \right\|_\infty \leq \epsilon^{-1} \tag{2.29}$$

Figure 2.4 - H_∞ robust stabilization problem with left coprime factorization.

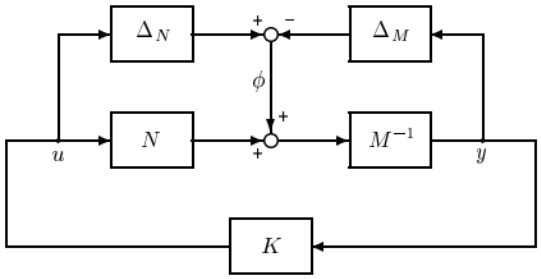

SOURCE: Skogestad and Postlethwaite (2005).

The maximum stability margin ϵ and the corresponding minimum γ (the exogenous signal w is locally attenuated by γ) are given by Glover and McFarlane (1989) as:

$$\gamma_{min} = \epsilon_{max}^{-1} = (1 + \rho(XZ))^{\frac{1}{2}} \tag{2.30}$$

where ρ denotes the spectral radius (maximum eigenvalue) and for the minimal state-space realization (A, B, C, D) of G - a state-space realization (A, B, C, D) of G is said to be a minimal realization of G if A has the smallest possible dimension, i.e., the fewest number of states; therefore, a state-space is minimal if and only if pair(A,B) is controllable and pair(A,C) is observable; moreover, being minimal $G(s) = C(sI - A)^{-1}B + D$ - , Z and X are the solutions to the AREs (GLOVER; MCFARLANE, 1989; SKOGESTAD; POSTLETHWAITE, 2005):

$$\begin{aligned} (A - BS^{-1}D^TC)Z + Z(A - BS^{-1}D^TC)^T - ZC^TR^{-1}CZ + BS^{-1}B^T = 0 \\ (A - BS^{-1}D^TC)^TX + X(A - BS^{-1}D^TC) - XBS^{-1}B^TX + C^TR^{-1}C = 0 \\ R = I + DD^T \\ S = I + D^TD \end{aligned} \tag{2.31}$$

A controller (the "central" controller in Glover and McFarlane (1989)) which guarantees that:

$$\left\| \begin{bmatrix} K \\ I \end{bmatrix} (I - GK)^{-1}M^{-1} \right\|_\infty \leq \gamma \tag{2.32}$$

for a specified $\gamma > \gamma_{min}$, is given by:

$$K_{H_\infty} = \begin{bmatrix} A + BF + \gamma^2 (L^T)^{-1} Z C^T (C + DF) & \gamma^2 (L^T)^{-1} Z C^T \\ B^T X & -D^T \end{bmatrix}$$
$$F = -S^{-1}(D^T C + B^T X) \tag{2.33}$$
$$L = (1 - \gamma^2) I + XZ$$

2.2.2 Nonlinear control

Linear optimal control theory takes the assumption that the system dynamics is indeed linearizable (as discussed in Subsection 2.2.1), furthermore, it relies on the key assumption of small range operation.

Starting from these assumptions (linearizable and small range operation), if the resulting linear time-invariant (LTI), in the form $\dot{x} = Ax + Bu$, has A nonsingular - i.e., one that has a matrix inverse, then the system has a *unique equilibrium point* and such equilibrium point is stable if all eigenvalues of A have negative real parts, regardless of initial conditions (SLOTINE; LI, 1991). Nonetheless, nonlinear systems can have much richer and more complex behaviors, e.g., multiple equilibrium points (nonlinear systems frequently have more than one equilibrium point), limit cycles (nonlinear systems can display oscillations of fixed amplitude and fixed period without external excitation), bifurcations (as the parameters of nonlinear dynamic systems are changed, the stability of the equilibrium points can change and so can the number of equilibrium points) and chaos (which may mean that the nonlinear system is extremely sensitive to initial conditions so the system output is unpredictable (TABOR, 1989)) (SLOTINE; LI, 1991; KHALIL, 2002).

Facing such richness of the nonlinear dynamical systems, the *qualitative theory of differential equations* studies the behavior of differential equations by means other than finding their closed form solutions. It originated from the works of Henri Poincaré and Aleksandr Lyapunov (LEIPHOLZ, 1970). An approach is to study the qualitative behavior of the system under *perturbations* of the *initial conditions* (initial value problem): (A) what happens if $x_0 \to x_0 + \Delta x_0$, (B) how close is the perturbed evolution to the nominal evolution, and, (C) under which conditions the two solutions tend to coincide for $t \to \infty$.

In the qualitative theory of differential equations, one is frequently interested in the **domain of attraction** (also called *region of attraction (ROA)* or *basin of at-*

traction), i.e., the region of the statespace in which the initial conditions of the trajectories lie in order to attain stable behavior (PARKS, 1966).

Equilibrium points, if exist, must lie in the domains of attraction, indeed, a state $x_e \in \mathcal{R}^n$ is an equilibrium point of a nonlinear dynamical system $\dot{x} = f(x)$ if $x_0 = x_e \implies x(t) = x_e, \forall\, t > 0$ so $f(x_e) = 0$. A nonlinear system can have an infinite number of equilibrium points, and, each one can be stable or unstable. Therefore, stability is a property of equilibrium points (PARKS, 1966). Additionally, to investigate the stability of a particular equilibrium point x_0 it is convenient to transform the equilibrium point to the origin $x^* = 0$ through the transformation $x^* = x - x_0$ (PARKS, 1966).

Such equilibrium points, if exist, lie in the domains of attraction, which are defined by their attractors. An *attractor* is a subset $A \in \mathcal{R}^n$ of the statespace characterized by the following three conditions: (i) $a \in A \implies f(a,t) \in A, \forall\, t > 0$; (ii) there exists a vicinity of A (*basin of attraction*) which consists of all trajectories that enter A for $t \to \infty$; and, (iii) there is no proper (non-empty) subset of A having the first two properties. The attractors can be classified in: (I) *Fixed point* - the final state that a dynamic system evolves towards corresponds to an attracting fixed point, i.e., stable equilibrium point; (II) Limit cycle - a periodic orbit; (III) Quasiperiodic - it exhibits irregular periodicity; (IV) Strange attractor - when such sets cannot be easily described.

Regarding the **fixed point attractor**, it can be defined by the following equation (BACCIOTTI A.; ROSIER, 2005).

$$A = \{x_0 \in \mathcal{R}^n : \lim_{t \to +\infty} x(t, x_0) = 0\} \tag{2.34}$$

It is important for practical reasons to have information about the size and/or the shape of A. Indeed, *the stability properties could be of scarce utility if the domain of attraction is very small, or if the equilibrium point is very close to its boundary.* There is a wide literature about theoretical methods for the determination of A, and about numerical methods for its approximate estimation (ERDEM; ALLEYNE, 2002; BACCIOTTI A.; ROSIER, 2005; BRACCI et al., 2006).

One can assess the existence of *fixed point attractors* in a given system, applying the qualitative theory of differential equations, in particular, the **Lyapunov's direct method**. The basic philosophy of Lyapunov's direct method is the mathematical extension of a fundamental physical observation: if the total energy of a mechanical

(or electrical) system is continuously dissipated, then the system, whether linear or nonlinear, must eventually settle down to an equilibrium point. Thus, one can conclude the stability of an equilibrium point, and, consequently, the existence of a fixed point attractor, by examining the variation of a single scalar funcion (SLOTINE; LI, 1991). If one consider $x = 0$ to be an equilibrium point of Equation (2.14), then it may prove possible to investigate the stability of such equilibrium point by examining a scalar positive-definite function $V = V(x)$, surrounding $x = 0$ with a nest of closed surfaces defined by $V(x) = c$ ($c > 0$; V positive definite). The rate of change with respect to time of V following a trajectory of Equation (2.14) is calculated as (PARKS, 1992):

$$\dot{V} = \sum_{i=1}^{n} \frac{\partial V}{\partial x_i} \frac{dx_i}{dt} = \sum_{i=1}^{n} \frac{\partial V}{\partial x_i} f_i(x) \tag{2.35}$$

If $\dot{V}$ is always negative (except at $x = 0$, where $V = 0$; $\dot{V}$ negative semi-definite), then it follows that the trajectories must cross the surface V in an inwards directions, and, consequently, tend to the point $x = 0$ as time $t \to \infty$. Thus **asymptotic stability** may be proven using a Lyapunov function V without any need to find explicit solutions of the nonlinear differential equations (PARKS, 1992).

2.2.2.1 Applying Lyapunov's direct method and obtaining the algebraic Riccati equation (ARE)

The problem of asymptotic stability verification of LQR can be performed applying qualitative theory of differential equation, in particular, the Lyapunov's direct method (KALMAN, 1960b; KUCERA, 1973) by means of certain auxiliary quadratic functions, i.e., Lyapunov candidate functions of the form in Equation (2.36).

$$\begin{aligned} V(x) &= x^T P x \\ \dot{V}(x) &= \dot{x}^T P x + x^T P \dot{x} \end{aligned} \tag{2.36}$$

where P is a symmetric positive definite matrix.

If the function $V(x)$ is positive definite (as assumed) and has continuous partial derivatives, and if its time derivative along any state trajectory of system is negative semi-definite, i.e., $\dot{V}(x) \leq 0$ then $V(x)$ is said to be a Lyapunov function for the system (SLOTINE; LI, 1991).

Regarding the *linear system* described in Equation (2.15), if such a system admits a linear controller $u = Kx$, then $\dot{x} = Ax + BKx$ can be tested by the Lyapunov's

direct method.

It is reasonable to make the inspired guess $K = -\frac{1}{2}R^{-1}B^TP$, which leads to the following equation:

$$\begin{aligned} \dot{x} &= (A + BK)x \\ &= (A - \frac{1}{2}BR^{-1}B^TP)x \end{aligned} \tag{2.37}$$

where R is a symmetric positive definite matrix and P is the unknown symmetric positive definite matrix.

Substituting Equation (2.37) in Equation (2.36) gives Equation (2.38).

$$\begin{aligned} \dot{V}(x) &= ((A - \frac{1}{2}BR^{-1}B^TP)x)^TPx + x^TP((A - \frac{1}{2}BR^{-1}B^TP)x) \\ &= (Ax - \frac{1}{2}BR^{-1}B^TPx)^TPx + x^TP(Ax - \frac{1}{2}BR^{-1}B^TPx) \\ &= (Ax)^TPx - \frac{1}{2}(BR^{-1}B^TPx)^TPx + x^TPAx - \frac{1}{2}x^TPBR^{-1}B^TPx \\ &= x^TA^TPx - \frac{1}{2}x^TPBR^{-1}B^TPx + x^TPAx - \frac{1}{2}x^TPBR^{-1}B^TPx \\ &= x^TA^TPx + x^TPAx - x^TPBR^{-1}B^TPx \\ &= x^T(A^TP + PA - PBR^{-1}B^TP)x \end{aligned} \tag{2.38}$$

using the following properties of matrices operations: (I) $(HI)^T = I^TH^T$; and (II) if M is any symmetric matrix, then $M^T = M$.

As $\dot{V}(x)$ must be negative semi-definite function for a Lyapunov function, then $\dot{V}(x) = x^T(-Q)x$ for a fixed positive definite matrix Q. Using Q in Equation (2.38) gives Equation (2.39).

$$\begin{aligned} -Q = A^TP + PA - PBR^{-1}B^TP \implies \\ A^TP + PA - PBR^{-1}B^TP + Q = 0 \end{aligned} \tag{2.39}$$

Consequently, through Lyapunov's direct method, the asymptotic stability is guaranteed if a unique symmetric positive definite matrix P is the solution for the algebraic Riccati equation (ARE) (2.39). The requirements for the existence of such a P are described in Subsection 2.2.1.1. Furthermore, if asymptotic stability is verified by Lyapunov's direct method, then it is guaranteed the existence of a *fixed point attractor* for the *linear system* described in Equation (2.15).

2.2.2.2 State-dependent Riccati equation (SDRE)

Still, in the 1960s, Pearson (PEARSON, 1962) observed that one of the difficulties of controlling a nonlinear dynamic system (one in which the assumptions of linearization do not hold) is that optimal control policies are not generally easy to implement so a lengthy preliminary computation is required which presents quite unwieldy solutions for the controller to realize. In other words, in general, the embedded required computations are too expensive as well as their certification so the idea is starting with a nonlinear control problem, a linear time and state varying model is constructed. Such a model is treated as an instantaneously stationary linear system and then optimized using the usual linear techniques. This approach later was called State-Dependent Riccati Equation (SDRE) since it leads towards one or more algebraic Riccati equations (ARE) (AUB A. J.; BITTANTI, 1991) of the state varying model (CLOUTIER et al., 1996; CLOUTIER, 1997).

Decades later, SDRE is explored in detail by (CLOUTIER et al., 1996; CLOUTIER, 1997). A good survey of the SDRE method can be found in (ÇIMEN, 2008) and its systematic application to deal with a nonlinear plant in (ÇIMEN, 2010).

The SDRE technique entails factorization (that is, parametrization) of the nonlinear dynamics into the state vector and the product of a matrix-valued function that depends on the state itself. In doing so, SDRE brings the nonlinear system to a (nonunique) linear structure having SDC matrices given by Equation (2.40).

$$\begin{aligned} \vec{\dot{x}} &= A(\vec{x})\vec{x} + B(\vec{x})\vec{u} \\ \vec{y} &= C\vec{x} \end{aligned} \tag{2.40}$$

where $\vec{x} \in \mathbb{R}^n$ is the state vector and $\vec{u} \in \mathbb{R}^m$ is the control vector. Notice that the state-dependent coefficient form (SDC) has the same structure as a linear system, but with the system matrices, A and B, being functions of the state vector. The nonuniqueness of the SDC matrices creates extra degrees of freedom, which can be used to enhance controller performance, however, it poses challenges since not all SDC matrices fulfill the SDRE requirements, e.g., the pair (A,B) must be pointwise stabilizable.

The system model in Equation (2.40) is subject to the cost functional described in Equation (2.41).

$$J(\vec{x_0}, \vec{u}) = \frac{1}{2}\int_0^\infty (\vec{x}^T Q(\vec{x})\vec{x} + \vec{u}^T R(\vec{x})\vec{u})dt \tag{2.41}$$

where $Q(\vec{x}) \in \mathbb{R}^{n \times n}$ and $R(\vec{x}) \in \mathbb{R}^{m \times m}$ are the state-dependent weighting matrices. In order to ensure local stability, $Q(\vec{x})$ is required to be positive semi-definite for all $\vec{x}$ and $R(\vec{x})$ is required to be positive for all $\vec{x}$ (MENON et al., 2002).

The SDRE controller linearizes the plant about the current operating point and creates constant statespace matrices so that the LQR method can be used. This process is repeated in all samplings steps, resulting in a pointwise linear model from a non-linear model, so that an ARE is solved and a control law is computed also in each step. Therefore, according to LQR theory and Equation (2.40) and (2.41), the state-feedback control law in each sampling step is $\vec{u} = -K(\vec{x})\vec{x}$ and the state-dependent gain $K(\vec{x})$ is obtained by Equation (2.42) (ÇIMEN, 2010).

$$K(\vec{x}) = R^{-1}(\vec{x})B^T(\vec{x})P(\vec{x}) \tag{2.42}$$

where $P(\vec{x})$ is the unique, symmetric, positive-definite solution of the algebraic state-dependent Riccati equation (SDRE) given by Equation (2.43) (ÇIMEN, 2010).

$$P(\vec{x})A(\vec{x}) + A^T(\vec{x})P(\vec{x}) - P(\vec{x})B(\vec{x})R^{-1}(\vec{x})B^T(\vec{x})P(\vec{x}) + Q(\vec{x}) = 0 \tag{2.43}$$

Considering that Equation (2.43) is solved in each sampling step, it is reduced to an ARE. Finally, the conditions for the application of the SDRE technique in a given system model are (ÇIMEN, 2010):

a) $A(\vec{x}) \in C^1(\mathbb{R}^w)$

b) $B(\vec{x}), C(\vec{x}), Q(\vec{x}), R(\vec{x}) \in C^0(\mathbb{R}^w)$

c) $Q(\vec{x})$ is positive semi-definite and $R(\vec{x})$ is symmetric positive definite

d) $A(\vec{x})x \implies A(0)0 = 0$, i.e., the origin is an equilibrium point

e) $pair(A, B)$ is pointwise stabilizable (a sufficient test for stabilizability is to check the rank of controllability matrix)

f) $pair(A, Q^{\frac{1}{2}})$ is pointwise detectable (a sufficient test for detectability is to check the rank of observability matrix)

According to (CLOUTIER et al., 1996), since the cost functional described in Equation (2.41) is convex, any stationary point is at least a local optimum. In general

(multivariable case), SDRE is not optimal but it is suboptimal. Indeed, the suboptimality property gives rise to the phenomenon that is observed in applications of the SDRE, that the control trajectories converge to the optimal control trajectories as the state is driven towards zero (CLOUTIER et al., 1996).

Finally, Çimen (2008) advocated that in the presence of hard nonlinearities, integral control can bring the system to the required structure given by Equation (2.40).

2.2.2.3 SDRE and H-infinity

Taking into account the general linear statespace dynamics defined by Equation (2.23), SDRE method can be readily extended to nonlinear H_∞ through the γ-iteration in each step in order to solve the general H_∞ problem (CLOUTIER et al., 1996).

It is known that if an SDRE controller can be found using H_∞, the exogenous signal (w) is locally attenuated by γ in each step (CLOUTIER et al., 1996).

3 RELATED WORKS

This chapter shares the selected research related to the current work.

3.1 Linear control

In the domain of attitude kinematics, it is well-known that quaternions representation has several advantages over the Euler angles representation, in particular, (i) it does not have any singular point at any attitude, (ii) it does not depend on any rotational sequence. However, the linearized attitude systems with all quaternion components are not fully controllable (detailed discussion available in Section 5.3). Therefore, the linear control theory including LQR and H_∞ cannot be directly applied to the attitude problem if a full quaternion-based linearized model is used (YANG, 2012).

3.1.1 LQR

In order to overcome the previously mentioned fundamental limitation, researches applied Euler angles for the designing of a linear controller based on LQR (GONZALES; SOUZA, 2009).

Nonetheless, as pointed out by Yang (2010), Yang (2012), Equation (2.5) defines a direct method to find q_4 (the scalar component of the quaternion), therefore, one option is to model the statespace without such component of the quaternion using sole the vectorial components of the quaternion. Furthermore, under mild assumptions (see Section 2.2.1.1 and disregarding hard nonlinearities), Yang (2012) argued using Lyapunov's direct method that the linearized model that involves three vectorial components of the quaternion globally stabilizes the nonlinear system (in other words, the region of attraction of the system is characterized by a fixed point attractor for the whole space spanned by x), whereas it locally optimizes the performance.

To support the argumentation, Yang (2012) shared Figure 3.1 showing the simulation result for a Monte Carlo perturbation model, described as follows: (1) in inertia tensor, the off-diagonal elements were randomly selected between [0, 310], (2) the initial Euler angle errors (converted into quaternions) of the system are randomly selected between $[0, 90]$ degrees, and (3) the initial angular rates are randomly selected between $[0, 0.00174]$ radians per second.

Figure 3.1 - 300 Monte Carlo runs of quaternion response of the system with nondiagonal inertia tensor.

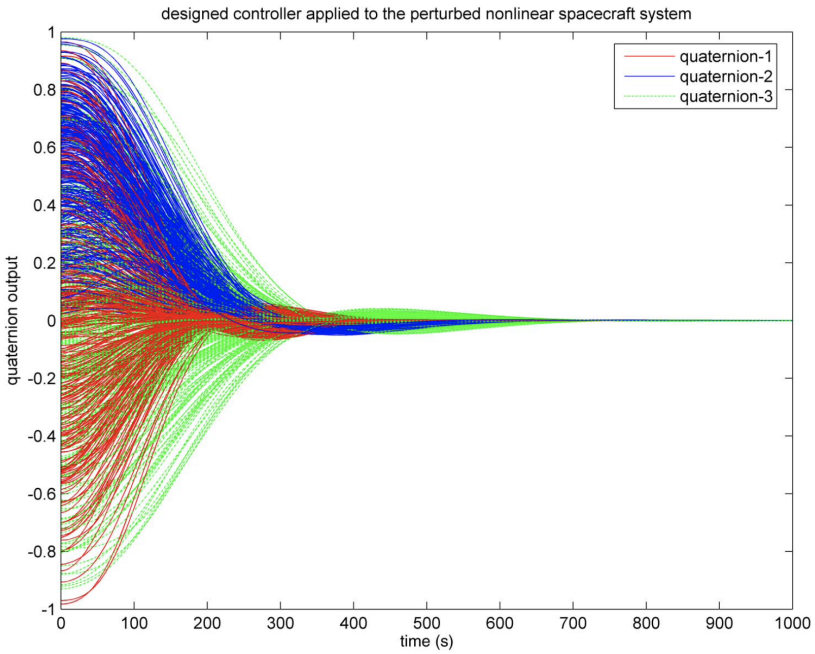

SOURCE: Yang (2012).

3.2 Nonlinear control

Recalling the reasons to investigate SDRE as the nonlinear control technique can be summarized as follows: (1) suboptimal results; (2) less known, consequently, it exhibits more opportunities for extension; (3) numerical tractability for embedded computation so it can be applied in the practical day to day; and (4) flexibility for the designer, being comparable to the flexibility in the LQR (DIMAURO et al., 2015).

3.2.1 SDRE

The application of the SDRE technique, and, consequently, the ARE problem that arises, have already been studied in the available literature, e.g., Menon et al. (2002) investigated the approaches for the ARE solving as well as the resource requirements for such online solving. DiMauro et al. (2015) proposed the usage of differential algebra to reduce the resource requirements for the real-time implementation of SDRE controllers. In fact, the intensive resource requirements for the online ARE solving is the major drawback of SDRE.

The SDRE technique was applied by research (GONZALES; SOUZA, 2009; DIMAURO et al., 2015; ROMERO et al., 2018; ROMERO; SOUZA, 2018; ROMERO; SOUZA, 2019c; ROMERO; SOUZA, 2019a; ROMERO; SOUZA, 2019b; ROMERO; SOUZA, 2019d; ROMERO, 2020a; ROMERO; SOUZA, 2020; ROMERO; SOUZA, 2021b; ROMERO; SOUZA, 2021a; YAO et al., 2021) for controlling a nonlinear system similar to the six-degree of freedom satellite model considered in this thesis. Gonzales and Souza (2009) defined a simulator using Euler angles based on commercial software, whereas, DiMauro et al. (2015) applied quaternions on commercial software. Romero et al. (2018), Romero and Souza (2018) showed, through simulation applying opensource software, using a Monte Carlo perturbation model, SDRE based on quaternions provides better performance than the PID controller.

3.2.1.1 State-dependent coefficients (SDC)

The nonuniqueness of the SDC matrices creates extra degrees of freedom, which can be used to enhance controller performance, however, it poses challenges since not all SDC matrices fulfill the SDRE requirements. Research is focused on the latter challenges.

Liang and Lin (2013) addressed the general problem of the lack of guidelines on the construction of the SDC matrix when the SDRE solvability conditions are violated, which may result in the SDRE scheme being terminated. Indeed, the authors highlighted that SDRE can be unsolvable when the state is at origin ($Cx = 0$).

Romero and Souza (2019a), Romero and Souza (2019b), Romero and Souza (2021a) tackled the SDC construction for the attitude control, in fact, regarding the attitude kinematics, there is a plethora of options, e.g., Euler angles, Gibbs vector, modified Rodrigues parameters (MRPs), quaternions, etc. The SDCs were evaluated according to Çimen (2010), in which is advocated that an effective approach for selecting the optimal state-space model for the SDRE is to attempt to maximize the pointwise stabilizability of the possible models since pointwise control effort can be directly linked with controllability. The controllability criterion requires the value of the determinant of the controllability matrix to be different from zero, therefore, a graphical comparison of the absolute value of the determinant of controllability matrix can be used to reveal when pointwise controllability is maximized. For multi-input systems, as the one studied in such research, the controllability matrix is nonsquare, then the controllability matrix multiplied by its transpose is used to evaluate the determinant.

Yao et al. (2021) proposed an SDC parametrization for the attitude control, in which the previously referred guideline from (ÇIMEN, 2010) is improved. Subsequently, at the region in which the derived SDC parametrization fails to operate, a complementary SDC parametrization is proposed.

3.2.1.2 Domain of attraction

The origin of an SDRE controlled system is a locally asymptotically stable equilibrium point (CLOUTIER et al., 1996). Furthermore, the knowledge of its region of attraction is fundamental due to the local stability even more in the presence of hard nonlinearities or uncertainties.

Indeed, much criticism has been leveled against SDRE technique because it does not provide assurance of global asymptotic stability. However, empirical experience shows that in many cases the fixed point attractor (or the region of attraction, ROA) may be as large as the domain of interest. Moreover, there are situations in which global asymptotic stability cannot be achieved (for example, systems with multiple equilibrium points). Therefore, especially in aerospace, estimating the region of attraction is fundamental (ÇIMEN, 2008).

Obtaining a good estimate of such a ROA, especially of higher order, is a challenging task in itself. In fact, Yao et al. (2021) states that analytical ROA for nonlinear systems with dimensions greater than two is usually unavailable. Such a task becomes even more difficult since the closed-loop matrix of SDRE is usually not available in the closed form (ERDEM; ALLEYNE, 2002).

The well-known Lyapunov approaches to estimate the region of attraction cannot be used for SDRE since the closed-loop system equations are usually not known explicitly. Erdem and Alleyne (2002), Bracci et al. (2006) proposed procedures to reduce the effort of ROA's computation focusing on the maximum and the minimum values of feedback gains over a chosen region of the statespace. The other alternative is to make time-domain simulations of the closed loop system, which is cumbersome and costly (ERDEM; ALLEYNE, 2002; BRACCI et al., 2006).

Yao et al. (2021) showed a domain of attraction based on time-domain simulations (464373 runs) of the closed loop system for the proposed SDC parametrizations. The initial conditions were (3-2-1 Cardan angles were converted into quaternions):

- Z - angles $[-90, 90]$ degrees and angular velocity $[-0.1, 0.1]$ radians per

Figure 3.2 - Region of attraction (ROA) for 50 simulation sets selected randomly among all runs.

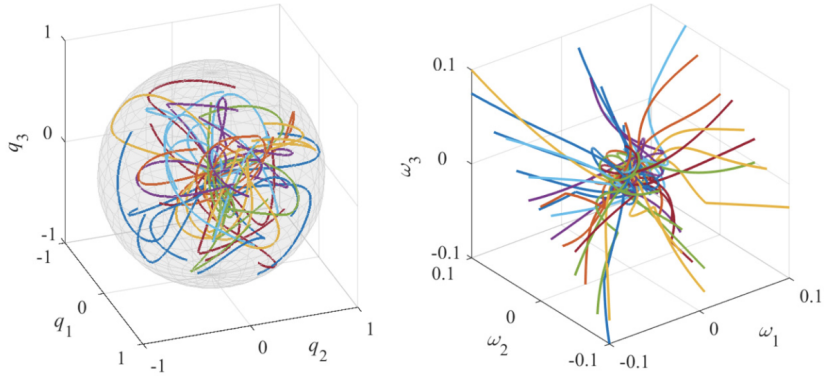

SOURCE: Yao et al. (2021).

second;

- Y - angles $[-90, 90]$ degrees and angular velocity $[-0.1, 0.1]$ radians per second;
- Z - angles $[0, 360]$ degrees and angular velocity $[-0.1, 0.1]$ radians per second;

and a part of the results was shown in Figure 3.2. The simulation results revealed that the proposed SDCs were able to guarantee the system stability in the interest ROA.

3.2.2 SDRE and H-infinity

In order to model uncertainties, Cloutier et al. (1996) proposed the extension of SDRE to nonlinear H_∞ through the γ-iteration and, subsequently, stated if a controller can be found using H_∞, the exogenous signal (w) is locally attenuated by γ in each step (CLOUTIER et al., 1996).

Nonetheless, it can be found in the literature propositions without an explicit rationale that sole SDRE can be robust to uncertainties, e.g., Çimen (2010) (pg. 43) *"... It is also worth mentioning that all three SDRE designs carried out above are robust to 5% variations in the cart-pendulum parameters, as well as unmodeled dynamics of friction and inertia, and attenuate external disturbances on the cart-pendulum*

system...".

Finally, as the extension of SDRE to H_∞ is done step-by-step, all the literature of H_∞ is available. For example, Wang et al. (2017) concluded that the suboptimal control solution achieves mixed performance objectives guaranteeing nonlinear quadratic optimality with inherent stability property in combination with H_∞ type of disturbance reduction; moreover, the SDRE extended with H_∞ showed a better capability of disturbance rejection, but slower response rate.

4 METHODOLOGY

> "One unerring mark of the love of truth is not entertaining any proposition with greater assurance than the proofs it is built upon will warrant." - John Locke

4.1 Toward the goals

Back in 2017, in the discipline CMC-202-4 (Movement of a Solid Body), the first prototype of the open-source software based on Java was defined. It was based on Orekit (OREKIT..., 2017) and Hipparchus (HIPPARCHUS..., 2018) open-source projects. The former for flight dynamics and the latter for mathematics, in particular, linear algebra. The dynamics was linearized enabling the application of LQR (linear-quadratic regulator), in which the matrix P was computed using commercial software.

In the sequel, such dependence on commercial software was removed from the previously mentioned prototype through the contribution for the open-source project Hipparchus (ROMERO, 2017). Such contribution enables the users of the Hipparchus project to solve the ARE easily (for details about the algorithm for solving AREs in Hipparchus, see Romero (2020a)).

In 2018, Romero and Souza (2019c) compared the performance of a PID controller and an SDRE controller applying a kinematic based on Euler Angles using the Amazonia-1 characteristics (SILVA et al., 2014). Applying a Monte Carlo perturbation model, the results showed that SDRE has better performance. Afterwards, Romero et al. (2018), Romero and Souza (2021a) extended the dynamics of the prototype to be based on quaternions and then compared the performance of a PID controller, an LQR controller, and an SDRE controller. Once again applying a Monte Carlo perturbation model, the results showed that SDRE had better performance and the LQR did not exhibit asymptotic stability.

Turning to CubeSats Romero and Souza (2019c), Romero and Souza (2019d), compared the performance of a PID controller and an SDRE controller, resulting in a better performance of the SDRE controller.

The next endeavor was to evaluate different SDCs since the nonuniqueness of the SDC matrices creates extra degrees of freedom, which can be used to enhance controller performance, however, it poses challenges since not all SDC matrices fulfill

the SDRE requirements. Moreover, regarding the satellite's kinematics, there are a plethora of options, e.g., Euler angles, Gibbs vector, modified Rodrigues parameters (MRPs), quaternions, etc. Therefore, Romero and Souza (2019a), Romero and Souza (2019b), Romero and Souza (2021a) evaluated which of these kinematic options resulted in better factorizations of the SDRE technique for the attitude control applying a given Monte Carlo perturbation model based on a set of parameters, initial conditions, and references for the controller. The results showed that different SDCs can produce extremely different results ranging from non-applicability of the SDRE technique to huge differences in the controllability and, consequently, in the robustness and performance of the system.

In 2020, the next fundamental problem was tackled: robustness (ROMERO; SOUZA, 2020; ROMERO; SOUZA, 2021b; ROMERO; SOUZA, 2021c). The robustness was evaluated using two perspectives: (1) structured (parametric) uncertainty of the inertia tensor and (2) a Monte Carlo perturbation model based on a uniform attitude probability distribution. Through the combination of these two perspectives, the robustness properties of the SDRE were grasped. In order to handle the uncertainty appropriately, SDRE was extended with H_∞, in such a way that a family of systems characterized by H_∞ bounded perturbations of a normalized left coprime factorization of a nominal system was computed for each step. Therefore, the attention was moved to the size of error signals and away from the size and bandwidth of selected closed-loop transfer function (GLOVER; MCFARLANE, 1989; SKOGESTAD; POSTLETHWAITE, 2005). To the best of our knowledge, the usage of exactly three AREs to find the sub-optimal controller was original since the SDRE's literature suggests the γ-iteration in each step to solve the general H_∞ problem (CLOUTIER et al., 1996).

The achievements up to the ending of 2019 were published as open-source software, under the license GPL v3.0, and are available at Romero (2020b). Moreover, a developer guide, to enable public extension, is available at Romero (2020a). The continuous development is publicly available, under the same license, at Romero (2021a).

4.2 Methodology

Firstly, the control laws, independent of the applied technique being linear or nonlinear, are modeled and too many time-domains simulations are available for their analysis. Furthermore, as explored in Section 2, in the presence of hard nonlinearities or uncertainties even the techniques that guarantee global asymptotically stability can lose such property. Therefore, the first major task is to assess the presence of a

fixed point attractor as well as its size and shape.

Nonetheless, it is somewhat difficult to depict the ROA for statespace systems with dimensions higher than three. Facing such difficulty, (YAO et al., 2021) chose to list the domain of interest and to plot a small subset of simulations in Figure 3.2. Such an approach offers restricted support for the comparison of different ROAs.

Inspired by the works of Henri Poincaré, in particular, Poincaré maps (LEIPHOLZ, 1970) which defines a lower-dimensional subspace for qualitative analysis. The present work applied two euclidean norms, namely L2-norm of Euler angles (three components) and L2-norm of angular velocities (three angular velocities), to define a two-dimensional space for quantitative analysis. In such a way that the area of the ROA (dimensionless) can be analytically computed and compared; and, the plot of the ROA can allow straightforward analysis.

Besides, as the current work pursues the evaluation of robustness, the definition of the fixed point attractor presented in Equation (2.34) is restricted by the definition of an explicit final time t_f and a numerical error ϵ, according to the following equation:

$$A = \{x_0 \in \mathcal{R}^n : \lim_{t \to t_f} ||x(t, x_0)||_2 < \epsilon\} \tag{4.1}$$

Equipped with these two tools, namely (A) the two-dimensional space for quantitative analysis of the up to seven-dimensional statespace and (B) Equation (4.1), simple polygons - they do not intersect themselves and have no holes - of ROAs are defined in the two-dimensional space for the initial conditions x_0. **The area of such polygons is the primary measure for the quantifiable comparison of different control laws**.

Secondly, inspired by the cost functionals defined by Equations (2.20) and (2.41), the **secondary and final measure applied for the quantifiable comparison of different control laws is** J_m defined by Equation (4.2):

$$J_m = \frac{1}{2} \int_0^{t_f} x^T Q x + u^T R u \, dt \tag{4.2}$$

where $Q = R = I$.

J_m is an approach for **quantifying time domain performance** in terms of the integral of the generalized norm of state (for regulator problem in which it is driven to zero) combined with the generalized norm of control. In this way, the various

objectives related to both speed and quality of response are combined into one measure (SKOGESTAD; POSTLETHWAITE, 2005).

Focusing on these two measures, area of ROAs A and J_m, one defines a Monte Carlo perturbation model for the interested initial conditions, performs the time-domain simulation until the predefined t_f, and, finally, computes the measures.

The last topic in the methodology of the evaluation of control laws is how to define the interest initial conditions.

Regarding *initial attitudes* defined by 3-2-1 Euler angles (Z-Y-X, nonclassical Euler angles), it is well-known that representing Y beyond ± 90 degrees (that means ± 180 degrees) would give two Euler angles solution for every rotation, so Y is limited to ± 90 degrees. X and Z are limited to ± 180 degrees. Therefore, independent distributions are applied for each Euler angle respecting the limits previously discussed in order to define the initial attitudes (3-2-1, Z-Y-X, nonclassical Euler angles, which are converted in quaternions) in a given Monte Carlo perturbation model.

Regarding *initial angular velocities*, they are defined by independent distributions based on the maximum angular velocity of satellite that is controllable by the reaction wheels (see Section 6.1).

In summary, the methodology for the evaluation of the robustness through the determination of the region of attraction as well as the quantifiable results of the control laws can be summarized as:

- Compute initial conditions for the Monte Carlo perturbation model

  Using independent distributions, compute the 3-2-1 Euler angles (Z-Y-X, nonclassical Euler angles) in the range (± 180, ± 90, ± 180)

  Using independent distributions, compute the angular velocities based on the maximum angular velocity of satellite that is controllable by the reaction wheels

- Perform the time-domain simulation until the predefined t_f
- Computes the primary and secondary measures
- Compare such measures

Finally, such a procedure can be extended to introduce structured uncertainty in

the simulation (typically, imprecision in the inertia tensor) as well as unstructured uncertainty (e.g., external torques).

4.3 Limitations

As the conclusions are based on analysis through simulations, they are neither valid for general cases nor for scenarios out of the range of the Monte Carlo perturbation models due to the underlining nonlinear dynamics.

5 MODELS

This chapter presents the models developed in the current work.

5.1 Satellite as rigid-bodies

In this work, satellites are defined to be three-axes stabilized attitude-maneuvering rigid-bodies, therefore, it is a *zero-bias-momentum* system. In the sense that, a major control requirement is to remove the unwanted accumulated angular momentum. Therefore, an active control system is needed. Note the existence of angular momentum in the satellite would cause control difficulties when attitude maneuvers in space would be executed since this superfluous momentum would provide the spacecraft with unwanted gyroscopic stability (SIDI, 2006).

Since an active control system is required, it is worthwhile to explore the techniques available to produce torques for attitude control. There are two types of actuators: (1) the inertial actuators - they change the overall inertial angular momentum of the satellite, in other words, they generate external torques; (2) the momentum exchange actuators - they do not change the inertial angular momentum; or, a symmetrical rotating body produces torque when accelerated about its axis of rotation since such change in the momentum is internal to the satellite, it transfers the momentum change to the satellite with a negative sign (*angular momentum is a conservative quantity*) (SIDI, 2006).

At least, three different ways of producing torque for the attitude control of the satellite are available:

a) Inertial actuators

   Earth's magnetic field - magnetorques provide continuous and smooth control, albeit, the low level of the control torques achieved, and, consequently, slow attitude maneuvers (SIDI, 2006)

   Reaction force produced by a thruster - no smooth control can be achieved owing to the inherent impulsive nature of the thrusters (SIDI, 2006), furthermore, there is no straightforward way to refuel such actuators

b) Momentum exchange actuators

   Reaction wheels - for very accurate control and for moderately fast maneuvers, the reaction wheels are preferred since they allow continuous and smooth control with the lowest possible disturbing torques (SIDI, 2006)

Focusing on the sensors, there are two principal types of attitude determination hardware: attitude sensors and angular velocity sensors (SIDI, 2006).

Figure 5.1 shows the decomposition of the satellite considered in the present work.

Figure 5.1 - Satellite hierarchical decomposition.

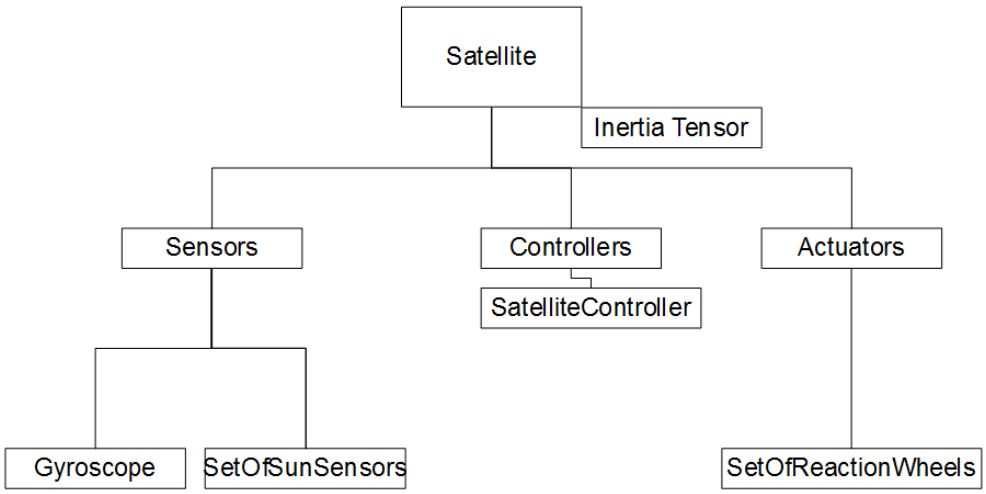

SOURCE: Author.

5.1.1 Sensors

In the Satellite Simulation, there are three types of sensors: (1) a set of attitude sensors, the set of sun sensors (quite-common on earth-orbiting satellites (SIDI, 2006)); and (2) an angular velocity sensor, a gyroscope. The sensors, available in the simulator, are ideal and simplified, in the sense that, they can read *the physical quantities at any moment with perfect accuracy and no noise*. In other words, it is always assumed that $x(t)$ is known exactly (KALMAN, 1960a). Additionally, the set of sun sensors provides through the entire simulation the same measure of the sun versor $\hat{s}_b$ ($\hat{s}_b = [0.323116\ 0.868285\ 0.376401]^T$) so there is no eclipse, the sun is not moving in the ECI reference frame and the sun is always visible by each individual sensor. Indeed, ECI is a quasi-inertial reference frame generally used in AOCS (HUGHES, 1986; SIDI, 2006).

5.1.2 Actuators

One type of actuator is applied, which is a set of reaction wheels. In this thesis, there is no *unloading* of the angular momentum of the reaction wheels perhaps through magnetorques.

Reaction wheels

Since an active control system is required, the simulator uses momentum exchange actuators - they do not change the inertial angular momentum; or, a symmetrical rotating body produces torque when accelerated about its axis of rotation since such change in the momentum is internal to the satellite, it transfers the momentum change to the satellite with a negative sign (*angular momentum is a conservative quantity*) (SIDI, 2006).

The type of the momentum exchange actuator used is reaction wheel, a rotating machine that is commonly applied for very accurate control and for moderately fast maneuvers since it allows continuous and smooth control with the lowest possible disturbing torques (SIDI, 2006). In particular, reaction wheels are often used in satellites that carry optical payloads, as in the previously discussed typical mission of the INPE. For example, a camera-pointing error creates a signal which increases the speed of the wheel, initially at zero. This torque corrects the satellite and leaves the wheel spinning at low speed until another pointing error speeds the wheel further or decreases its speed. If the error is cyclic during each orbit, the wheel may not approach saturation speed for several orbits.

Figure 5.2 - Three reactions wheels mounted in a satellite.

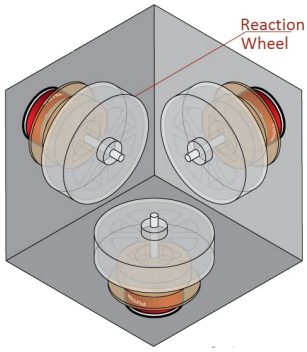

SOURCE: Adapted from Futek... (2018).

Reaction wheels are essentially torque motors with high-inertia rotors. They can spin in either direction and provide one axis of control for each wheel. The basic technical features of a reaction wheel are: maximum achievable torque, maximum momentum capacity (or maximum speed), low torque noise, and low coulomb friction (SIDI, 2006).

Reaction wheels and hard nonlinearities

The reaction wheel models: maximum achievable torque ($M_t \in \mathbb{R}$) and maximum speed ($M_s \in \mathbb{R}$). These two characteristics are physically defined for each reaction wheel apparatus and are described in their supplier's datasheet usually.

According to the Euler-Newton formulation of the rotational motion, angular acceleration is caused by torques, in other words, the change in the angular momentum $\vec{h}$ is equal to the net torques, see Equation 2.7. Moreover, the reaction wheel has constant inertia moment (I), therefore, in the scalar form, the control torque u generated by a reaction wheel is $I\dot{\omega} = \dot{h} = u$. Assuming the reaction wheel has a control mode driven by speed (e.g., the reaction wheel from Futek... (2018), which is commanded by rotational speed), the equation is $\dot{\omega} = uI^{-1}$, which leads to $\omega = \int uI^{-1}$.

A controller computes the commanded control torque ($u_c \in \mathbb{R}$) to be generated by a reaction wheel, which is constrained by M_t due to its physical limitations, in other words, **hard constraints**. In order to model such hard constraints, discrete behavior must be introduced.

Discrete behaviors are modeled using conditional functions, which may be activated at certain points or during some interval of points. These conditional functions may change instantaneously the state when a predicate holds, e.g., a variable x (current value) assumes a new value x'(next value). The ODEs augmented with conditional functions are called **hybrid ODEs**.

The following hybrid ODE models the maximum achievable torque:

$$\omega(t, u_c) := \begin{cases} \int u_c I^{-1}, & \text{if } -M_t \leq \int u_c I^{-1} \leq M_t \\ \int (M_t \, sign(u_c)) I^{-1}, & \text{otherwise} \end{cases} \tag{5.1}$$

where *sign* returns the signal of a given real number.

Note $\omega(t, u_c)$ is continuous because for any given pair $(t, u_c) \in \mathbb{R}^2$ the limit exists

and converges.

Going further, in order to model the maximum speed of a given reaction wheel the model (5.1) must be stacked with the following one:

$$\omega_c(t, u_c) := \begin{cases} \omega(t, u_c), & \text{if } -M_s \leq \omega(t, u_c) \leq M_s \\ M_s \, sign(\omega(t, u_c)), & \text{otherwise} \end{cases} \tag{5.2}$$

Note $\omega_c(t, u_c)$ is still continuous because for any given pair $(t, u_c) \in \mathbb{R}^2$ the limit exists and converges. Nevertheless, such a model (5.2) is **nonlinear** since some changes in u_c do not produce the linear expected effect (due to the constraints), i.e., it does not exhibit the superposition principle, the net response caused by two or more stimuli is not always the sum of the responses that would have been caused by each stimulus individually.

In conclusion, hybrid ODE (5.2) states that the commanded control torque (u_c) is not always achievable so for any given step the actual control torque generated by the reaction wheel can be different from the commanded (smaller). Moreover, hybrid ODE (5.2) is also known as **hard nonlinear** since it is bounded by hard constraints which then lead to nonlinearities (SLOTINE; LI, 1991). Finally, continuity is maintained in such hybrid ODEs, therefore, the conditions for the existence and uniqueness of a solution are maintained; however, global stability properties of linear controllers are easily missed due to such hard nonlinearities.

5.2 Satellite's attitude control

In a *zero-bias-momentum* system, two dynamics states must be controlled: (1) the attitude (perhaps described by Euler angles θ or unit quaternions Q) and (2) its stability ($\dot{\theta}$, in other words, the angular velocity ω of the satellite). Taking into account Satellite Simulation, the following high-level requirements are: (1) is refined in "REQ01 - the attitude must be stabilized and must follow the sun according to a given sun vector in the satellite" and (2) is refined in "REQ02 - the angular momentum must be as close as possible of 0". An additional third (3) requirement would be the unloading of the angular momentum of the reaction wheels, which is not explored in the current work. These high-level requirements lead to a possible control loop described in Figure5.3. Note the main control loop is exclusively based on the set of reaction wheels as actuators, and an additional control-loop could be defined to unload the angular momentum of the reaction wheels. Consequently,

Figure 5.3 - Satellite's attitude control.

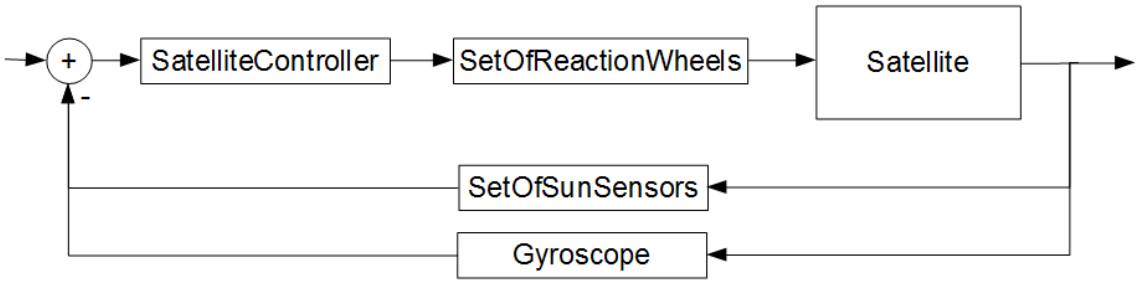

SOURCE: Author.

the state and the control vectors, for the main control loop, can be defined by Equation 5.3.

$$\begin{bmatrix} x_1 \\ x_2 \end{bmatrix} = \begin{bmatrix} Q \\ \omega \end{bmatrix} \qquad \left[u_1\right] = \left[T_c = \sum_{n=1}^{3} g_n a_n\right] \tag{5.3}$$

The control regulator problem requires that errors in the attitude and angular velocity must be obtained. The error in the angular velocity is directly obtained from the gyroscope readings, nonetheless, the error in the attitude must be computed. The applied approach for the computation of the error in the attitude is: (I) in the initial iteration of the simulation, given two versors, namely (a) the actual sun versor $\hat{s}_b$ in the satellite coordinate frame (constant during the simulation) and (b) the reference versor in the satellite coordinate frame, to compute a rotation (there are many) from the actual sun versor to the reference versor (this computed rotation can be described by the unit quaternion Q_t); afterwards, (II) the usual quaternion error is applied as defined by Equation 5.4 (WERTZ; LARSON, 1999).

$$Q_o^{-1} Q_t \equiv Q_e = \begin{bmatrix} Q_{t4} & Q_{t3} & -Q_{t2} & Q_{t1} \\ -Q_{t3} & Q_{t4} & Q_{t1} & Q_{t2} \\ Q_{t2} & -Q_{t1} & Q_{t4} & Q_{t3} \\ -Q_{t1} & -Q_{t2} & -Q_{t3} & Q_{t4} \end{bmatrix} \begin{bmatrix} -Q_{o1} \\ -Q_{o2} \\ -Q_{o3} \\ Q_{o4} \end{bmatrix} \tag{5.4}$$

where Q_o is the quaternion that describes the observed attitude (propagated during

Table 5.1 - Satellite characteristics of Amazonia-1.

Name	Value
Characteristics	
inertia tensor ($kg.m^2$)	$\begin{bmatrix} 310.0 & 1.11 & 1.01 \\ 1.11 & 360.0 & -0.35 \\ 1.01 & -0.35 & 530.7 \end{bmatrix}$
Actuators Characteristics - Reaction Wheels	
inertia ($kg.m^2$)	0.01911
inertia tensor of 3 reaction wheels ($kg.m^2$)	$\begin{bmatrix} 0.01911 & 0 & 0 \\ 0 & 0.01911 & 0 \\ 0 & 0 & 0.01911 \end{bmatrix}$
maximum achievable torque ($N.m$)	0.075
maximum speed (RPM)	6000
References for the controller	
solar vector in the body (XYZ)	$\begin{bmatrix} 1 & 0 & 0 \end{bmatrix}^T$
angular velocity ($radians/second$, XYZ)	$\begin{bmatrix} 0 & 0 & 0 \end{bmatrix}^T$

SOURCE: Adapted from Silva et al. (2014).

the simulation), Q_t is the quaternion that describes the target attitude (as described above) and Q_e is the quaternion error (the actual state for the regulator problem).

5.2.1 Satellite characteristics

Table 5.1 shows the satellite characteristics of **Amazonia-1** (SILVA et al., 2014).

5.3 Linear control

The following subsections share the models for linear control.

5.3.1 LQR based on full quaternions

Equation 2.4 and Equation 2.5 can be used to linearize the system around the stationary point ($\omega = 0$ and $Q = [0\,0\,0\,-1]^T$), assuming also that there are no net

external torques ($g_{cm} = 0$) lead to Equation 5.5.

$$\begin{bmatrix} x_1 \\ x_2 \end{bmatrix} = \begin{bmatrix} Q \\ \omega \end{bmatrix}$$

$$\begin{bmatrix} \dot{x_1} \\ \dot{x_2} \end{bmatrix} = \begin{bmatrix} 0 & -\frac{1}{2}I_{3x3} \\ 0 & 0 \\ 0 & 0 \end{bmatrix} \begin{bmatrix} x_1 \\ x_2 \end{bmatrix} + \begin{bmatrix} 0 \\ -I_b^{-1} \end{bmatrix} \begin{bmatrix} u_1 \end{bmatrix} \tag{5.5}$$

$$\begin{bmatrix} y \end{bmatrix} = I \begin{bmatrix} x_1 \\ x_2 \end{bmatrix}$$

The expansion of the Equation 5.5 generates the Equation 5.6, which defines the constant matrixes A, B e C (taking into account Amazonia-1).

$$\begin{bmatrix} \dot{q_1} \\ \dot{q_2} \\ \dot{q_3} \\ \dot{q_4} \\ \dot{\omega_1} \\ \dot{\omega_2} \\ \dot{\omega_3} \end{bmatrix} = \begin{bmatrix} 0 & 0 & 0 & 0 & -\frac{1}{2} & 0 & 0 \\ 0 & 0 & 0 & 0 & 0 & -\frac{1}{2} & 0 \\ 0 & 0 & 0 & 0 & 0 & 0 & -\frac{1}{2} \\ 0 & 0 & 0 & 0 & 0 & 0 & 0 \\ 0 & 0 & 0 & 0 & 0 & 0 & 0 \\ 0 & 0 & 0 & 0 & 0 & 0 & 0 \\ 0 & 0 & 0 & 0 & 0 & 0 & 0 \end{bmatrix} \begin{bmatrix} q_1 \\ q_2 \\ q_3 \\ q_4 \\ \omega_1 \\ \omega_2 \\ \omega_3 \end{bmatrix} + \begin{bmatrix} 0 & 0 & 0 \\ 0 & 0 & 0 \\ 0 & 0 & 0 \\ 0 & 0 & 0 \\ -0.0032 & 0 & 0 \\ 0 & -0.0028 & 0 \\ 0 & 0 & -0.0019 \end{bmatrix} \begin{bmatrix} u_1 \end{bmatrix}$$

$$\begin{bmatrix} y \end{bmatrix} = I \begin{bmatrix} q_1 \\ q_2 \\ q_3 \\ q_4 \\ \omega_1 \\ \omega_2 \\ \omega_3 \end{bmatrix} \tag{5.6}$$

However, the constant matrices A and B are *not stabilizable* since the controllability matrix of the pair(A,B) has no full rank. Indeed, (YANG, 2012) shown that *this linearized model with all quaternion components is not stabilizable, meaning that LQR is not applicable.*

5.3.2 LQR based on partial quaternions

Since Equation 2.5 defines a direct method to find q_4, therefore, one option is to model the state of the system without such component of the quaternion (YANG, 2012), which leads to the following equation:

$$\begin{bmatrix} x_3 \\ x_2 \end{bmatrix} = \begin{bmatrix} q_1 \\ q_2 \\ q_3 \\ \omega \end{bmatrix}$$

$$\begin{bmatrix} \dot{x_3} \\ \dot{x_2} \end{bmatrix} = \begin{bmatrix} 0 & -\frac{1}{2}I_{3x3} \\ 0 & 0 \end{bmatrix} \begin{bmatrix} x_3 \\ x_2 \end{bmatrix} + \begin{bmatrix} 0 \\ -I_b^{-1} \end{bmatrix} \begin{bmatrix} u_1 \end{bmatrix} \tag{5.7}$$

$$\begin{bmatrix} y \end{bmatrix} = I \begin{bmatrix} x_3 \\ x_2 \end{bmatrix}$$

The expansion of the Equation 5.7 generates the Equation 5.8, which defines the constant matrixes A, B e C (taking into account Amazonia-1).

$$\begin{bmatrix} \dot{q_1} \\ \dot{q_2} \\ \dot{q_3} \\ \dot{\omega_1} \\ \dot{\omega_2} \\ \dot{\omega_3} \end{bmatrix} = \begin{bmatrix} 0 & 0 & 0 & -\frac{1}{2} & 0 & 0 \\ 0 & 0 & 0 & 0 & -\frac{1}{2} & 0 \\ 0 & 0 & 0 & 0 & 0 & -\frac{1}{2} \\ 0 & 0 & 0 & 0 & 0 & 0 \\ 0 & 0 & 0 & 0 & 0 & 0 \\ 0 & 0 & 0 & 0 & 0 & 0 \end{bmatrix} \begin{bmatrix} q_1 \\ q_2 \\ q_3 \\ \omega_1 \\ \omega_2 \\ \omega_3 \end{bmatrix} + \begin{bmatrix} 0 & 0 & 0 \\ 0 & 0 & 0 \\ 0 & 0 & 0 \\ -0.0032 & 0 & 0 \\ 0 & -0.0028 & 0 \\ 0 & 0 & -0.0019 \end{bmatrix} \begin{bmatrix} u_1 \end{bmatrix}$$

$$\begin{bmatrix} y \end{bmatrix} = I \begin{bmatrix} q_1 \\ q_2 \\ q_3 \\ \omega_1 \\ \omega_2 \\ \omega_3 \end{bmatrix} \tag{5.8}$$

In such statespace, the constant matrices A and B, defined by Equation 5.8, are *stabilizable*.

5.4 Nonlinear control

For small maneuvers a linear controller can be used, however, for large maneuvers, the linearized equations do not hold and discontinuities compromise the system (e.g., saturation of the actuators) (SIDI, 2006). In order to avoid linearization, the nonlinear control technique SDRE is applied.

Assuming that there are no net external torques ($g_{cm} = 0$), kinetics defined by Equation 2.13 can be rearranged as defined by Equation 5.9 using the property $v^{\times}w = -w^{\times}v$.

$$\begin{aligned}\dot{\omega} &= -I_b^{-1}\omega^{\times}I_b\omega - I_b^{-1}\omega^{\times}\sum_{n=1}^{3} h_{w,n}a_n - I_b^{-1}\sum_{n=1}^{3} g_n a_n \\ &= (-I_b^{-1}\omega^{\times}I_b + I_b^{-1}(\sum_{n=1}^{3} h_{w,n}a_n)^{\times})\omega - I_b^{-1}\sum_{n=1}^{3} g_n a_n\end{aligned} \tag{5.9}$$

5.4.1 SDRE based on quaternions

Taking into account the state and control vectors defined in Equation 5.3, the state space model can be defined using Equation 2.4 (Ω) and Equation 5.9 in Equation 5.10.

$$\begin{bmatrix} x_0 \\ x_2 \end{bmatrix} = \begin{bmatrix} Q \\ \omega \end{bmatrix}$$

$$\begin{bmatrix} \dot{x_0} \\ \dot{x_2} \end{bmatrix} = \begin{bmatrix} \frac{1}{2}\Omega & 0 \\ 0 & -I_b^{-1}\omega^{\times}I_b + I_b^{-1}(\sum_{n=1}^{3} h_{w,n}a_n)^{\times} \end{bmatrix} \begin{bmatrix} x_0 \\ x_2 \end{bmatrix} + \begin{bmatrix} 0 \\ -I_b^{-1} \end{bmatrix} \begin{bmatrix} u_1 \end{bmatrix} \tag{5.10}$$

$$\begin{bmatrix} y \end{bmatrix} = I \begin{bmatrix} x_0 \\ x_2 \end{bmatrix}$$

However, the SDC matrices (in Equation 5.10) do not fulfill the SDRE requirements, in particular, the *pair (A,B) is not pointwise stabilizable*. Another option for the definition of the SDC matrices is to use Equation 2.4 based on Ξ, which leads to Equation 5.11.

$$\begin{bmatrix} x_0 \\ x_2 \end{bmatrix} = \begin{bmatrix} Q \\ \omega \end{bmatrix}$$

$$\begin{bmatrix} \dot{x_0} \\ \dot{x_2} \end{bmatrix} = \begin{bmatrix} 0 & \frac{1}{2}\Xi \\ 0 & -I_b^{-1}\omega^{\times} I_b + I_b^{-1}(\sum_{n=1}^{3} h_{w,n} a_n)^{\times} \end{bmatrix} \begin{bmatrix} x_0 \\ x_2 \end{bmatrix} + \begin{bmatrix} 0 \\ -I_b^{-1} \end{bmatrix} \begin{bmatrix} u_1 \end{bmatrix} \tag{5.11}$$

$$\begin{bmatrix} y \end{bmatrix} = I \begin{bmatrix} x_0 \\ x_2 \end{bmatrix}$$

Nonetheless, the SDC matrices (in Equation 5.11) do not fulfill the SDRE requirements, in particular, the *pair (A,B) is not pointwise stabilizable.*

5.4.2 SDRE based on Gibb's vector

An alternative option for the definition of the SDC matrices is to use Equation 2.6, which leads to Equation 5.12.

$$\begin{bmatrix} x_0 \\ x_2 \end{bmatrix} = \begin{bmatrix} Q \\ \omega \end{bmatrix}$$

$$\begin{bmatrix} \dot{x_0} \\ \dot{x_2} \end{bmatrix} = \begin{bmatrix} -\frac{1}{2}\begin{bmatrix} \omega^{\times} \\ \omega^T \end{bmatrix} & 0 & \begin{bmatrix} \frac{1}{2} q_4 I_{3\times 3} \\ 0_{1\times 3} \end{bmatrix} \\ 0 & 0 & -I_b^{-1}\omega^{\times} I_b + I_b^{-1}(\sum_{n=1}^{3} h_{w,n} a_n)^{\times} \end{bmatrix} \begin{bmatrix} x_0 \\ x_2 \end{bmatrix} + \begin{bmatrix} 0 \\ -I_b^{-1} \end{bmatrix} \begin{bmatrix} u_1 \end{bmatrix}$$

$$\begin{bmatrix} y \end{bmatrix} = I \begin{bmatrix} x_0 \\ x_2 \end{bmatrix} \tag{5.12}$$

Equation 5.12 has been shown to satisfy SDRE conditions in the majority of statespace with exception of the region on which the angular velocity is close to 0 (the pair(A,B) loses rank in such region). In practical problems, regarding such a region, one approach is to switch to another SDC parametrization (YAO et al., 2021) or to resort to LQR. Note such the known limitation of this particular parametrization of SDRE imposes laxity as the REQ01 is not satisfied. Nonetheless, as the goal of this thesis is to evaluate the control laws in the presence of hard nonlinearities and

uncertainties such a limitation is accepted.

Finally, equation 5.12 can be factored to produce infinity parametrizations. Moreover, other kinematic equations (e.g., MRPs) can result in statespace models with different properties.

5.4.3 SDRE and H-infinity based on Gibb's vector

In the same spirit of the performance index studied by (KALMAN, 1960b) for LQR in the early 1960s, the current work chooses to focus on the size of error signals z in the statespace described by Equation (2.23) but not on the size and bandwidth of transfer functions (frequency response techniques; (SKOGESTAD; POSTLETHWAITE, 2005)).

The SDRE extended with H_∞ uses Equation (5.12) and the following procedure to compute the controller that maximizes the stability margin for the perturbed plants in each step, which is:

a) Reconstruct the matrices using the SDC form;

b) Solve the two ARES of Equation (2.31) computing X and Z;

c) Compute γ_{min} using Equation (2.30);

d) Define a state-space model (A,B,C,D) using X, Z and a $\gamma > \gamma_{min}$ by Equation (2.33);

e) Solve the third ARE that results from state-space model described by Equation (2.33), which leads to $P_{K_{H_\infty}}$ as the unique, symmetric, positive-definite solution of such ARE;

f) Compute the controller K for the original system using $K(\vec{x}) = R^{-1}(\vec{x})B_2(\vec{x})P_{K_{H_\infty}}(\vec{x})$.

Such a procedure requires the solving of three AREs in each step, instead of one ARE as usual in the SDRE controller. Nonetheless, it avoids the λ-iteration in each step.

Concluding, the limitations and reflections discussed in the previous subsection apply to this control law since it is based on the same Equation (5.12).

6 RESULTS

This section shares the evaluation of four scenarios of the control laws under analysis:

- Primary and secondary measures for a Monte Carlo perturbation model as described by Section 4.2 without the hard nonlinearities in the reaction wheels as modeled in Equation 5.2, see Section 6.2;
- Primary and secondary measures for a Monte Carlo perturbation model as described by Section 4.2 with the hard nonlinearities in the reaction wheels as modeled in Equation 5.2, see Section 6.3;
- Primary measure for a Monte Carlo perturbation model as described by Section 4.2 with the hard nonlinearities in the reaction wheels as modeled in Equation 5.2 extended by *structured uncertainties* modeled as variations in the inertia tensor, see Section 6.4;
- Primary measure for a Monte Carlo perturbation model as described by Section 4.2 with the hard nonlinearities in the reaction wheels as modeled in Equation 5.2 extended by *unstructured uncertainties* modeled as a net external torque, see Section 6.5;

6.1 Preliminaries

Taking into account the limitations of the control laws previously stated in Section 5, the definition of the fixed point attractor presented in Equation (4.1) is once restricted by the selection of sole angular velocities (x_2 in Equation (5.5)), ω-stability in Hughes (1986), according to the following equation:

$$A = \{x_0 \in \mathcal{R}^n : \lim_{t \to t_f} ||x_2(t, x_0)||_2 < \epsilon\} \tag{6.1}$$

All the results are based on the satellite Amazonia-1, which is characterized by Table 5.1, furthermore, the simulations were conducted with the full Monte Carlo perturbation model (see Section 4.2) tuned with the parameters shared in Table 6.1.

The parameters are self-evident with except of the angular velocities. Using Section 2.1.2, the maximum angular momentum of the set of reactions wheels was computed ($\vec{h_{w_{max}}} = \vec{I_w}.\vec{\omega_{w_{max}}}$) and then the corresponding maximum angular velocity of the satellite was found solving a matrix equation ($\vec{h_{w_{max}}} = \vec{I}.\vec{\omega_{max}}$). The result

Table 6.1 - Monte Carlo perturbation model parameters.

Name	Value
3-2-1 Euler angles (degrees)	$Z : U(-180, 180)$ $Y : U(-90, 90)$ $X : U(-180, 180)$
angular velocities (rad/s)	$X : U(-0.0385, 0.0385)$ $Y : U(-0.0385, 0.0385)$ $Z : U(-0.0385, 0.0385)$
Q	I
R	I
ϵ (rad/s)	0.0001
samples	150
t_f (seconds)	3600
fixed step size (seconds)	0.05

SOURCE: Author.

in radians per second was $\vec{\omega_{max}} = \{0.0385,\ 0.0332,\ 0.0225\}$, the norm (L2) is 0.0556, and the infinity norm was 0.0385, which is the value used as parameter.

The initial conditions uniformly distributed computed using such parameters by the Monte Carlo perturbation model are depicted in the next sections using a two-dimensional space, in which the norm of Euler angles is along the X axis and the norm of angular velocities is along the Y axis for each initial condition. This space has its bounds constrained by the norm of Euler Angles ranging from 0 to 270 degrees and the norm of angular velocities ranging from 0 to 0.066 radians per second, following the parameters presented in Table 6.1. However, as there is no mechanism to desaturate the reactions wheels, the limit expected for the norm of the angular velocities of the initial conditions inside any ROA is the previously shared 0.0556 radians per second (in the presence of the hard nonlinearities). From here on NS is used in the sense that such a predicted upper bound for the norm of the angular velocities is achieved; furthermore, NP is used in the sense of the convergence in the defined t_f.

The same two-dimensional space is applied in the next sections to depict ROA (primary measure). In the same spirit, the secondary measure defined by Equation (4.2) is shown using another two dimensional space, in which the integral of the generalized norm of statespace is along the X axis and the integral of the generalized norm of control is along the Y axis for each sample; furthermore, the statistics for the

measure, as defined by Equation (4.2) and computed using the samples, are shared.

Additionally, Appendix B shares the simulations of the control laws for two relevant maneuvers, a Y and a Z "pure-spins", which provide complementary engineering insights.

Finally, the data, as generated by the simulator, are completely available at Romero (2021b).

6.2 Primary and secondary measures evaluated without hard nonlinearities

This section evaluates the satellite (modeled as a nonlinear system) and the control laws (LQR, SDRE based on Gibb's vector, and SDRE and H-infinity based on Gibb's vector) without hard nonlinearities in the reaction wheels. Therefore, the reaction wheels are linear and can achieve any torque as well as any speed as opposed to Equation 5.2.

Figure 6.1 shows the initial conditions uniformly distributed by such a Monte Carlo perturbation model execution (450 simulations, three different control laws for each initial condition).

Figure 6.1 - Initial conditions without hard nonlinearities.

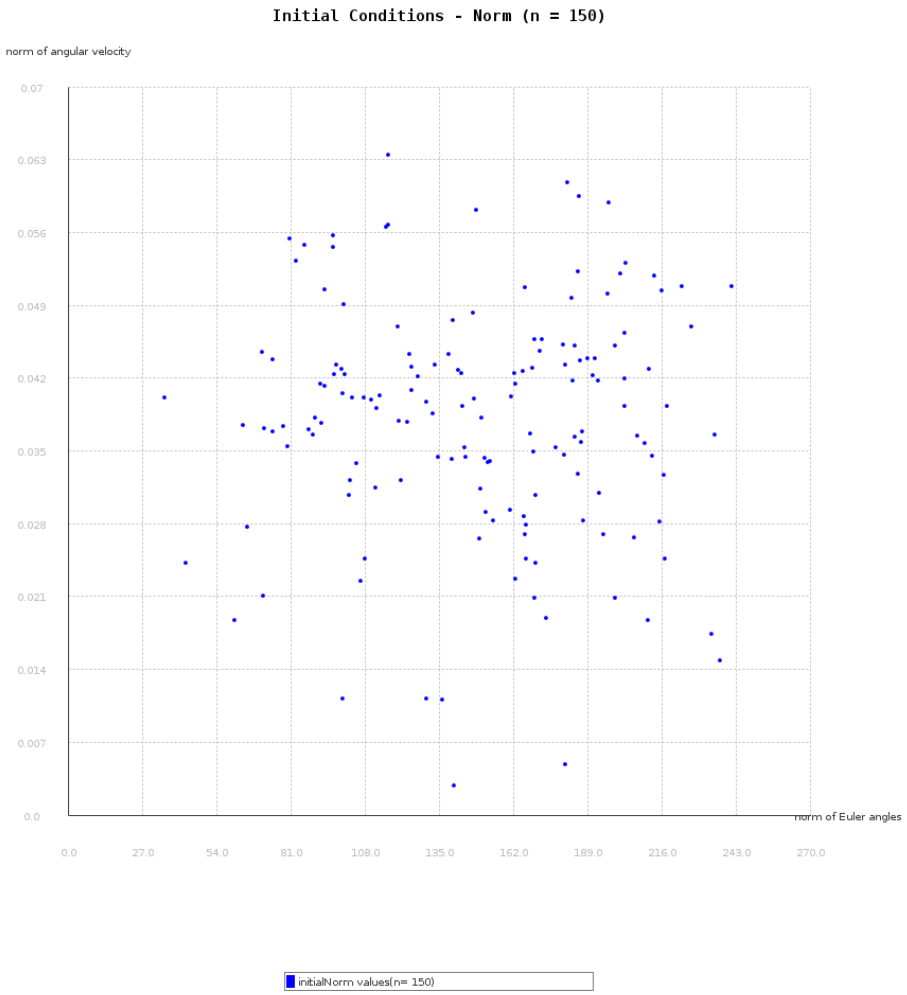

SOURCE: Author.

Figure 6.2 shows the ROA of LQR (in blue, legend ProportionalLinearQuatuernionPartialLQRController), SDRE based on Gibb's vector (in green, legend ProportionalNonLinearQuaternionSDREController_GIBBS), and SDRE and H-infinity based on Gibb's vector (in red, legend ProportionalNonLinearQuaternionFullSDREHinfinityController), which were identical. In particular, all the 150 initial conditions converged in t_f according to Equation (6.1); consequently, the area of the three polygons was the same (primary measure). Note the upper bound for angular velocities (in the presence of hard nonlinearities) established as a criterion for NS was overpassed since the hard nonlinearities were turned off.

Figure 6.2 - ROA without hard nonlinearities.

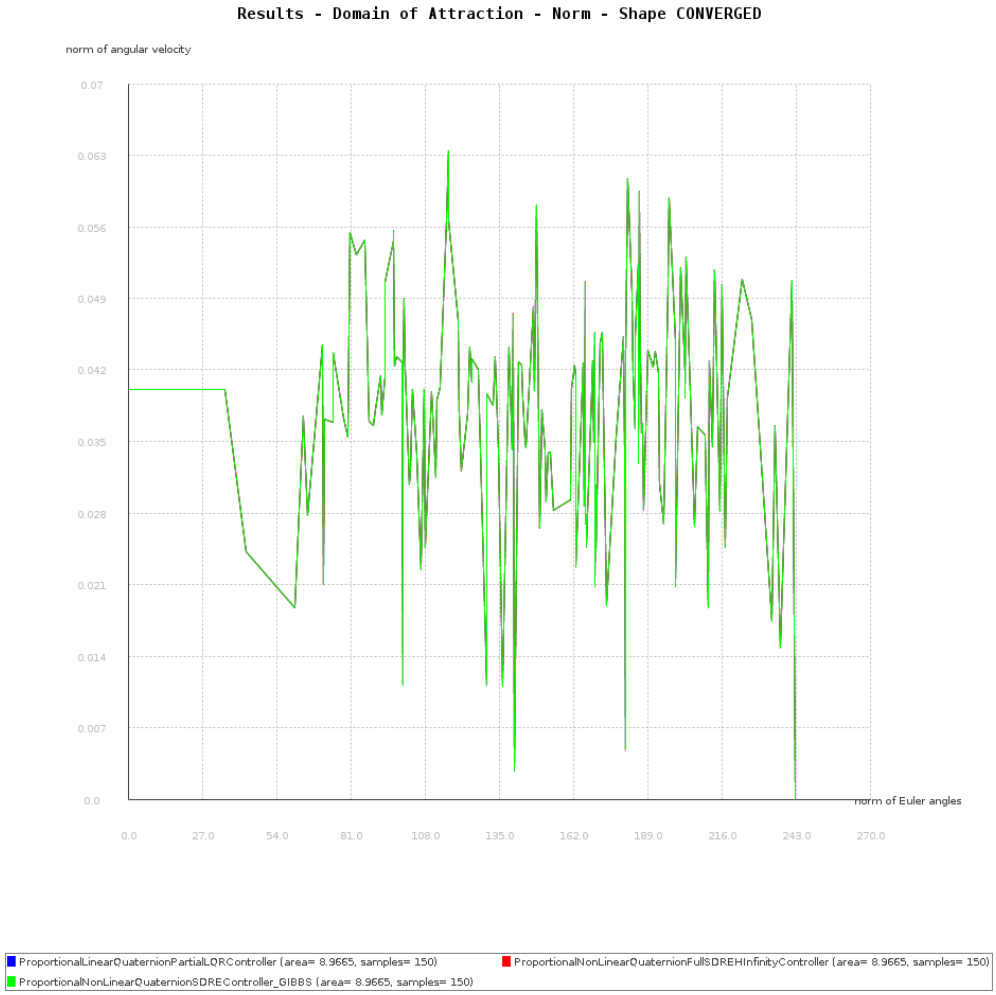

SOURCE: Author.

Figure 6.3 depicts the secondary measure. Recall LQR, in blue, legend ProportionalLinearQuatuernionPartialLQRController; SDRE based on Gibb's vector, in green, legend ProportionalNonLinearQuaternionSDREController_GIBBS; and, SDRE and H-infinity based on Gibb's vector, in red, legend ProportionalNonLinearQuaternionFullSDREHinfinityController.

Figure 6.3 - Statistics of Optimality without hard nonlinearities.

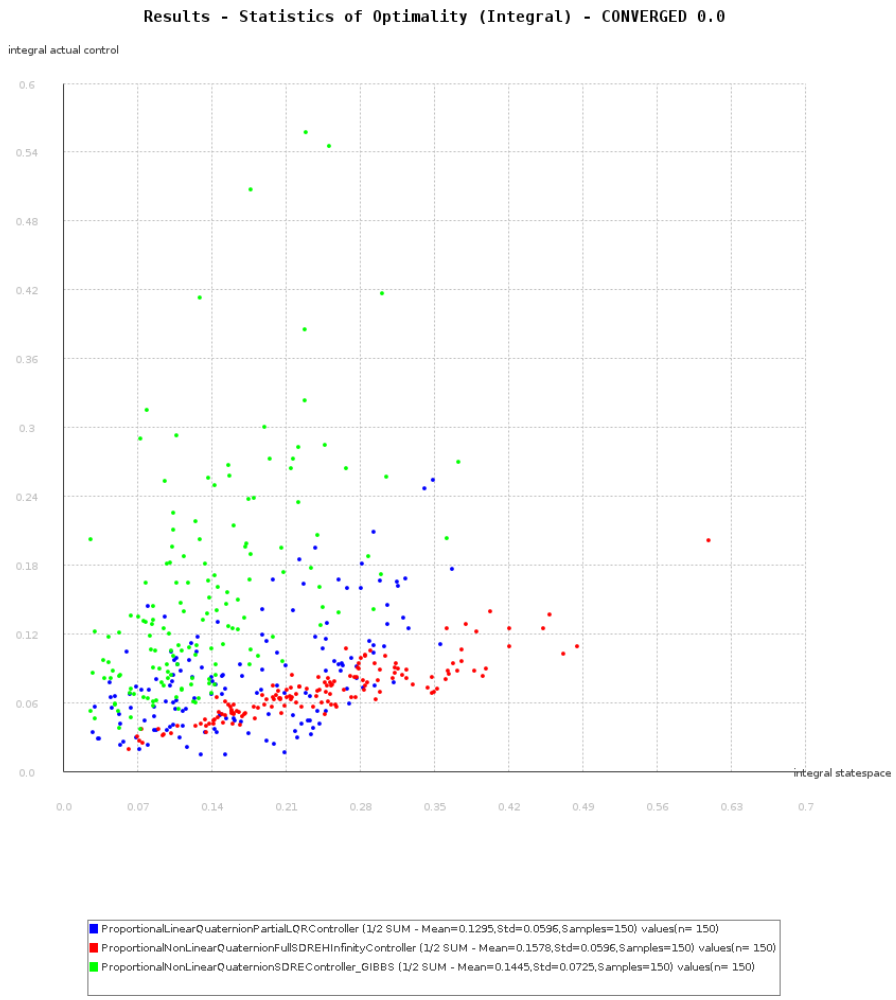

SOURCE: Author.

Without hard nonlinearities, LQR exhibited the best compromise regarding Equation (4.2). In fact, it had the smallest mean and standard deviation.

SDRE based on Gibb's vector had the second best mean and the worst standard deviation, in the sense that, it demanded more control from the actuators. On the other hand, SDRE and H-infinity based on Gibb's vector demanded less control from the actuators with the expenditure of the largest amplitude in the statespace.

Concluding this section, Figure 6.4 plots the integral of the generalized norm of computed control along the X axis and along the Y axis for the actual control applied for each control law and sample. Note, without hard nonlinearities, the computed

and actual control were the same for all samples.

Figure 6.4 - Actual versus computed control without hard nonlinearities.

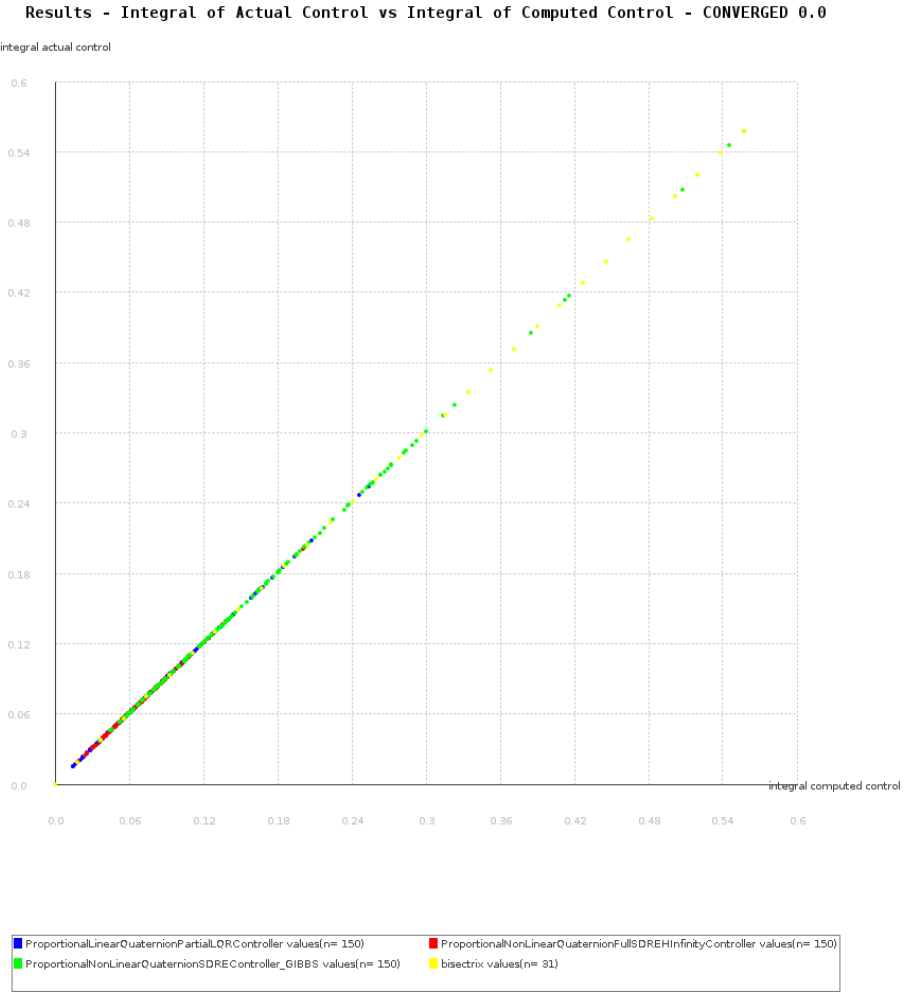

SOURCE: Author.

In summary, taking into account the Amazonia-1 modeled as a nonlinear system but without hard nonlinearities and the full Monte Carlo perturbation model previously shared, the linear control law, LQR, exhibited NS and NP (highlighted by the primary measure) and the best performance (highlighted by the secondary measure). Furthermore, the nonlinear control laws (SDRE based on Gibb's vector, and SDRE and H-infinity based on Gibb's vector) exhibited NS and NP (highlighted by the primary measure) and the worst performance (highlighted by the secondary

measure).

6.3 Primary and secondary measures evaluated with hard nonlinearities

As opposed to the previous section, this section evaluates the satellite (modeled as a nonlinear system) and the control laws (LQR, SDRE based on Gibb's vector, and SDRE and H-infinity based on Gibb's vector) with hard nonlinearities in the reaction wheels (see Equation 5.2).

Figure 6.5 shows the initial conditions uniformly distributed by such a Monte Carlo perturbation model execution (450 simulations, three different control laws for each initial condition).

Figure 6.5 - Initial conditions with hard nonlinearities.

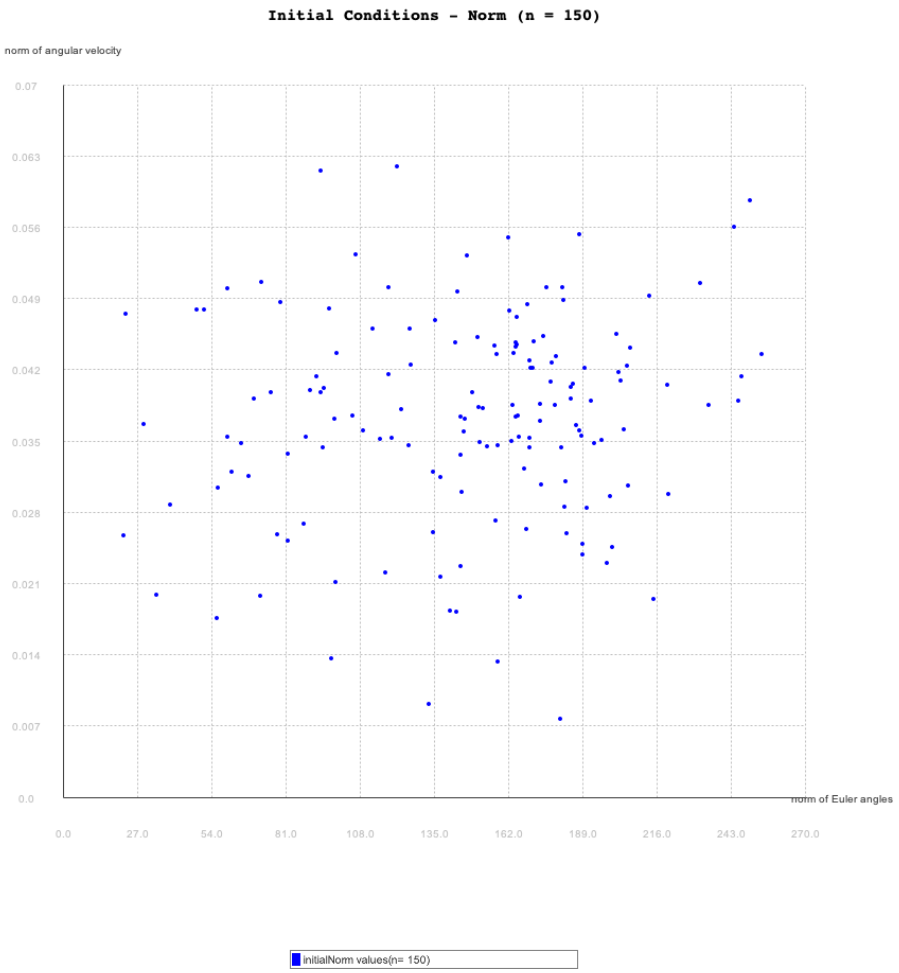

SOURCE: Author.

The applied hard nonlinearities are those described by Equation (5.2) and so for any step of a given maneuver the actual control torque generated by the reaction wheels could be smaller than the computed control. Indeed, with hard nonlinearities, the actual control was smaller than the computed control in the simulations as shown in Figure 6.6. Note points are close to the X axis in the sense that actual control was much smaller than the bisectrix (where actual equals computed control).

Figure 6.6 - Actual versus computed control with hard nonlinearities.

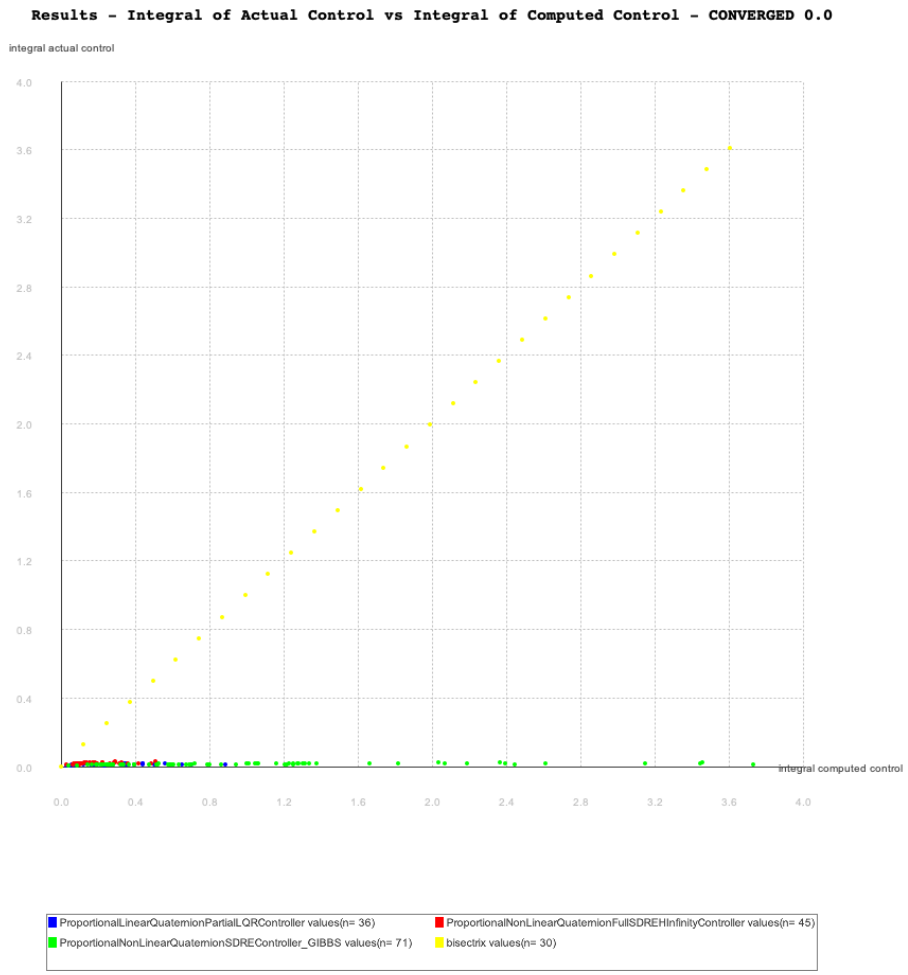

SOURCE: Author.

The result of such a "lack of control" is depicted in Figure 6.7 that shows the ROA of LQR (in blue, legend ProportionalLinearQuatuernionPartialLQRController), SDRE based on Gibb's vector (in green, legend ProportionalNonLinearQuaternionS-

DREController_GIBBS), and SDRE and H-infinity based on Gibb's vector (in red, legend ProportionalNonLinearQuaternionFullSDREHinfinityController).

Figure 6.7 - ROA with hard nonlinearities.

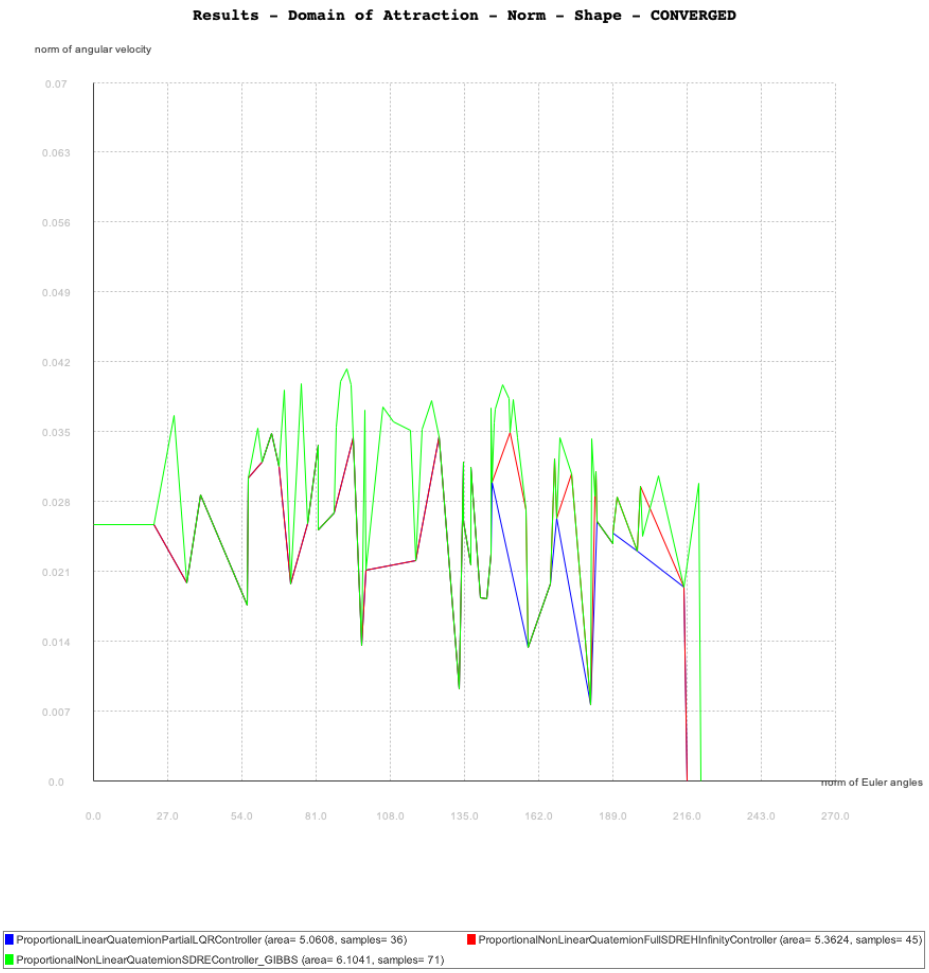

SOURCE: Author.

Firstly, the number of samples that converged, as modeled by Equation (6.1), are less than one-half, even for the better control law, regarding the 150 initial conditions shown in Figure 6.5. **Hence, the NS of the three control laws was lost by the introduction of the hard nonlinearities modeled by Equation** (5.2)**.** Moreover, the three control laws are able to control the whole range of Euler angles, henceforth, the angular velocities are the critical aspects to be constrained in the initial conditions perhaps through requirements for the launch vehicle. Such

a fact corroborates asymptotic ω-stability (HUGHES, 1986) as the major concern in accordance with Equation (6.1). Furthermore, it confirms the common sense the controlling of angular velocities is constrained by hard nonlinearities in the actuators (reaction wheels, see Table 5.1) leading to phenomena as saturation.

In a quantitative analysis, using the primary measure (see Equation (6.1)) shown in Figure 6.7, the ROA of LQR had the smallest area in the sense that some extra initial conditions did not respect Equation (6.1) in the specified t_f. Moreover, SDRE based on Gibb's vector had the largest ROA (35 more samples converged). Finally, SDRE and H-infinity based on Gibb's vector had the intermediary ROA.

Figure 6.8 depicts the secondary measure using the previously presented two dimensional space. Recall LQR, in blue, legend ProportionalLinearQuatuernionPartialLQRController; SDRE based on Gibb's vector, in green, legend ProportionalNonLinearQuaternionSDREController_GIBBS; and, SDRE and H-infinity based on Gibb's vector, in red, legend ProportionalNonLinearQuaternionFullSDREHinfinityController.

Figure 6.8 - Statistics of Optimality with hard nonlinearities.

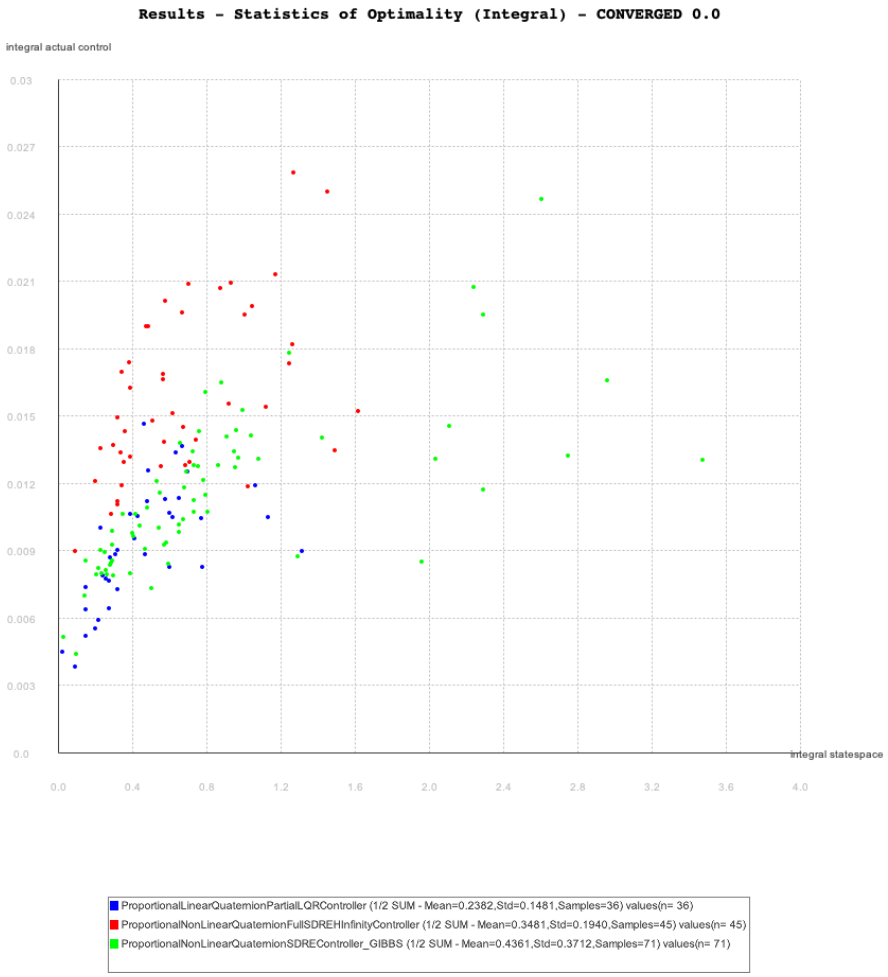

SOURCE: Author.

The first fact to be highlighted is that the statistics were computed with different sample sizes, which demands caution in the further analysis since the control laws based on SDRE were able to control initial conditions with the largest angular velocities. In addition, the previously discussed limitations of control laws have as consequence possible penalties for the control laws based on SDRE due to the arbitrary final quaternions.

The smallest mean and standard deviation was exhibited by LQR (in blue) in the sense that it was the optimal regulator for the smallest subset of the initial conditions. SDRE based on Gibb's vector (in green) had the largest mean and standard deviation, i.e., in the presence of hard nonlinearities SDRE was suboptimal. The

SDRE and H-infinity based on Gibb's vector (in red) showed the intermediary values for mean and standard deviation, which was an indication of a compromise between state and control.

In fact, in the realm of H-infinity, Equation (2.30) predicts the maximum stability margin (ϵ_{max}) for a given minimum gamma (γ_{min}). Therefore, Figure 6.9 plots a point (X: minimum gamma, Y: maximum gamma) for each sample that converged with SDRE and H-infinity based on Gibb's vector (in red, the sole control law that defines gamma). Additionally, Figure 6.9 shows the overall minimum and maximum gamma in the legend.

Figure 6.9 - Min-Max Gamma with hard nonlinearities.

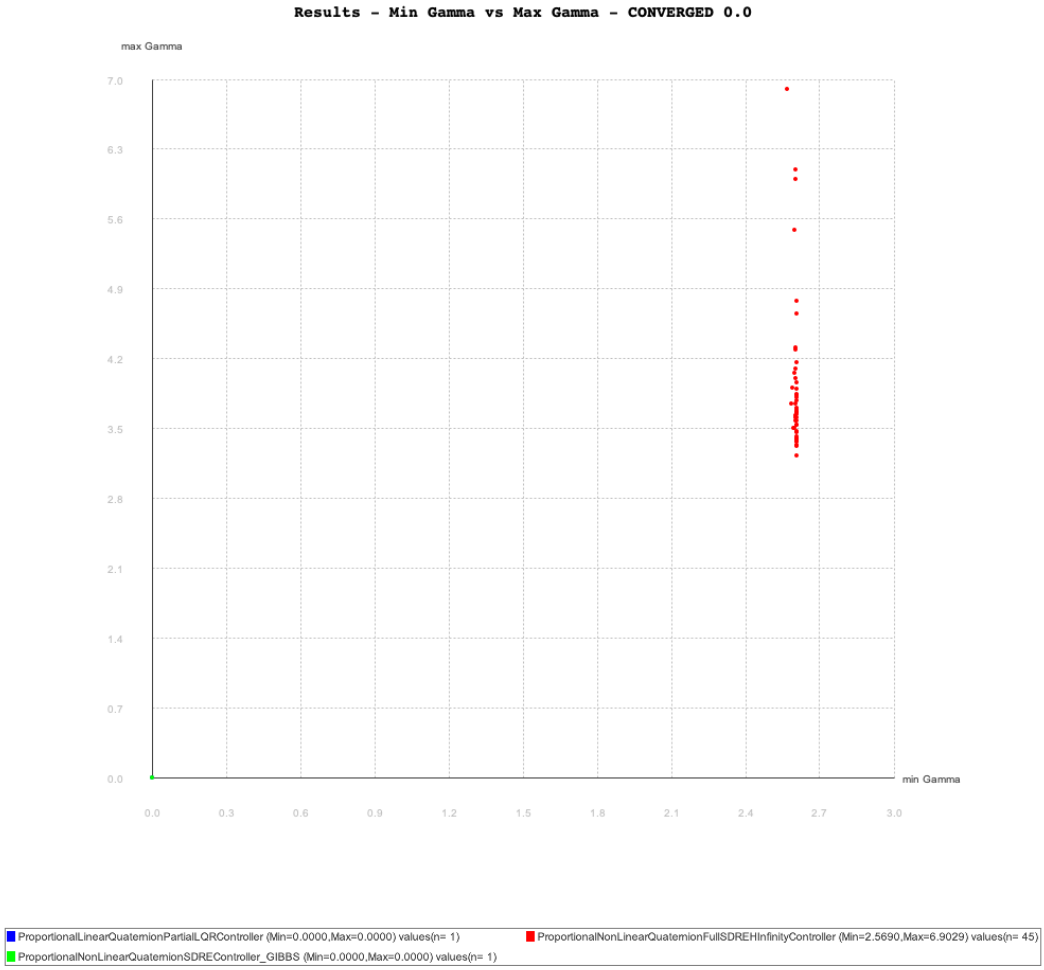

SOURCE: Author.

It was remarkable that the lower bound was close to 2.5 for all samples; whereas, the upper bound was close to 6.9 with a larger variation. Henceforth, for the approximation of a maximum stability margin (ϵ_{max}), the upper bound of the minimum gamma for all simulations could be used so the predicted maximum stability margin (ϵ_{max}) is approximately 0.14 ($\epsilon_{max} \approx 0.14$).

In summary, taking into account the Amazonia-1 modeled as a nonlinear system with hard nonlinearities and the full Monte Carlo perturbation model previously shared, the linear control law (LQR) lost its NS (highlighted by the primary measure) with the worst ROA. In fact, the nonlinear control laws (SDRE based on Gibb's vector, and SDRE and H-infinity based on Gibb's vector) also lost their NS (highlighted by the primary measure) but they exhibited the largest ROAs. Regarding performance, the three control laws lost NP with the secondary measure compromised by such a difference in the sample sizes.

6.4 Primary measure evaluated with structured uncertainties

This section assesses structured uncertainty into the model evaluated in the last section. The structured uncertainty is assessed by varying the inertia tensor of the satellite (assumed as time-invariant), in particular, an additive percentage is applied in each entry of the inertia tensor.

There is a plethora of valid goals regarding the definition of the additive percentage to be evaluated, e.g., what is the percentage that maintains NS (recall NS was lost in the previous section), what is the control law that provides better ROA for a wider range of percentage, what is the control law that provides better ROA for a relevant range of percentage, what is a relevant range of percentage, etc... This section chose to evaluate "what is the control law that provides better ROA for a wider range of percentage" in the sense that the range applied was at most 150%.

Taking into account the satellite Amazonia-1, which is characterized by Table 5.1, the simulations were conducted with the full Monte Carlo perturbation model (see Section 4.2) tuned with the parameters shared in Table 6.1. Such a Monte Carlo perturbation model was executed five times (2250 simulations, five times three different control laws for each initial condition), each one using the same set of initial conditions with a varying additive percentage ($p, \%$) applied to the inertia tensor in the range $p = \{-1.5, -0.75, 0.0, 0.75, 1.5\}$, in which 0.0 is the nominal case.

Figure 6.10 shows the initial conditions uniformly distributed by such a Monte Carlo

perturbation model execution in the two-dimensional space described in the previous sections.

Figure 6.10 - Initial conditions with hard nonlinearities and structured uncertainties.

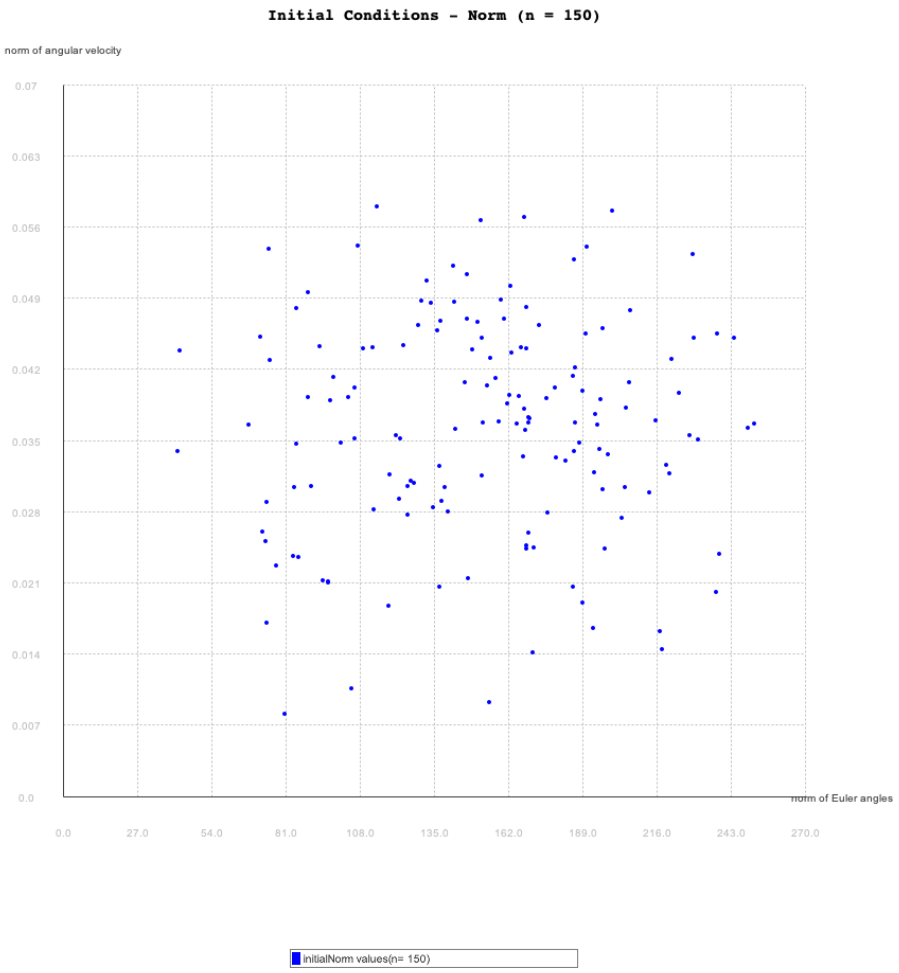

SOURCE: Author.

As previously discussed, focusing on ROA only primary measure matters (area of ROA). Moreover, varying the additive percentage applied to the nominal inertia tensor ($p = 0$), a set of ROAs is obtained. The natural way to visualize such a set of ROAs is to stack them perhaps with a proper computational power a polytope could be obtained and its area calculated. With restricted computational power as the range previously defined, the ROAs can be stacked and the area of each one can be summed up. Therefore, Figure 6.11 shows the stacked ROAs for each p and

control law.

Figure 6.11 - Stacked ROAs with hard nonlinearities and structured uncertainties (p, %).

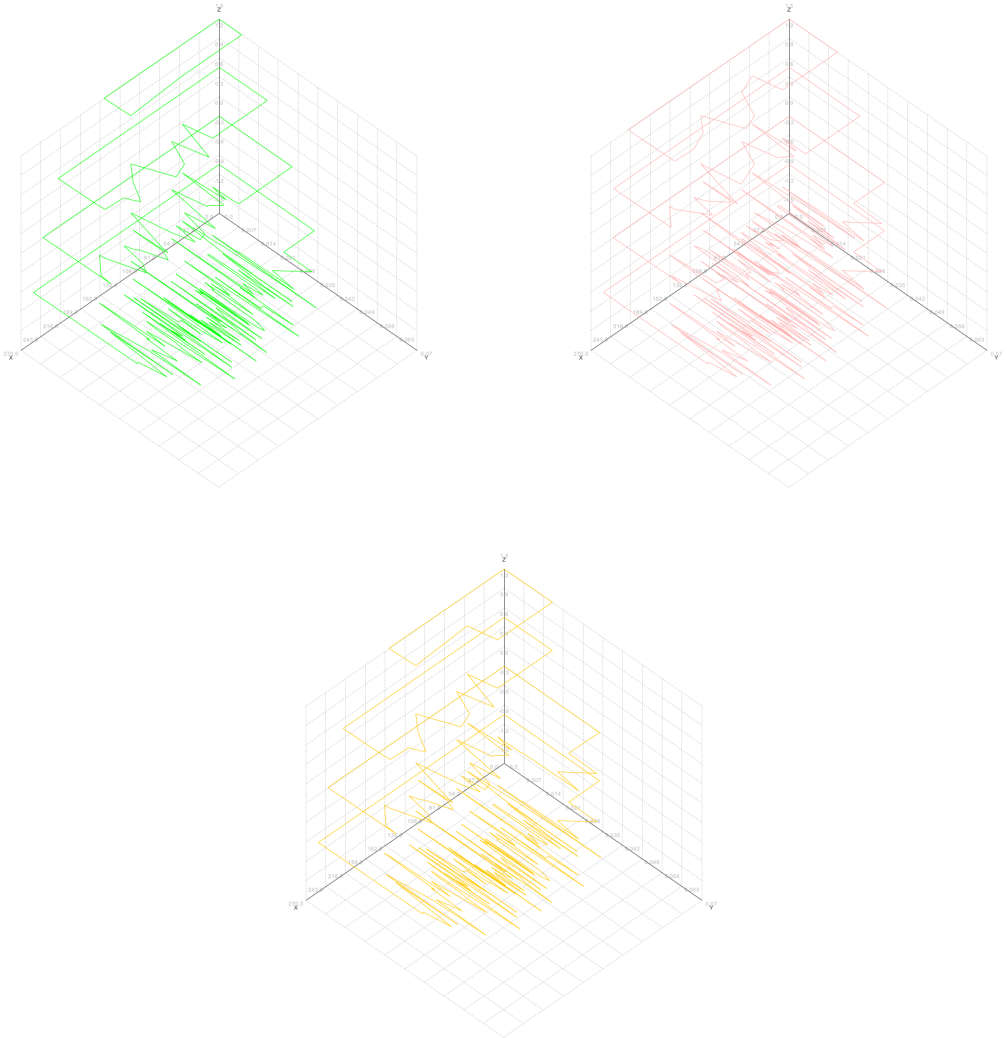

The first graph shows the stacked ROA for LQR (sum of areas=19.29), the second graph shows the stacked ROA for SDRE based on Gibb's vector (sum of areas=24.99), and the thrid graph shows the stacked ROA for SDRE and H-Infinity based on Gibb's vector (sum of areas=20.76) (X: norm of Euler angles - degrees, Y: norm of angular velocities - rad/s, Z: p - %).

SOURCE: Author.

The lowest $p = -1.5$ prevented the convergence of the three control laws. When $p = -0.75$, the control laws had an additional gain due to the smaller inertia tensor

so all the samples converged (as in Section 6.2). At the nominal case ($p = 0$), the control laws exhibited the same pattern discussed in Section 6.3. Beyond the nominal case, the norm of angular velocities was decreasing as p increased.

In conclusion, evaluating the "sum of areas of ROAs" (primary measure), SDRE based on Gibb's vector provided the largest ROA followed by SDRE and H-Infinity based on Gibb's vector. LQR provided the smallest ROA. Figure 6.12 shares the ROA for each p.

Figure 6.12 - ROA with hard nonlinearities and structured uncertainties (p, %).

SOURCE: Author.

6.5 Primary measure evaluated with unstructured uncertainties

This section evaluates unstructured uncertainty into the model presented in Section 6.3. The unstructured uncertainty is introduced as an additive white Gaussian noise (AWGN) net external torque applied to the center of mass of the satellite.

Recall Section 6.3 shared $\epsilon_{max} \approx 0.14$ for the SDRE and H-infinity based on Gibb's vector, therefore, it is reasonable to assess such a net external torque as upper bound. Moreover, the AWGN is computed for each axis so the infinity norm of such net external torque should have an upper bound close to the ϵ_{max}.

Taking into account the satellite Amazonia-1, which is characterized by Table 5.1, the simulations were conducted with the full Monte Carlo perturbation model (see Section 4.2) tuned with the parameters shared in Table 6.1. Such a Monte Carlo perturbation model was executed five times (2250 simulations, five times three different control laws for each initial condition), each one using the same set of initial conditions with the AWGN $(p, N.m)$ applied as net external torque (g_{cm}, see Equation (2.13)) in the range $p = \{0.0, N(0, 0.0375/7), N(0, 0.075/7), N(0, 0.1125/7), N(0, 0.15/7)\}$ for each axis, in which 0.0 is the nominal case. Once computed, the same set of AWGN was applied for each initial condition in a given execution, in a way that there was no difference between the AWGN applied for the three control laws during the simulations. The σ was computed using a division by seven so it was unlikely to have a net external torque out of the predefined upper bound.

Figure 6.13 shows the initial conditions uniformly distributed by such a Monte Carlo perturbation model execution in the two-dimensional space described in the previous sections.

Figure 6.13 - Initial conditions with hard nonlinearities and unstructured uncertainties.

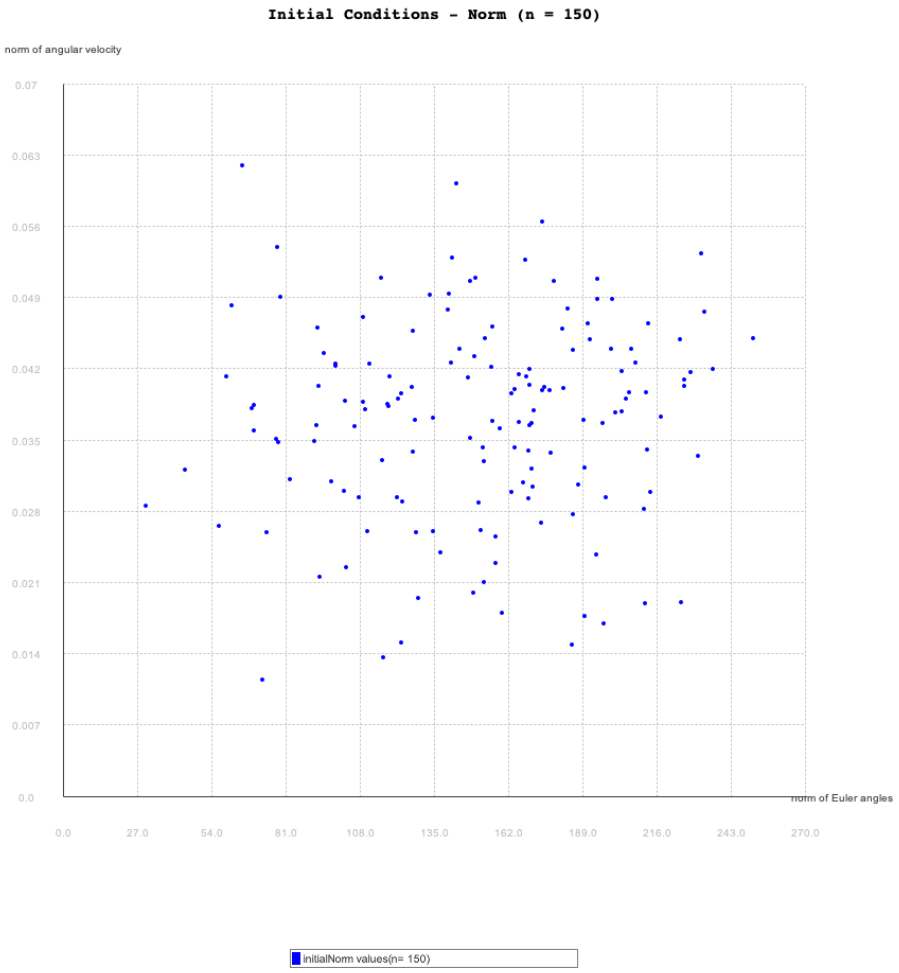

SOURCE: Author.

As previously discussed, focusing on ROA only primary measure matters (area of ROA). Moreover, varying the AWGN a set of ROAs is obtained. With restricted computational power as the range previously defined, the ROAs can be stacked and the area of each one can be summed up. Therefore, Figure 6.14 shows the stacked ROAs for each p and control law.

Figure 6.14 - Stacked ROAs with hard nonlinearities and unstructured uncertainties (p, $N.m$).

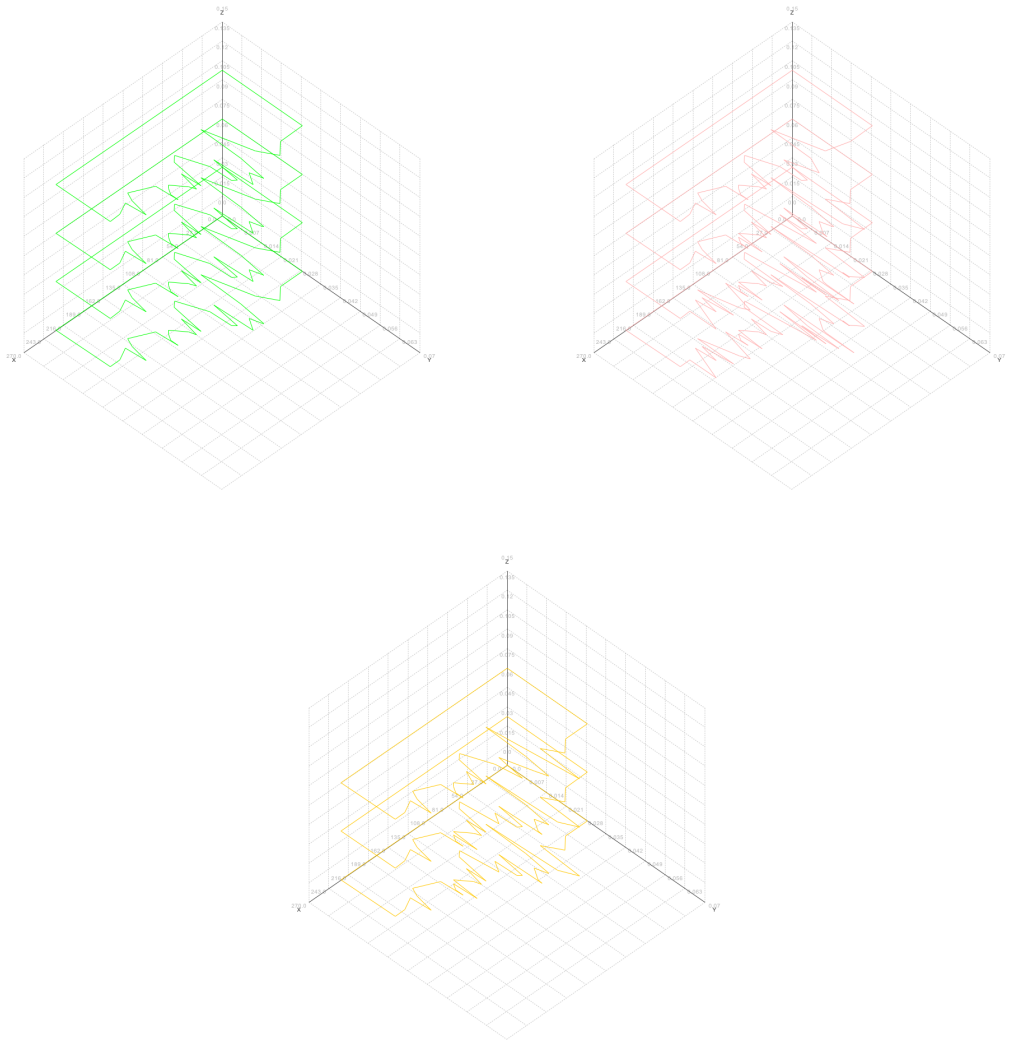

The first graph shows the stacked ROA for LQR (sum of areas=20.71), the second graph shows the stacked ROA for SDRE based on Gibb's vector (sum of areas=22.42), and the thrid graph shows the stacked ROA for SDRE and H-Infinity based on Gibb's vector (sum of areas=16.24) (X: norm of Euler angles - degrees, Y: norm of angular velocities - rad/s, Z: p - $N.m$).

SOURCE: Author.

The highest $p = 0.15$ prevented the convergence of the three control laws. At the nominal case ($p = 0$), the control laws exhibited the similar pattern discussed in Section 6.3. LQR exhibited the same ROA for all p that converged. Beyond the nominal case, the norm of angular velocities was decreasing as p increased for the control laws based on SDRE. In particular, the ROA of SDRE and H-infinity based on Gibb's vector vanished at $p = 0.1125$.

In conclusion, evaluating the "sum of areas of ROAs" (primary measure), SDRE based on Gibb's vector provided the largest ROA followed by LQR. SDRE and H-Infinity based on Gibb's vector provided the smallest ROA failing to satisfy the $\epsilon_{max} \approx 0.14$ shared in Section 6.3. Figure 6.15 shares the ROA for each p.

Figure 6.15 - ROA with hard nonlinearities and unstructured uncertainties (p, $N/.m$).

SOURCE: Author.

6.6 Discussion

Firstly, the comparison of ROAs between the current work and Yao et al. (2021) is not applicable (see Subsection 3.2.1.2) since the ROA is consequence of the satellite and control models, which includes hard nonlinearities in the present work, and the SDC parametrizations which are different.

Table 6.2 collects the primary and secondary (if applicable) measures for each scenario assessed in this chapter.

Table 6.2 - Measures collected for each scenario.

Hard nonlinearities	Uncertainty	Control	**Primary**	**Secondary**
without uncertainty				
No	-	LQR	8.96	$\mu = 0.12\,, \sigma = 0.05$
No	-	SDRE	8.96	$\mu = 0.14\,, \sigma = 0.07$
No	-	SDRE+H_∞	8.96	$\mu = 0.15\,, \sigma = 0.05$
Yes	-	LQR	5.06	$\mu = 0.23\,, \sigma = 0.14$
Yes	-	SDRE	6.10	$\mu = 0.43\,, \sigma = 0.37$
Yes	-	SDRE+H_∞	5.36	$\mu = 0.34\,, \sigma = 0.19$
with uncertainty				
Yes	Structured	LQR	19.29	-
Yes	Structured	SDRE	24.99	-
Yes	Structured	SDRE+H_∞	20.76	-
Yes	Unstructured	LQR	20.71	-
Yes	Unstructured	SDRE	22.42	-
Yes	Unstructured	SDRE+H_∞	16.24	-

SOURCE: Author.

Note the difference presented in the scale of the primary measure between the group "without uncertainty" and the group "with uncertainty" highlights that such a measure is a sum of areas in the latter group.

Focusing on the group "without uncertainty", with the infinity norm of angular velocities in the range analyzed and without hard nonlinearities, the linear control technique (LQR) was able to control the nonlinear system (linear technique controlling a nonlinear system) exhibiting the same primary measure (ROA) of the nonlinear control techniques based on SDRE. Moreover, since the secondary measure is defined by Equation (4.2) (the same cost functional of LQR in Equation (2.41)), LQR is the optimal control law in such a scenario.

Once introduced the hard nonlinearities defined by Equation 5.2, SDRE based on Gibb's vector exhibited the largest primary measure (ROA, 6.10) whereas LQR exhibited the smallest one (5.06). Henceforth, the applicability of a linear control technique is conditioned to the degree of nonlinearity of the system in control. Indeed, there is research investigating how to quantify the degree of nonlinearity of a nonlinear system as well as how adequate is a linear model for the representation of a nonlinear system (NIKOLAOU; HANAGANDI, 1998). Although such an issue is beyond the scope of the current thesis, such a degree of nonlinearity played a role once the

hard nonlinearities, as well as the uncertainties, were introduced in the models since the linear control technique (LQR) exhibited the worst ROAs consistently, which turned out the analysis of the second measure innocuous.

Moving to the group "with uncertainty", SDRE based on Gibb's vector exhibited the largest primary measure (ROA) consistently. Therefore, it provided better robustness to the structured (perturbations in the inertia tensor) and the unstructured (net external torques) uncertainties. It was remarkable the control laws based on SDRE (SDRE based on Gibb's, and SDRE and H-infinity based on Gibb's vector) had a bigger advantage in the presence of structured uncertainty regarding ROA. In fact, SDRE and H-infinity based on Gibb's vector showed the worst ROA for unstructured uncertainty due to the complete lack of control in the presence of AWGN of $p = 0.1125$ (see Figure 6.15).

6.6.1 Main result

The comparison of the **primary measure** (ROA) **rejected the null hypothesis** H_0 since there was empirical quantitative data about a significant quantifiable increment of robustness comparing the linear control technique (LQR) and the nonlinear control technique (SDRE based on Gibb's) in the Amazonia-1 INPE's mission. In particular, with hard nonlinearities and without uncertainty the increment was from 5.06 (LQR) to 6.10 (SDRE based on Gibb's) approximately 20%; with hard nonlinearities and with structured uncertainty the increment was from 19.29 (LQR) to 24.99 (SDRE based on Gibb's) approximately 29%; and, finally, with hard nonlinearities and with unstructured uncertainty the increment was from 20.71 (LQR) to 22.42 (SDRE based on Gibb's) approximately 8% (see Table 6.2).

The alternative hypothesis H_1 and the null hypothesis H_0 were mutually exclusive, which means that only one of the two hypotheses could be true. Therefore, H_1 **was accepted**.

7 CONCLUSIONS

In accordance with Subsection 6.6.1, the results provided a sufficient condition to the rejection of the null hypothesis (H_0) and, consequently, the acceptance of the alternative hypothesis (H_1).

The specific goals - namely (I) mathematical modeling and evaluation of uncertainties using SDRE and SDRE extended with H_∞ in the presence of hard nonlinearities); (II) evaluation of the stability through the determination of the region of attraction of LQR, SDRE and SDRE extended with H_∞ in the presence of hard nonlinearities and uncertainties; and (III) compare the quantifiable results, using Monte Carlo perturbation models, between a linear control technique (LQR) and its counterpart nonlinear technique SDRE as well as SDRE extended with H_∞ in the presence of hard nonlinearities and uncertainties - were completely achieved, documented in the present work and publicly available under the license GPL v3.0 at (ROMERO, 2021a).

Although the H_0 and H_1 were focused on the INPE's missions, the following contributions are original, general, and widely applicable.

The modeling of hard nonlinearities, as applied in Equation 5.2, using hybrid ODEs is *per se* a contribution in the context of robustness and performance of nonlinear control techniques, in particular, for SDRE. In addition, the evidence that such hard-nonlinearities can compromise theoretical properties - e.g, the global asymptotic stability of LQR as shown in Section 6.3 - emphasizes the importance of the estimation of ROAs. Indeed, from the engineering perspective, it is crucial to have information about the size and/or the shape of ROA since the local stability properties could be of scarce utility if the domain of attraction is very small, or if the equilibrium point is very close to its boundary. Furthermore, such estimation of ROAs can confirm valuable insights for engineering, e.g., angular velocities were the critical aspects to be constrained in the initial conditions perhaps through requirements for the launch vehicle of the satellite.

The appropriately tackling of uncertainties for nonlinear systems in the context of SDRE and SDRE extended with H_∞ as applied by this thesis is a significant contribution to the research field of control engineering. In fact, this thesis provides the missing rationale for the propositions of Çimen (2010) about the robustness of SDRE.

The approach for SDRE extended with H_∞ based on left coprime factorizations is also a control engineering contribution in the realm of SDRE since the attention was moved to the size of error signals and away from the size and bandwidth of selected closed-loop transfer function (ROMERO; SOUZA, 2020; ROMERO; SOUZA, 2021b; ROMERO; SOUZA, 2021c). Additionally, left coprime factorizations enable the finding of the suboptimal controller solving exactly three AREs whereas the SDRE's literature suggests the γ-iteration (CLOUTIER et al., 1996).

Another contribution to the field of control engineering is the evaluation of different kinematic options of SDRE technique for the attitude control since the results showed that different SDCs can produce extremely different results ranging from non-applicability of the SDRE technique to huge differences in the controllability and, consequently, in the robustness and the performance of the system (ROMERO; SOUZA, 2019a; ROMERO; SOUZA, 2019b; ROMERO; SOUZA, 2021a).

Finally, the methodology (Section 4.2) applied in this work also presents itself as a contribution since it applies experimental mathematics, in which computation is used to investigate mathematical objects and identify properties and patterns (BAILEY; BORWEIN, 2005). In particular, the abstraction of the statespace from the six dimensions (three Euler angles plus three angular velocities) to the two-dimensional space based on L2 norms of Euler angles and angular velocities allowed quantifiable comparison and visualization of ROAs (compared with Section 3).

7.1 Future works

Focusing on the engineering perspective, an envisioned future work is to evaluate different step sizes for the simulation itself and the control loop. Such enhancement would definitely turn the system under analysis (plant plus controller) into a hybrid system.

Regarding the hard nonlinearities, a relevant question for further analysis is how the degree of nonlinearity of a given system is impacted by the introduction of hard-nonlinearities (NIKOLAOU; HANAGANDI, 1998).

Another relevant aspect that would require further investigation is why SDRE extended with H_∞ based on left coprime factorization exhibited a lack of control in the presence of AWGN $p = 0.1125$ (see Figure 6.15) while the other control laws were able to control some initial conditions with the same AWGN. Although it is well-known SDRE extended with H_∞ exhibits a slower response (WANG et al., 2017)

due to its capability of disturbance rejection, it remains as a future work such an issue.

Indeed, a related issue that would require further investigation is the sensitivity of the control laws faced with a state observer (state estimator), which would provide an estimate of the internal state of a given system. Recall this work assumed that the state is always available (see Subsection 5.1.1). It is notorious LQR when faced with uncertainties may have arbitrarily small stability margins (DORATO et al., 2000).

Finally, as advocated by Çimen (2008), integral control could be evaluated to bring the system to the required structure given by Equation (2.40) and then to appropriately handle hard nonlinearities.

REFERENCES

AERONAUTICS, N.; (NASA), S. A. **NASA open source software**. 2020. Available from: <https://code.nasa.gov/>. Access in: 08.Jun.2020. 8

ARMBRUSTER, A.; BAKER, J.; CUNEI, A.; FLACK, C.; HOLMES, D.; PIZLO, F.; PLA, E.; PROCHAZKA, M.; VITEK, J. A real-time java virtual machine with applications in avionics. **ACM Transactions on Embedded Computing Systems**, v. 7, n. 1, p. 5:1–5:49, dec. 2007. ISSN 1539-9087. Available from: <http://doi.acm.org/10.1145/1324969.1324974>. 5, 7

AUB A. J.; BITTANTI, S. e. **Riccati equation**. Berlin, Germany: Springer, 1991. 30

BACCIOTTI A.; ROSIER, L. **Liapunov functions and stability in control theory**. 2. ed. Berlin, Germany: Springer, 2005. ISBN 3-540-21332-5. 4, 27

BAILEY, D. H.; BORWEIN, J. M. **Future Prospects for Computer-Assisted Mathematics**. 2005. 82

BENNETT, S. **A history of control engineering 1800-1930**. [S.l.]: Institution of Engineering & Technology, 1979. ISBN 0863410472. 13, 14, 15

BRACCI, A.; INNOCENTI, M.; POLLINI, L. Estimation of the region of attraction for state-dependent riccati equation controllers. **Journal of Guidance, Control, and Dynamics**, v. 29, n. 6, p. 1427–1430, 2006. 27, 36

CARRARA, V. **Cinemática e dinâmica da atitude de satélites artificiais**. São José dos Campos: Instituto Nacional de Pesquisas Espaciais, 2012. 111 p. Available from: <http://urlib.net/sid.inpe.br/mtc-m19/2012/01.26.19.13>. Access in: 02.May.2017. 9, 10, 12

CARVALHO, M. J. M. de. **Estudo de uma missão espacial para coleta de dados ambientais baseada em nano satélites**. 2010. 1, 2

ÇIMEN, T. State-Dependent Riccati Equation (SDRE) control: a survey. **IFAC Proceedings Volumes (IFAC-PapersOnline)**, v. 17, n. 1 pt. 1, p. 3761–3775, 2008. ISSN 14746670. 1, 4, 30, 32, 36, 83

_____. Systematic and effective design of nonlinear feedback controllers via the state-dependent Riccati equation (SDRE) method. **Annual Reviews in Control**, v. 34, n. 1, p. 32–51, 2010. ISSN 13675788. 1, 4, 19, 30, 31, 35, 36, 37, 81

CLOUTIER, J. R. State-dependent riccati equation techniques: an overview. In: AMERICAN CONTROL CONFERENCE. **Proceedings...** [S.l.], 1997. p. 932–936. 1, 4, 30

CLOUTIER, J. R.; D'SOUZA, C. N.; MRACEK, C. P. Nonlinear regulation and nonlinear H-infinity control via the state-dependent Riccati equation technique. **Conference on Nonlinear Problems in Aviation**, 1996. 1, 4, 30, 31, 32, 36, 37, 40, 82

CNES. **Open space for everyone**. 2020. Available from: <https://www.federation-openspacemakers.com/en/decouvrir/about/>. Access in: 08.Jun.2020. 8

DIMAURO, G.; SCHLOTTERER, M.; THEIL, S.; LAVAGNA, M. Nonlinear control for proximity operations based on differential algebra. **Journal of Guidance, Control, and Dynamics**, v. 38, n. 11, p. 2173–2187, apr 2015. ISSN 0731-5090. Available from: <https://doi.org/10.2514/1.G000842>. 34, 35

DORATO, P.; ABDALLAH, C.; CERONE, V. **Linear quadratic control: an introduction**. Krieger Publishing Company, 2000. ISBN 9781575241562. Available from: <https://books.google.com.br/books?id=tuYFAAAACAAJ>. 19, 83

ERDEM, E.; ALLEYNE, A. Estimation of stability regions of sdre controlled systems using vector norms. In: AMERICAN CONTROL CONFERENCE. **Proceedings...** [S.l.], 2002. v. 1, p. 80–85 vol.1. 27, 36

(ESA), E. S. A. **ESA open source policy**. 2020. Available from: <https://essr.esa.int/esa-open-source-policy>. Access in: 08.Jun.2020. 7

FORTESCUE, P. W.; SWINERD, G. G. Attitude control. **Spacecraft Systems Engineering**, p. 289–326, 2011. Available from: <http://doi.wiley.com/10.1002/9781119971009.ch9>. 11, 12

FUTEK: Torque sensor - application 317. 2018. Available from: <http://www.futek.com/application/torque-sensor/Satellite-Reaction-Wheel-Torque>. Access in: 13.Apr.2018. 47, 48

GITHUT. **Languages in Github - Pull Requests**. 2020. Available from: <https://madnight.github.io/githut/#/pull_requests/2020/1>. Access in: 07.Jun.2020. 5

GLOVER, K.; MCFARLANE, D. Robust stabilization of normalized coprime factor plant descriptions with h/sub infinity /-bounded uncertainty. **IEEE Transactions on Automatic Control**, v. 34, n. 8, p. 821–830, Aug 1989. ISSN 2334-3303. 23, 24, 25, 40

GONZALES, R. G.; SOUZA, L. C. G. d. Application of the sdre method to design a attitude control system simulator. **Advances in the Astronautical Sciences**, v. 134, n. Part 1-3, p. 2251–2258, 2009. ISSN 0065-3438. 33, 35

GOOGLE, I. **Creating an android app**. 2020. Available from: <https://developer.android.com/training/basics/firstapp/creating-project>. Access in: 07.Jun.2020. 5

HIPPARCHUS (version 1.3-SNAPSHOT). 2018. Available from: <https://github.com/Hipparchus-Math/hipparchus>. Access in: 28.Jan.2018. 39

HUGHES, P. C. **Spacecraft attitude dynamics**. [S.l.]: New York, 1986. 7, 9, 10, 12, 46, 57, 67, 103

KALMAN, R. Contributions to the theory of optimal control. In: . [S.l.: s.n.], 1960. 4, 17, 18, 19, 46

_____. On the general theory of control systems. **IFAC Proceedings Volumes**, v. 1, p. 491–502, 1960. ISSN 14746670. Available from: <http://dx.doi.org/10.1016/S1474-6670(17)70094-8>. 16, 17, 18, 19, 23, 28, 56

KHALIL, H. **Nonlinear systems**. Prentice Hall, 2002. (Pearson Education). ISBN 9780130673893. Available from: <https://books.google.com.br/books?id=t_d1QgAACAAJ>. 4, 26

KUCERA, V. A review of the matrix riccati equation. **Kybernetika**, v. 9, p. 42–61, 1973. Available from: <http://www.kybernetika.cz/content/1973/1/42/paper.pdf>. 19, 28

LEIPHOLZ, H. **Stability theory: an introduction to the stability of dynamic systems and rigid bodies**. [S.l.]: Academic Press, 1970. ISBN 012442550X. 26, 41

LIANG, Y.-W.; LIN, L.-G. Analysis of sdc matrices for successfully implementing the sdre scheme. **Automatica**, v. 49, n. 10, p. 3120–3124, 2013. ISSN 0005-1098.

Available from: <https://www.sciencedirect.com/science/article/pii/S0005109813003749>. 35

MATU, R.; PROKOP, R.; PEKA, L. Parametric and unstructured approach to uncertainty modelling and robust stability analysis. **International Journal of Mathematical Models and Methods in Applied Sciences**, v. 5, n. 6, p. 1011–1018, 2011. 23

MENON, P. K.; LAM, T.; CRAWFORD, L. S.; CHENG, V. H. Real-time computational methods for SDRE nonlinear control of missiles. **Proceedings of the American Control Conference**, v. 1, p. 232–237, 2002. ISSN 07431619. 7, 31, 34

MESQUITA, B. D. R. de; KUGA, H. K.; CARRARA, V. Estimation and attitude control in CONASAT nominal operation mode: an approach for SDRE Filter and PID control. **IEEE Latin America Transactions**, v. 15, n. 5, p. 835–842, 2017. 1, 2

NIKOLAOU, M.; HANAGANDI, V. Nonlinearity quantification and its application to nonlinear system identification. **Chemical Engineering Communications**, v. 166, n. 1, p. 1–33, 1998. Available from: <https://doi.org/10.1080/00986449808912379>. 79, 82

OREKIT (version 8.0). 2017. Available from: <https://www.orekit.org>. Access in: 01.Apr.2017. 7, 8, 39

PARKS, H. **Stability Theory**. [S.l.: s.n.], 1966. 15, 16, 27

PARKS, P. C. A. M. Lyapunov's stability theory—100 years on *. **IMA Journal of Mathematical Control and Information**, v. 9, n. 4, p. 275–303, 12 1992. ISSN 0265-0754. Available from: <https://doi.org/10.1093/imamci/9.4.275>. 28

PEARSON, J. D. Approximation methods in optimal control i. sub-optimal control. **Journal of Electronics and Control**, v. 13, n. 5, p. 453–469, 1962. Available from: <https://doi.org/10.1080/00207216208937454>. 1, 4, 30

ROMERO, A. G. **Hipparchus contributions**. Hipparchus.org, 2017. Available from: <https://github.com/Hipparchus-Math/hipparchus/commit/b9d19a715993bb82b9711e7910a4dd238d7bb91b>. Access in: 03.Nov.2019. 39

_____. **Satellite simulation developer's guide - attitude dynamics and control of nonlinear satellite simulations**. São José dos Campos: Instituto Nacional de Pesquisas Espaciais, 2020. 89 p. Available from: <http://urlib.net/rep/8JMKD3MGP3W34R/3UCPLUE>. Access in: 06 jun. 2020. 35, 39, 40, 93

_____. **Satellite simulation v0.1.0 - sources**. National Institute for Space Research, 2020. Available from: <http://urlib.net/rep/8JMKD3MGP3W34R/3SNSQ7L>. Access in: 07.Jun.2020. 40

_____. **Satellite Simulation v0.2.2 - Sources**. Github, 2021. Available from: <https://github.com/romgerale/satellitesimulator>. Access in: 14.Nov.2021. 40, 81

_____. **Thesis data**. Github, 2021. Available from: <https://github.com/romgerale/2021ThesisData>. Access in: 14.Nov.2021. 59, 103

ROMERO, A. G.; SOUZA, L. C. G. Application of the sdre technique based on java in a cubesat attitude and orbit control subsystem. In: IAA LATIN AMERICAN CUBESAT, 3., 2018. **Proceedings...** [S.l.], 2018. 35, 94

ROMERO, A. G.; SOUZA, L. C. G.; CHAGAS, R. A. Application of the sdre technique in the satellite attitude and orbit control system with nonlinear dynamics. In: SPACEOPS CONFERENCE, 2018. **Proceedings...** 2018. Available from: <https://arc.aiaa.org/doi/abs/10.2514/6.2018-2536>. 35, 39, 95

ROMERO, A. G.; SOUZA, L. C. G. de. Application of a new optimal factorization of the sdre method in the satellite attitude and orbit control system design with nonlinear dynamics. In: INTERNATIONAL CONFERENCE ON ADVANCES IN SATELLITE AND SPACE COMMUNICATIONS, 11., 2019. **Proceedings...** Valencia, Spain, 2019. 35, 40, 82, 99

_____. Optimal factorization of the state-dependent riccati equation technique in a satellite attitude and orbit control system. In: INTERNATIONAL CONFERENCE ON STRUCTURAL ENGINEERING DYNAMICS, 2019. **Proceedings...** Viana do Castelo, Portugal, 2019. 35, 40, 82, 98

_____. Satellite controller system based on reaction wheels using the state-dependent riccati equation (sdre) on java. In: CAVALCA, K. L.; WEBER, H. I. (Ed.). **Proceedings...** Cham: Springer International Publishing, 2019. p. 547–561. ISBN 978-3-319-99268-6. 35, 39, 100

_____. State-dependent Riccati equation controller using Java in remote sensing CubeSats. **Journal of Applied Remote Sensing**, v. 13, n. 3, p. 1 – 10, 2019. ISSN 19313195. Available from: <https://doi.org/10.1117/1.JRS.13.032509>. 35, 39, 93

_____. Suboptimal control on nonlinear satellite simulations using sdre and h-infinity. In: IBERO-LATIN-AMERICAN CONGRESS ON COMPUTATIONAL METHODS IN ENGINEERING, 41., 2020. **Proceedings...** Foz do Iguaću, Brazil, 2020. 35, 40, 82, 97

_____. Optimal factorization of the state-dependent Riccati equation technique in a satellite attitude and orbit control system. **WSEAS Transactions on Systems**, v. 20, p. 98 – 107, 2021. ISSN 1109-2777. Available from: <https://doi.org/10.37394/23202.2021.20.12>. 35, 39, 40, 82, 96

_____. Suboptimal control on nonlinear satellite simulations using sdre and h-infinity. **WSEAS Transactions on Systems**, v. 20, p. 1 – 8, 2021. ISSN 1109-2777. Available from: <https://doi.org/10.37394/23202.2021.20.1>. 35, 40, 82, 97

_____. Suboptimal control on nonlinear satellite simulations using sdre and h-infinity. In: **MARTINS, E. R. (Org.). Coleção Desafios das Engenharias: Engenharia de Computação**. Ponta Grossa, Paraná, Brazil: Atena Editora, 2021. p. 181–192. ISBN 978-65-5983-387-0. 40, 82, 100

SHARP, D. C.; PLA, E.; LUECKE, K. R.; HASSAN, R. J. Evaluating real-time java for mission-critical large-scale embedded systems. In: IEEE REAL-TIME AND EMBEDDED TECHNOLOGY AND APPLICATIONS SYMPOSIUM, 9., 2003. **Proceedings...** [S.l.], 2003. p. 30–36. ISSN 1545-3421. 5, 7

SIDI, M. J. **Spacecraft dynamics and control - a practical engineering approach**. [S.l.]: Cambridge University Press, 2006. 7, 45, 46, 47, 48, 54

SILVA, D. F. d.; MURAOKA, I.; GARCIA, E. C. Thermal control design conception of the Amazonia-1 satellite. **Journal of Aerospace Technology and Management**, v. 6, p. 169 – 176, 06 2014. ISSN 2175-9146. Available from: <http://www.scielo.br/scielo.php?script=sci_arttext&pid=S2175-91462014000200169&nrm=iso>. 1, 2, 39, 51

SKOGESTAD, S.; POSTLETHWAITE, I. **Multivariable feedback control: analysis and design**. Hoboken, NJ, USA: John Wiley & Sons, 2005. ISBN 0470011688. 14, 17, 20, 21, 22, 23, 24, 25, 40, 42, 56

SLOTINE, J.; LI, W. **Applied nonlinear control**. Prentice Hall, 1991. ISBN 9780130408907. Available from: <https://books.google.com.br/books?id=cwpRAAAAMAAJ>. 4, 18, 26, 28, 49

TABOR, M. **Chaos and integrability in nonlinear dynamics**. NY, USA: John Wiley & Sons, 1989. ISBN 0471827282. 26

WANG, X.; YAZ, E. E.; SCHNEIDER, S. C.; YAZ, Y. I. H2-h-infinity control of continuous-time nonlinear systems using the state-dependent riccati equation approach. **Systems Science & Control Engineering**, v. 5, n. 1, p. 224–231, 2017. 38, 82

WERTZ, J. R.; LARSON, W. **Space mission analysis and design**. [S.l.: s.n.], 1999. 976 p. ISBN 9780792359012. 50

YANG, Y. Quaternion based model for momentum biased nadir pointing spacecraft. **Aerospace Science and Technology**, v. 14, n. 3, p. 199–202, 2010. ISSN 12709638. 33

_____. Analytic LQR design for spacecraft control system based on quaternion model. **Journal of Aerospace Engineering**, v. 25, n. 3, p. 448–453, 2012. ISSN 0893-1321. Available from: <http://ascelibrary.org/doi/abs/10.1061/{%}28ASCE{%}29AS.1943-5525.0000142>. 33, 34, 52, 53

YAO, J.; HU, Q.; ZHENG, J. Nonlinear optimal attitude control of spacecraft using novel state-dependent coefficient parameterizations. **Aerospace Science and Technology**, v. 112, p. 106586, 2021. ISSN 1270-9638. Available from: <https://www.sciencedirect.com/science/article/pii/S1270963821000973>. 35, 36, 37, 41, 55, 78

ZAMES, G. Feedback and optimal sensitivity: model reference transformations, multiplicative seminorms, and approximate inverses. **IEEE Transactions on Automatic Control**, v. 26, n. 2, p. 301–320, April 1981. ISSN 2334-3303. 20

APPENDIX A - LIST OF PUBLICATIONS

A.1 Space engineering

A.1.1 2020

Satellite Simulation Developer's Guide - Attitude Dynamics and Control of Nonlinear Satellite Simulations (ROMERO, 2020a)

Abstract: The satellite attitude and orbit control subsystem (AOCS), that one in charge of the attitude control, can be designed with success by linear control theory if the satellite has slow angular motions and small attitude maneuver. However, for large and fast maneuvers, the linearized models are not able to represent all the perturbations due to the effects of the nonlinear terms present in the dynamics and in the actuators (e.g., saturation) which can damage the system's performance. Therefore, in such cases, it is expected that nonlinear control techniques yield better performance than the linear control techniques, improving the AOCS pointing accuracy without requiring a new set of sensors and actuators. One candidate technique for the design of AOCS control law under a large and fast maneuver is the State-Dependent Riccati Equation (SDRE). SDRE provides an effective algorithm for synthesizing nonlinear feedback control by allowing nonlinearities in the system states while offering great design flexibility through state-dependent weighting matrices. The Brazilian National Institute for Space Research (INPE, in Portuguese) was demanded by the Brazilian government to build remote-sensing satellites, such as the Amazonia-1 and CONASAT mission. In such missions, the AOCS must stabilize the satellite in three-axes so that the optical payload can point to the desired target. Currently, the control laws of AOCS are designed and analyzed using linear control techniques in commercial software. In this work, we report an open-source nonlinear satellite simulator built to analyze control laws and their stability and robustness. This satellite simulator is implemented in Java using Hipparchus (linear algebra library; which was extended in order to support the SDRE technique) and Orekit (flight dynamics framework). The initial results ratify that SDRE yields better performance in the INPE's missions.

A.1.2 2019

State-dependent Riccati equation controller using Java in remote sensing CubeSats (ROMERO; SOUZA, 2019d)

Qualis: B1 (Engineering III, Quadrennium 2013-2016)

Abstract: STRaND and PhoneSat programs have attracted the attention of the

aerospace community by applying, in CubeSats, commercial off-the-shelf smartphones based on Google's Android. In Android, the development commonly applies Java hence this language is a natural candidate for the attitude and orbit control subsystem (AOCS). Moreover, such AOCS can be designed with success by linear control theory; however, the linearized models are not able to represent all the effects of the nonlinear terms present in the dynamics. Therefore, nonlinear control techniques can yield better performance. An example is the Nano-Satellite Constellation for Environmental Data Collection, used as the reference in this work, a set of remote sensing CubeSats from the Brazilian National Institute for Space Research, in which the AOCS must stabilize the satellite in three-axes. We present the investigation of a state-dependent Riccati equation (SDRE) controller, a nonlinear controller, based on attitude errors given by quaternions. The investigation uses Java, accordingly, it can run on an Android operating system in a CubeSat, and it has low cost. Two controllers (linear and SDRE) were evaluated using a Monte Carlo perturbation model. The initial results show that the SDRE controller provides better performance.

A.1.3 2018

Application of the SDRE technique based on Java in a Cubesat Attitude and Orbit Control Subsystem (ROMERO; SOUZA, 2018)

Abstract: In 2013, the STRaND (University of Surrey and Surrey Satellite Technology Ltd) and the PhoneSat (NASA) programs attracted attention of the aerospace community applying commercial off-the-shelf smartphones in CubeSats. Both programs deployed CubeSats using smartphones based on Google's Android, in which application development is mainly based on Java programming language. Some of these CubeSats had actuators, e.g., STRaND-1 had three reaction wheels mounted in an orthogonal configuration to provide three-axis control, whereas PhoneSat 2.0 beta had magnetorquers to de-tumble the spacecraft. Taking into account a CubeSat that runs Android operating system (based on a smartphone), it is natural to evaluate the attitude and orbit control subsystem (AOCS) based on Java. Moreover, such AOCS can be designed with success by linear control theory, if the satellite has slow angular motions and small attitude maneuver. However, the linearized models are not able to represent all the perturbations due to the effects of th e nonlinear terms present in the dynamics and in the actuators (e.g., saturation) which can damage the system's performance. Therefore, it is expected that nonlinear control techniques yield better performance than the linear control techniques, improving the AOCS pointing accuracy. One nonlinear candidate technique for the design of AOCS control law is the State-Dependent Riccati Equation (SDRE). SDRE pro-

vides an effective algorithm for synthesizing nonlinear feedback control by allowing nonlinearities in the system states while offering great design flexibility through statedependent weighting matrices. In this paper, we present a simulator and the investigation of a SDRE control law based on attitude errors given by quaternion error. The simulator is based on Java and related open-source software libraries (Hipparchus - linear algebra library, and Orekit - flight dynamics library), therefore, it can run on a variety of platforms - including an Android operating system in a CubeSat - and it has low cost. The Java open-source libraries were extended in order to solve the optimization problem that is the cornerstone of the SDRE method. Two control laws (a linear and a SDRE based) were simulated using a Monte Carlo perturbation model. The Nano satellite Constellation for Environmental Data Collection (CONASAT), a CubeSat from the Brazilian National Institute for Space Research (INPE), provided the parameters for the simulations. The initial results of the simulations shown that the SDRE-based controller provides better performance.

Application of the SDRE Technique in the Satellite Attitude and Orbit Control System with Nonlinear Dynamics (ROMERO et al., 2018)

Abstract: The satellite attitude and orbit control subsystem (AOCS) can be designed with success by linear control theory if the satellite has slow angular motions and small attitude maneuver. However, for large and fast maneuvers, the linearized models are not able to represent all the perturbations due to the effects of the nonlinear terms present in the dynamics and in the actuators (e.g., saturation) which can damage the system's performance. Therefore, in such cases, it is expected that nonlinear control techniques yield better performance than the linear control techniques, improving the AOCS pointing accuracy without requiring a new set of sensors and actuators. One candidate technique for the design of AOCS control law under a large and fast maneuver is the State-Dependent Riccati Equation (SDRE). SDRE provides an effective algorithm for synthesizing nonlinear feedback control by allowing nonlinearities in the system states while offering great design flexibility through state-dependent weighting matrices. The Brazilian National Institute for Space Research (INPE, in Portuguese) was demanded by the Brazilian government to build remote-sensing satellites, such as the Amazonia-1 mission. In such missions, the AOCS must stabilize the satellite in three-axes so that the optical payload can point to the desired target. Currently, the control laws of AOCS are designed and analyzed using linear control techniques in commercial software. In this paper, we discuss whether the application of the SDRE technique in the AOCS design can yield gains in the missions developed by INPE. Moreover, we report a proof of concept of an open-source satellite simulator built to analyze control laws based on SDRE. This

satellite simulator is implemented in Java using Hipparchus (linear algebra library; which was extended in order to support the SDRE technique) and Orekit (flight dynamics framework).

A.2 Control engineering

A.2.1 2021

Optimal Factorization of the State-Dependent Riccati Equation Technique in a Satellite Attitude and Orbit Control System (ROMERO; SOUZA, 2021a)

Qualis: C (Engineering III, Quadrennium 2013-2016)

Abstract: The satellite attitude and orbit control system (AOCS) can be designed with success by linear control theory if the satellite has slow angular motions and small attitude maneuver. However, for large and fast maneu- vers, the linearized models are not able to represent all the perturbations due to the effects of the nonlinear terms present in the dynamics and in the actuators (e.g., saturation). Therefore, in such cases, it is expected that nonlin- ear control techniques yield better performance than the linear control techniques. One candidate technique for the design of AOCS control law under a large maneuver is the State-Dependent Riccati Equation (SDRE). SDRE entails factorization (that is, parameterization) of the nonlinear dynamics into the state vector and the product of a matrix-valued function that depends on the state itself. In doing so, SDRE brings the nonlinear system to a (nonunique) linear structure having state-dependent coefficient (SDC) matrices and then it minimizes a nonlinear performance index having a quadratic-like structure. The nonuniqueness of the SDC matrices creates extra degrees of freedom, which can be used to enhance controller performance, however, it poses challenges since not all SDC matrices fulfill the SDRE requirements. Moreover, regarding the satellite's kinematics, there is a plethora of options, e.g., Euler angles, Gibbs vector, modified Rodrigues parameters (MRPs), quaternions, etc. Once again, some kinematics formulation of the AOCS do not fulfill the SDRE requirements. In this paper, we evaluate the factorization options (SDC matrices) for the AOCS exploring the requirements of the SDRE technique. Consid- ering a Brazilian National Institute for Space Research (INPE) typical mission, in which the AOCS must stabilize a satellite in three-axis, the application of the SDRE technique equipped with the optimal SDC matrices can yield gains in the missions. The initial results show that MRPs for kinematics provides an optimal SDC matrix.

Stability Evaluation of the SDRE Technique based on Java in a CubeSat Attitude and Orbit Control Subsystem (ROMERO; SOUZA, 2021b)
Qualis: C (Engineering III, Quadrennium 2013-2016)
Abstract: In 2013, the STRaND (University of Surrey and Surrey Satellite Technology Ltd) and the PhoneSat (NASA) programs attracted the attention of the aerospace community applying commercial off-the-shelf smartphones in CubeSats. Both programs deployed CubeSats using smartphones based on Google's Android, in which application development is mainly based on Java programming language. Some of these CubeSats had actuators, e.g., STRaND-1 had three reaction wheels mounted in an orthogonal configuration to provide three-axis control, whereas PhoneSat 2.0 beta had magnetorquers to de-tumble the spacecraft. Taking into account a CubeSat that runs Android operating system (based on a smartphone), it is natural to evaluate the attitude and orbit control subsystem (AOCS) based on Java. Elsewhere, we shown State-Dependent Riccati Equation (SDRE) is a feasible non-linear control technique that can be applied in such CubeSats using Java. Moreover, we shown, through simulation using a Monte Carlo perturbation model, SDRE provides better performance than the PID controller, a linear control technique. In this paper, we tackle the next fundamental problem: stability. We evaluate stability from two perspectives: (1) parametric uncertainty of the inertia tensor and (2) a Monte Carlo perturbation model based on a uniform attitude probability distribution. Through the combination of these two perspectives, we grasp the stability properties of SDRE in a broader sense. In order to handle the uncertainty appropriately, we combine SDRE with H-infinity. The Nanosatellite Constellation for Environmental Data Collection (CONASAT), a CubeSat from the Brazilian National Institute for Space Research (INPE), provided the nominal parameters for the simulations. The initial results of the simulations shown that the SDRE controller is stable to $\pm$ 20% uncertainty in the inertia tensor for attitudes uniformly distributed and angular velocity up to 0.15 radians/second.

A.2.2 2020

Suboptimal Control on Nonlinear Satellite Simulations using SDRE and H-infinity (ROMERO; SOUZA, 2020)
Abstract: The control of a satellite can be designed with success by linear control theory if the satellite has slow angular motions. However, for fast maneuvers, the linearized models are not able to represent all the perturbations due to the effects of the nonlinear terms present in the dynamics which compromises the system's performance. Therefore, a nonlinear control technique yields better performance.

Nonetheless, these nonlinear control techniques can be more sensitive to uncertainties. One candidate technique for the design of the satellite's control law under a fast maneuver is the State-Dependent Riccati Equation (SDRE). SDRE provides an effective algorithm for synthesizing nonlinear feedback control by allowing nonlinearities in the system states. The Brazilian National Institute for Space Research (INPE, in Portuguese) was demanded by the Brazilian government to build remote-sensing satellites, such as the Amazonia-1 mission. In such missions, the satellite must be stabilized in three-axes so that the optical payload can point to the desired target. Although elsewhere the application of the SDRE technique has shown to yield better performance for the missions developed by INPE, a subsequent important question is whether such better performance is robust to uncertainties. In this paper, we investigate whether the application of the SDRE technique in the AOCS is robust stable to uncertainties in the missions developed by INPE. Moreover, in order to handle such uncertainty appropriately, we propose a combination of SDRE with H-infinity based on a left coprime factorization. In such a way that the attention is moved to the size of error signals and away from the size and bandwidth of selected closed-loop transfer function. The initial results showed that SDRE controller is robust to 5%, at least, variations in the inertia tensor of the satellite.

A.2.3 2019

Optimal Factorization of the State-Dependent Riccati Equation Technique in a Satellite Attitude and Orbit Control System (ROMERO; SOUZA, 2019b)

Abstract: The satellite attitude and orbit control system (AOCS) can be designed with success by linear control theory if the satellite has slow angular motions and small attitude maneuver. However, for large and fast maneuvers, the linearized models are not able to represent all the perturbations due to the effects of the nonlinear terms present in the dynamics and in the actuators (e.g., saturation). Therefore, in such cases, it is expected that nonlinear control techniques yield better performance than the linear control techniques. One candidate technique for the design of AOCS control law under a large maneuver is the State-Dependent Riccati Equation (SDRE). SDRE entails factorization (that is, parameterization) of the nonlinear dynamics into the state vector and the product of a matrix-valued function that depends on the state itself. In doing so, SDRE brings the nonlinear system to a (nonunique) linear structure having state-dependent coefficient (SDC) matrices and then it minimizes a nonlinear performance index having a quadratic-like structure. The nonuniqueness of the SDC matrices creates extra degrees of freedom, which can

be used to enhance controller performance, however, it poses challenges since not all SDC matrices fulfill the SDRE requirements. Moreover, regarding the satellite's kinematics, there is a plethora of options, e.g., Euler angles, Gibbs vector, modified Rodrigues parameters (MRPs), quaternions, etc. Once again, some kinematics formulation of the AOCS do not fulfill the SDRE requirements. In this paper, we evaluate the factorization options (SDC matrices) for the AOCS exploring the requirements of the SDRE technique. Considering a Brazilian National Institute for Space Research (INPE) typical mission, in which the AOCS must stabilize a satellite in three-axis, the application of the SDRE technique equipped with the optimal SDC matrices can yield gains in the missions. The initial results show that MRPs for kinematics provides an optimal SDC matrix.

Application of a New Optimal Factorization of the SDRE Method in the Satellite Attitude and Orbit Control System Design with Nonlinear Dynamics (ROMERO; SOUZA, 2019a)

Abstract: The satellite Attitude and Orbit Control System (AOCS) can be designed with success by linear control theory if the satellite has slow angular motions and small attitude maneuver. However, for large and fast maneuvers, the linearized models are not able to represent all the perturbations due to the effects of the nonlinear terms present in the dynamics and in the actuators. Therefore, in such cases, it is expected that nonlinear control techniques yield better performance than the linear control techniques. One candidate technique for the design of AOCS control law under a large maneuver is the State-Dependent Riccati Equation (SDRE). SDRE entails factorization (that is, parameterization) of the nonlinear dynamics into the state vector and the product of a matrix-valued function that depends on the state itself. In doing so, SDRE brings the nonlinear system to a (not unique) linear structure having State-Dependent Coefficient (SDC) matrices and then it minimizes a nonlinear performance index having a quadratic-like structure. The non uniqueness of the SDC matrices creates extra degrees of freedom, which can be used to enhance controller performance; however, it poses challenges since not all SDC matrices fulfill the SDRE requirements. Moreover, regarding the satellite's kinematics, there is a plethora of options, e.g., Euler angles, Gibbs vector, Modified Rodrigues Parameters (MRPs), quaternions, etc. Once again, some kinematics formulations of the AOCS do not fulfill the SDRE requirements. In this paper, we evaluate the factorization options of SDC matrices for the AOCS exploring the requirements of the SDRE technique. Considering a Brazilian National Institute for Space Research (INPE) typical mission, in which the AOCS must stabilize a satellite in three-axis, the application of the SDRE technique equipped with the optimal SDC matrices can yield

gains in the missions. The initial results show that MRPs for kinematics provides an optimal SDC matrix.

Satellite Controller System Based on Reaction Wheels Using the State-Dependent Riccati Equation (SDRE) on Java: Vol. 2 (ROMERO; SOUZA, 2019c)

Abstract: Complex space missions involving large angle maneuvers and fast attitude control require nonlinear control methods to design the Satellite Controller System (SCS) in order to satisfy robustness and performance requirements. One candidate method for a nonlinear SCS control law is the State-Dependent Riccati Equation (SDRE). SDRE provides an effective algorithm for synthesizing nonlinear feedback control by allowing nonlinearities in the system states while offering great design flexibility through state-dependent weighting matrices. In that context, analysis by simulation of nonlinear control methods can save money and time. Although, commercial 3D simulators exist that can accommodate various satellites components including the controllers, in this paper, we present a 3D simulator and the investigation of a SDRE control law performance by simulations. The simulator is implemented based on Java and related open-source software libraries (Hipparchus - linear algebra library, and Orekit - flight dynamics library), therefore, it can run in a variety of platforms and it has low cost. These open-source libraries were extended in order to solve the optimization problem that is the cornerstone of the SDRE method, a major contribution of the simulator. The simulator is evaluated taking into account a typical mission of the Brazilian National Institute for Space Research (INPE), in which the SCS must stabilize a satellite in three-axis using reaction wheels so that the optical payload can point to the desired target. Two SCS control laws (a linear and a SDRE based) were simulated for an attitude maneuver in the launch and early orbit phase (LEOP), the upside-down maneuver. The results of simulations shown that SDRE-based controller provides better performance.

A.3 Computer engineering

A.3.1 2021

Suboptimal Control on Nonlinear Satellite Simulations using SDRE and H-Infinity (ROMERO; SOUZA, 2021c)

Abstract: The control of a satellite can be designed with success by linear control theory if the satellite has slow angular motions. However, for fast maneuvers, the linearized models are not able to represent all the perturbations due to the effects of the nonlinear terms present in the dynamics which compromises the system's

performance. Therefore, a nonlinear control technique yields better performance. Nonetheless, these nonlinear control techniques can be more sensitive to uncertainties. One candidate technique for the design of the satellite's control law under a fast maneuver is the State-Dependent Riccati Equation (SDRE). SDRE provides an effective algorithm for synthesizing nonlinear feedback control by allowing nonlinearities in the system states. The Brazilian National Institute for Space Research (INPE, in Portuguese) was demanded by the Brazilian government to build remote-sensing satellites, such as the Amazonia-1 mission. In such missions, the satellite must be stabilized in three-axes so that the optical payload can point to the desired target. Although elsewhere the application of the SDRE technique has shown to yield better performance for the missions developed by INPE, a subsequent important question is whether such better performance is robust to uncertainties. In this paper, we investigate whether the application of the SDRE technique in the AOCS is robust stable to uncertainties in the missions developed by INPE. Moreover, in order to handle such uncertainty appropriately, we propose a combination of SDRE with H-infinity based on a left coprime factorization. In such a way that the attention is moved to the size of error signals and away from the size and bandwidth of selected closed-loop transfer function. The initial results showed that SDRE controller is robust to 5%, at least, variations in the inertia tensor of the satellite.

APPENDIX B - PURE-SPIN MANEUVERS

This appendix reports the results of simulations for two particular maneuvers (without any source of perturbation) that provide complementary engineering insights. The data, as generated by the simulator, are completely available at Romero (2021b).

Firstly, the classical results, e.g., Hughes (1986), define ω-stability(sub-statespace covering only ω, angular velocities) regarding the so called "pure-spins" of a rigid-body. These results are based on the magnitude of the inertia component of each axis in the inertia tensor. Taking into account three axes, (1) the major-axis is the one that has the greatest component in the diagonal of the inertia tensor, (2) the minor-axis is the one that has the lesser component in the diagonal of the inertia tensor, and (3) the intermediary-axis spin is the other.

Taking into account the "pure-spins" and *ω-stability*: (1) the major-axis spin is Lyapunov stable, (2) the minor-axis spin is Lyapunov stable, and (3) the intermediary-axis spin is not Lyapunov stable (HUGHES, 1986).

Therefore, a maneuver that poses an additional challenge for the control laws studied is a "pure-spin" around the intermediary-axis - in other words, initial angular velocity presents sole on the intermediary-axis - since such a state is unstable. Regarding Amazonia-1, which is characterized by Table 5.1, the intermediary-axis is Y. Consequently, an initial condition, in which a pure-spin around Y at the norm (L2) of maximum controllable velocity (according to Section 6.1, the upper bound expected for the norm of the angular velocities of the initial conditions inside any ROA is the previously shared 0.0556 rad/s - in the presence of the hard-nonlinearities), is a particular maneuver that provides complementary engineering insights, see Section B.1.

A maneuver that poses also a challenge for the control laws studied is a "pure-spin" around the major-axis since such a state is stable but offers the greater "resistance" to movement. Regarding the satellite Amazonia-1, which is characterized by Table 5.1, the major-axis is Z. Consequently, an initial condition, in which a pure-spin around Z at the norm (L2) of maximum controllable velocity (0.0556 rad/s, according to Section 6.1) would be a maneuver that could provide complementary engineering insights. Nonetheless, the three control laws did not provide ω-stability for such maneuver as would be expected since this axis has the greater "resistance" to movement. The next maneuver evaluated was one with pure-spin around Z at the angular velocity defined by the infinity norm of maximum controllable velocity

(0.0385 rad/s, according to Section 6.1). For such a maneuver a control law provided asymptotic ω-stability, see Section B.2.

Finally, the "pure-spin" around the final minor-axis does not pose a challenge once the satellite could be stabilized around the other axes.

B.1 Y pure-spin

One simulation ran for each control law using the following parameters: initial Euler Angles (ZYX, degrees) $\{0, 0, 0\}$ and initial angular velocities (rad/s) $\{0, 0.0556, 0\}$. Q and R equals to identity, $t_f = 3600$s, fixed step size 0.05s and the hard-nonlinearities in accordance with Equation (5.2).

Figure B.1 shows the results for LQR control law. It turned out that the control law was not able to provide ω-stability for the satellite, moreover, the reaction wheels exhibited saturation with their maximum velocity ($\pm 628\, rad/s$) due to the hard-nonlinearities.

Figure B.1 - Y “pure-spin” controlled by LQR.

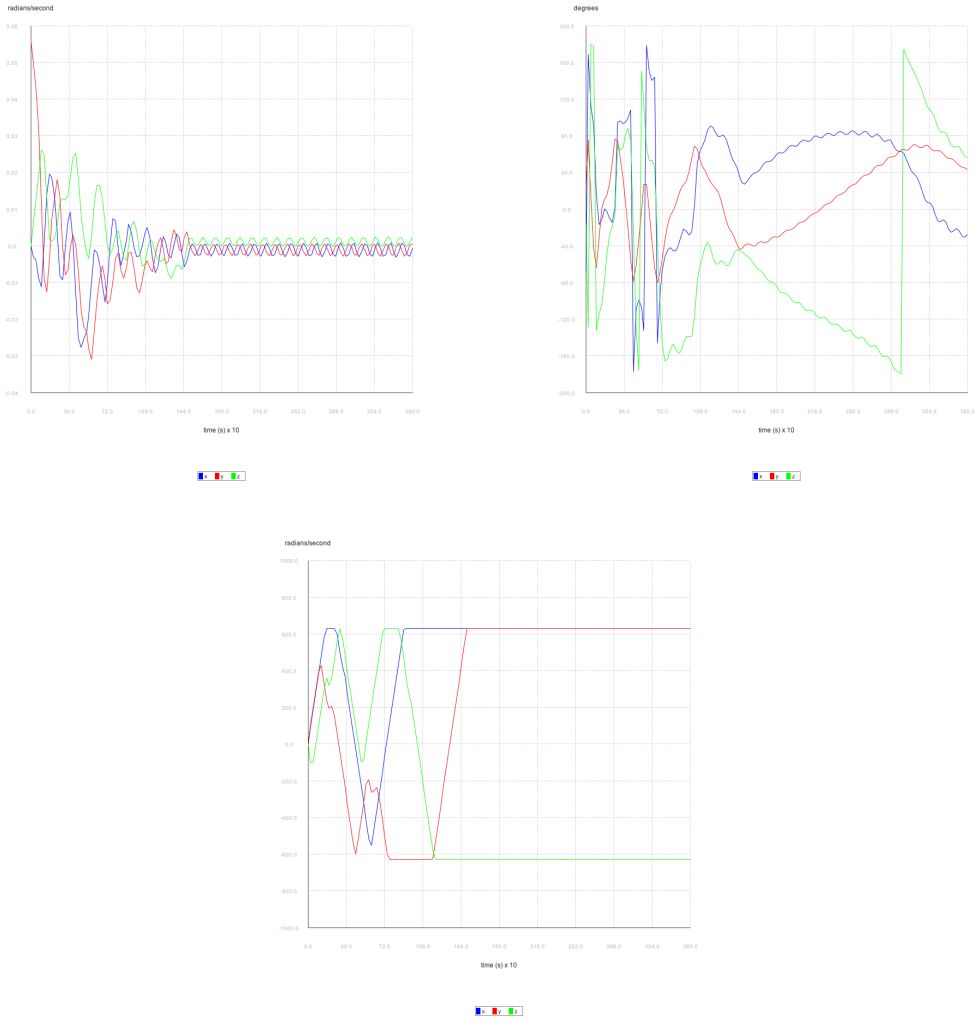

The first graph shows the angular velocities (rad/s), the second one the error of the solar vector (degrees) and the last one the reaction wheels angular velocities (rad/s).

SOURCE: Author.

Figure B.2 shows the results for SDRE based on Gibb’s vector control law. It turned out that the control law was able to provide asymptotic ω-stability for the satellite. Furthermore, using the nonlinearity, the saturation of reaction wheels did not prevent from the control law to extract torques that lead to ω-stability.

Figure B.2 - Y “pure-spin” controlled by SDRE based on Gibb’s vector.

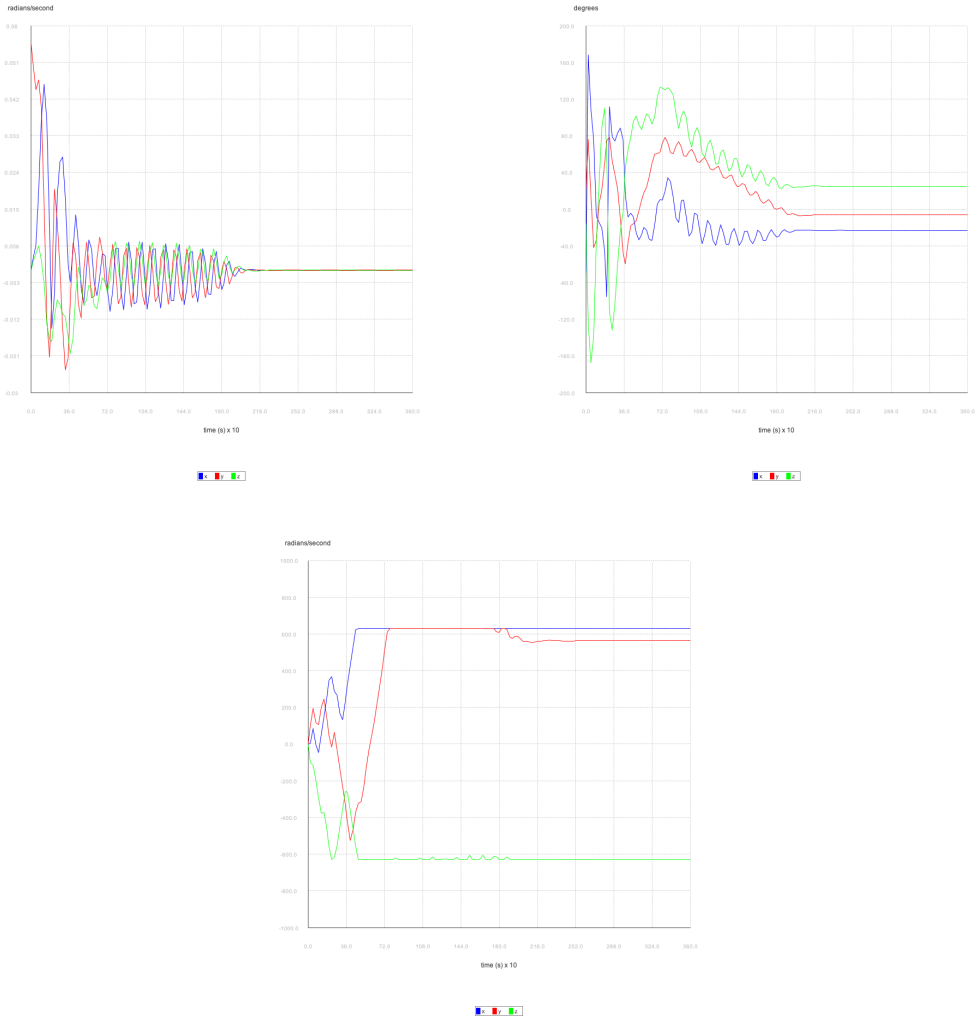

The first graph shows the angular velocities (rad/s), the second one the error of the solar vector (degrees) and the last one the reaction wheels angular velocities (rad/s).

SOURCE: Author.

Although asymptotic ω-stability was achieved, as discussed in Subsection 5.4.2, the region on which the angular velocity is close to 0 rad/s poses challenges to SDRE based on Gibb’s vector. Therefore, the error of the solar vector exhibited a pointing error.

Figure B.3 shows the results for SDRE and H-infinity based on Gibb’s vector control law. It turned out that the control law was not able to provide ω-stability for the satellite, moreover, using the nonlinearity, in the presence of the saturation of reaction wheels the control law was able to extract torques but they did not lead to

ω-stability.

Figure B.3 - Y “pure-spin” controlled by SDRE and H-infinity based on Gibb’s vector.

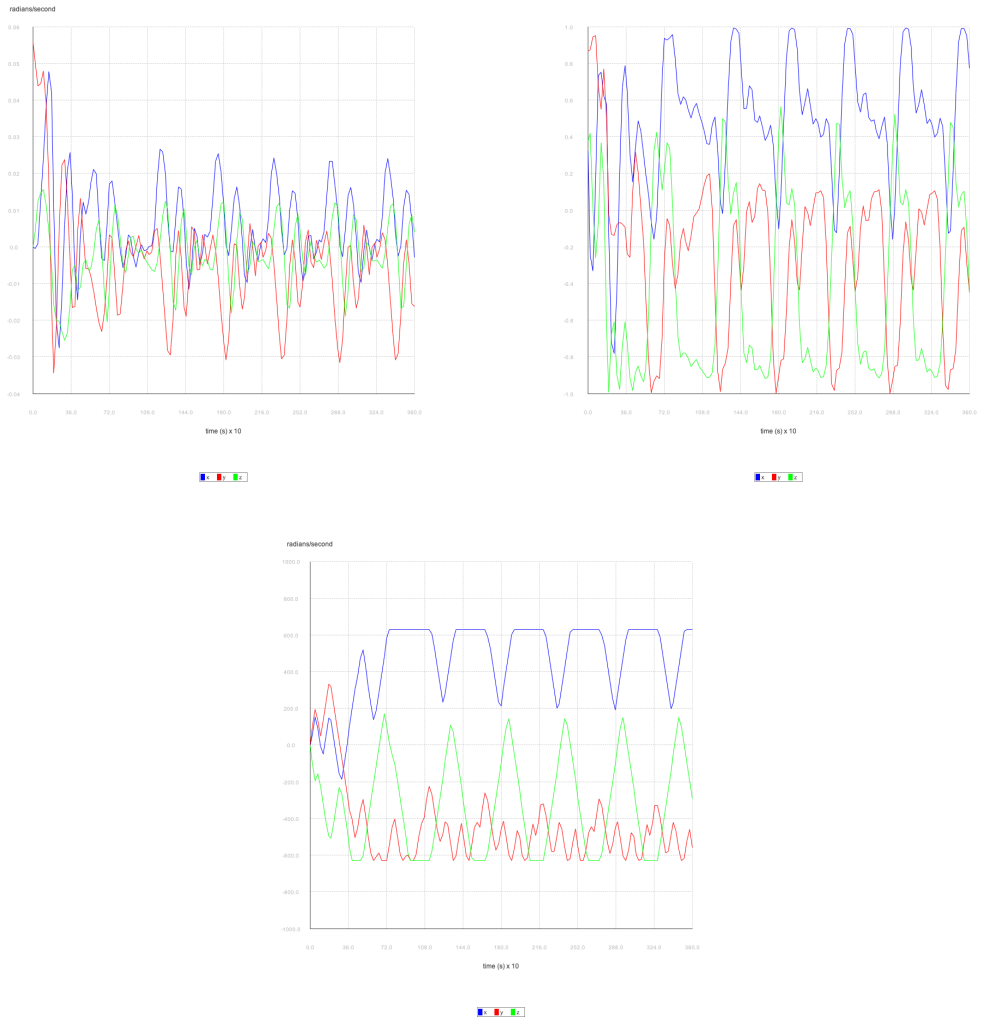

The first graph shows the angular velocities (rad/s), the second one the error of the solar vector (degrees) and the last one the reaction wheels angular velocities (rad/s).

SOURCE: Author.

In conclusion, SDRE based on Gibb’s vector was the only control law that provided asymptotic ω-stability. Clearly, the Y “pure-spin” was outside of the ROA of the SDRE and H-infinity based on Gibb’s vector control law. Due to the linearity in LQR explicitly, once the saturation was in place the control law was ineffective.

B.2 Z pure-spin

One simulation ran for each control law using the following parameters: initial Euler Angles (ZYX, degrees) $\{0, 0, 0\}$ and initial angular velocities (rad/s) $\{0, 0, 0.0385\}$. Q and R equals to identity, $t_f = 3600$s, fixed step size 0.05s and the hard-nonlinearities in accordance with Equation (5.2).

Figure B.4 shows the results for LQR control law. It turned out that the control law was not able to provide ω-stability for the satellite, moreover, the reaction wheels exhibited saturation with their maximum velocity ($\pm 628\, rad/s$) due to the hard-nonlinearities.

Figure B.4 - Z “pure-spin” controlled by LQR.

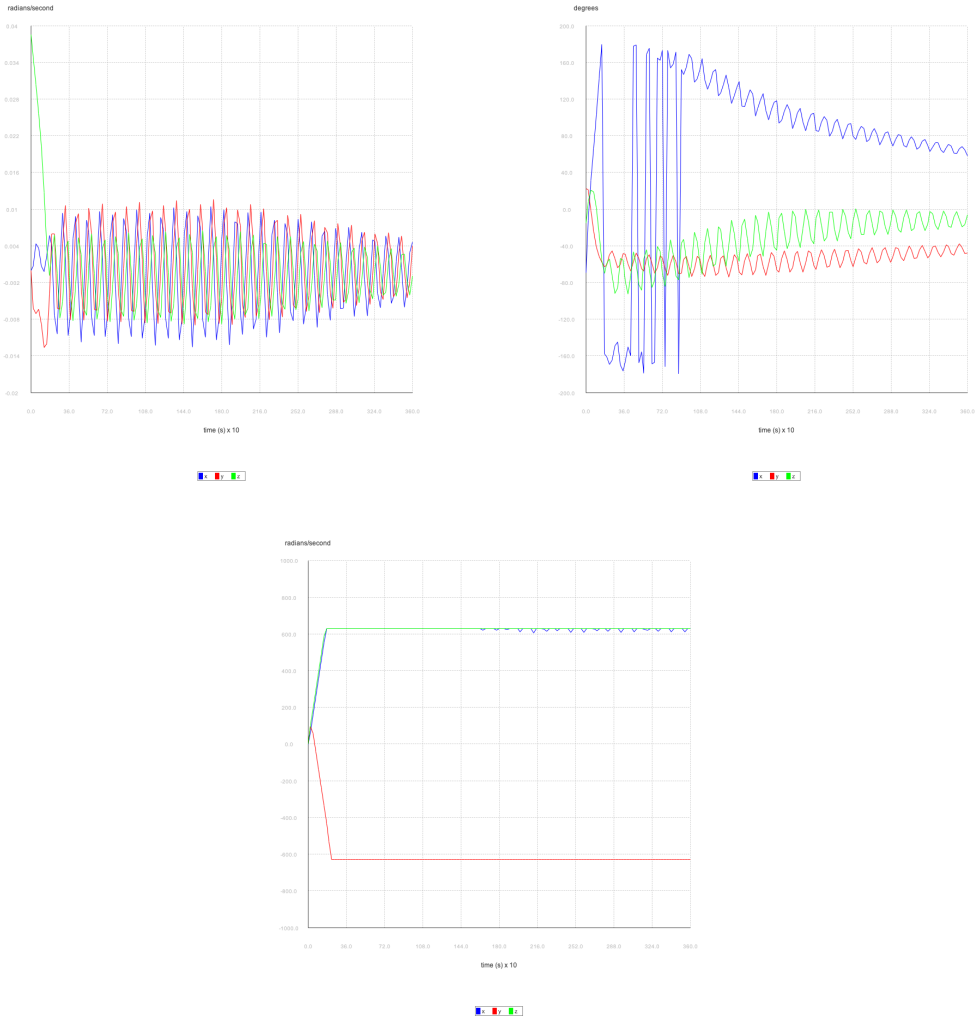

The first graph shows the angular velocities (rad/s), the second one the error of the solar vector (degrees) and the last one the reaction wheels angular velocities (rad/s).

SOURCE: Author.

Figure B.5 shows the results for SDRE based on Gibb’s vector control law. It turned out that the control law was able to provide asymptotic ω-stability for the satellite. Furthermore, using the nonlinearity, the saturation of reaction wheels did not prevent from the control law to extract torques that lead to ω-stability.

Figure B.5 - Z “pure-spin” controlled by SDRE based on Gibb’s vector.

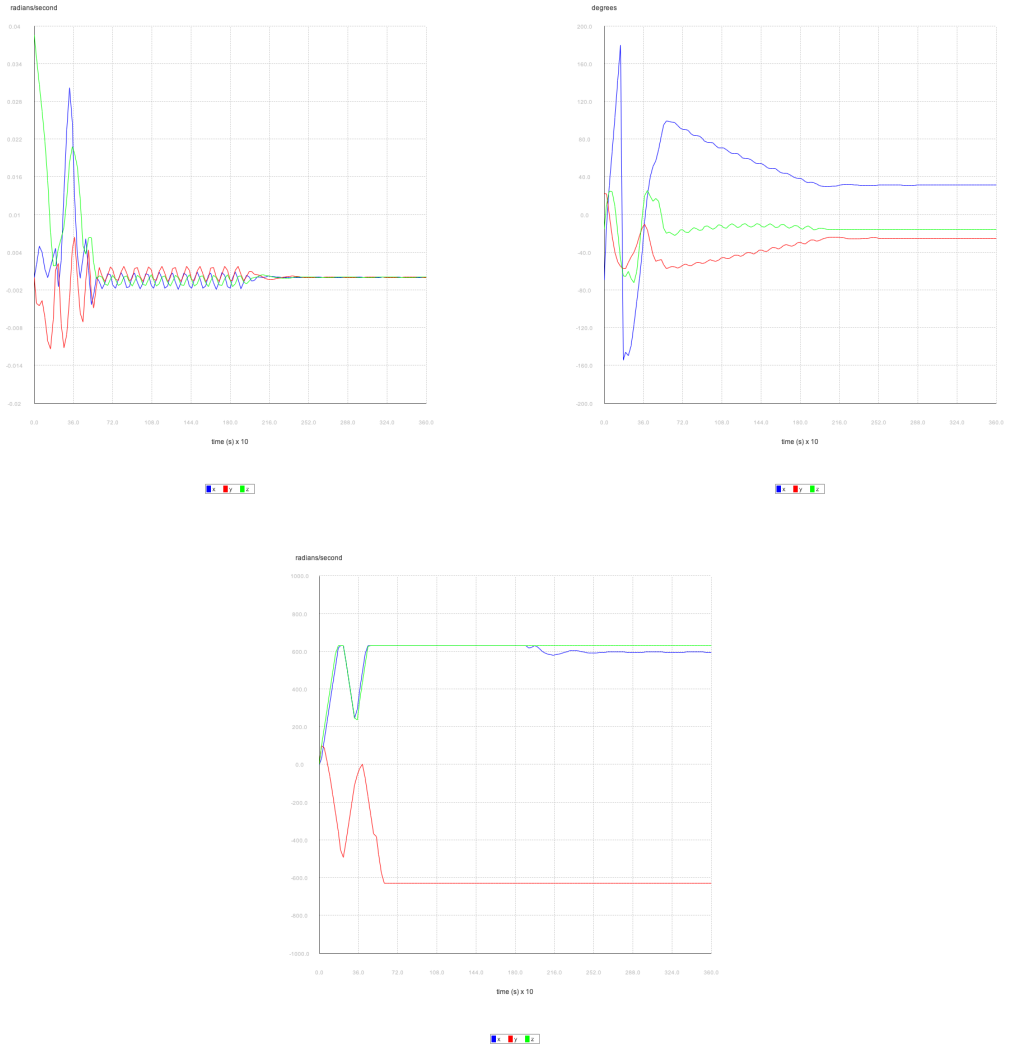

The first graph shows the angular velocities (rad/s), the second one the error of the solar vector (degrees) and the last one the reaction wheels angular velocities (rad/s).

SOURCE: Author.

Although asymptotic ω-stability was achieved, as discussed in Subsection 5.4.2, the region on which the angular velocity is close to 0 rad/s poses challenges to SDRE based on Gibb’s vector. Therefore, the error of the solar vector exhibited a pointing error.

Figure B.6 shows the results for SDRE and H-infinity based on Gibb’s vector control law. It turned out that the control law was not able to provide ω-stability for the satellite.

Figure B.6 - Z “pure-spin” controlled by SDRE and H-infinity based on Gibb’s vector.

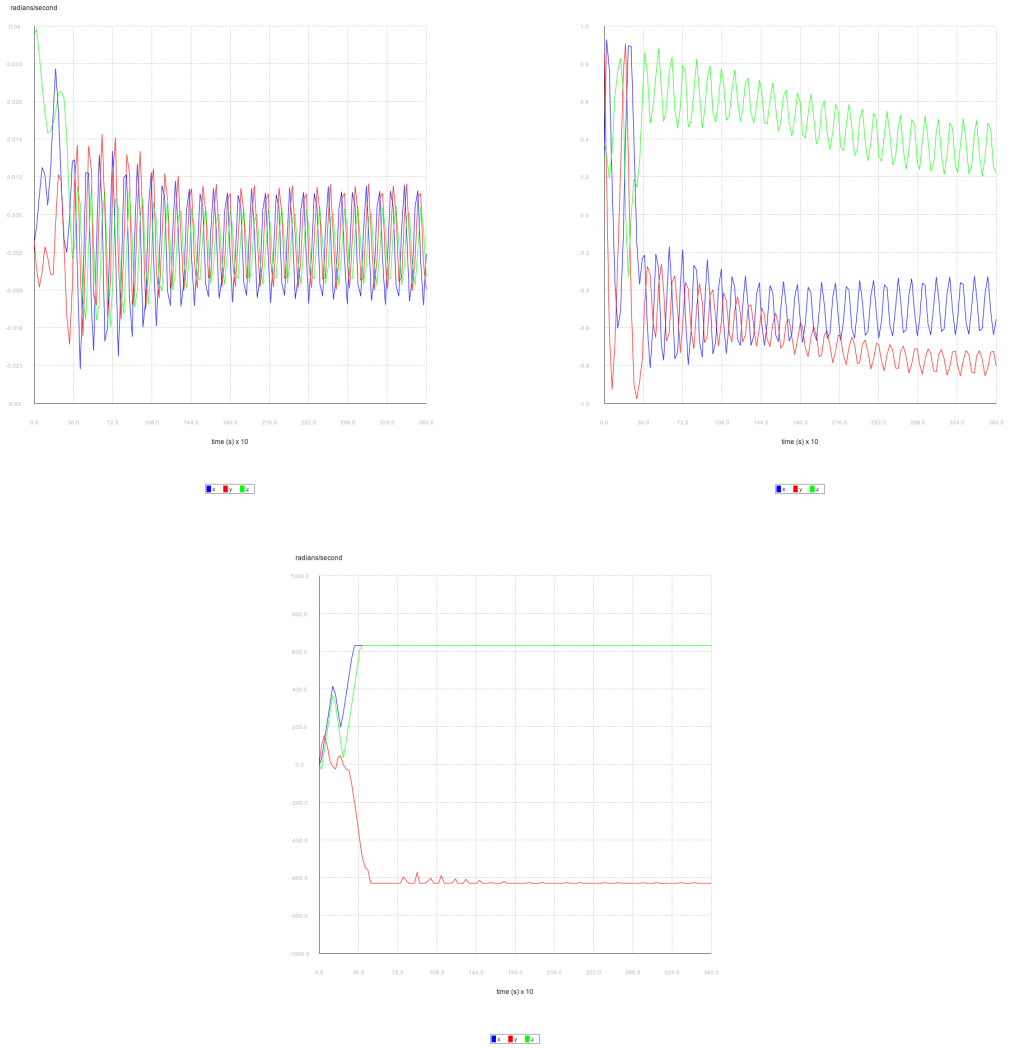

The first graph shows the angular velocities (rad/s), the second one the error of the solar vector (degrees) and the last one the reaction wheels angular velocities (rad/s).

SOURCE: Author.

In conclusion, SDRE based on Gibb’s vector was the only control law that provided asymptotic ω-stability. Clearly, the Z “pure-spin” was outside of the ROA of the SDRE and H-infinity based on Gibb’s vector control law. Due to the linearity in LQR, once the saturation was in place the control law was ineffective.